

CLEAN COAL TECHNOLOGIES, CLEAN AIR LEGISLATION,  
AND NATIONAL ENERGY STRATEGY

by

C. Lowell Miller, Ph.D.  
Associate Deputy Assistant Secretary for Clean Coal  
Office of Fossil Energy (FE-22)  
U.S. Department of Energy  
Washington, D.C., 20585

## Introduction

Over the last year or two, several new phrases have become part of our lexicon, and have become so well known that they are now "household words"; included are phrases like:

- Acid rain,
- Ozone depletion, and
- Global warming.

These words all conjur up a frightening image of withering trees, dying lakes, sunburn, rising oceans, and flooded coasts. As a response, however, in 1989 the Bush Administration strove to familiarize the American public with two more phrases; these were:

- The Clean Air Act Amendments of 1989, and
- National Energy Strategy.

If the job is done right, the image that these words will conjur up will be reduced pollution, environmental protection, and a reliable supply of energy at an affordable price. That's where the Clean Coal Technology (CCT) Program comes in, because the CCT Program is the single most potent means at our disposal with which to overcome the global dilemma of how to use our abundant fossil fuels — not just America's, but indeed the world's — without simultaneously impairing the very quality of life we are working to improve with readily available electrical and other forms of energy.

There is no point in pretending that coal is what it is not, nor that it is not what it is. Coal is naturally endowed with the elements and minerals of the living organisms that define its primordial origins, and that means the carbon for which it is valued. But, to some degree, it also must mean sulfur, and nitrogen, and incombustible impurities. It is an incontrovertible fact that the uncontrolled burning of coal will release into the environment carbon dioxide (CO<sub>2</sub>), sulfur dioxide (SO<sub>2</sub>), oxides of nitrogen (NO<sub>x</sub>), particulate matter, and ash.

It is the business of the CCT Program to develop the means of burning this coal with attendant minimal emissions of these undesirable pollutants; we know that there can never be none. So, if not literally "clean" coal, then certainly we mean "cleaner" coal, and it is in this sense that the Program uses the shorthand term, Clean Coal Technology.

### **What Are Clean Coal Technologies?**

Now, having said that, what are Clean Coal **Technologies**? When we refer to CCTs, we mean advanced coal-based systems that can offer significant benefits when used to generate power, control pollution, or to convert coal into other alternative energy products.

For electric utilities, the characteristics of these technologies, including such attributes as higher thermal efficiency, modular construction, improved environmental performance, fuel flexibility, and repowering capability, will help them adapt to the decade of the 90's — a time of difficult and even conflicting pressures from regulatory reform, uncertain growth in power demand, environmental concerns, and increasing competition from independent power producers and cogenerators.

With regard to pollution control, CCTs have the ability to produce less, or to directly remove from the combustion process, SO<sub>2</sub> and NO<sub>x</sub> acid rain precursors, and to reduce the amount of CO<sub>2</sub> generated by coal combustion. The types and quantities of pollutants removed will, of course, be a function of the specific CCT under consideration. In fact, some CCTs (e.g., pressurized fluidized bed combustion [PFBC] and integrated gasification combined cycle [IGCC]) even have the ability to remove SO<sub>2</sub> and NO<sub>x</sub> while at the same time increasing the power output of the facility itself from 50-150 percent. Table 1 lists the environmental performance of CCTs as compared to conventional (uncontrolled) pulverized coal-fired power plants.

Finally, CCTs can afford us the opportunity to produce coal-derived liquid fuels to replace oil and gas in numerous important applications. This capability could permit coal to play a much greater role in providing energy to the industrial, commercial, and transportation sectors.

### **The Projects That Comprise the CCT Program**

On December 19, 1985, Congress passed Pub. L. No. 99-190, *An Act Making Appropriations for the Department of the Interior and Related Agencies for the Fiscal Year Ending September 30, 1986, and for Other Purposes*. Included in this Act were provisions for funds to conduct cost-shared, clean coal technology, projects for constructing and operating facilities demonstrating the feasibility of future commercial clean coal applications.

## ENVIRONMENTAL PERFORMANCE OF CLEAN COAL TECHNOLOGIES RELATIVE TO CONVENTIONAL COAL-FIRED POWER PLANTS

| Technology                    | SO <sub>2</sub> Reduction | NO <sub>x</sub> Emissions | Waste Characteristics      |
|-------------------------------|---------------------------|---------------------------|----------------------------|
| Coal Cleaning:                | 10 - 30%                  | No change.                | Solids disposal.           |
| Flue Gas Desulfurization:     | 90+ %                     | No change.                | Sludge disposal.           |
| Advanced Flue Gas Cleaning    | 90+ %                     | Large reduction.          | Usable byproduct.          |
| Lime. Inj. Ms. Burner (LIMB): | 50 - 60 %                 | Moderate reduction.       | Dry pwdr. ok for landfill. |
| Slagging Combustor:           | 50 - 90 %                 | Moderate reduction.       | Dry pwdr. ok for landfill. |
| Gas Reburning:                | 10 - 20 %                 | Moderate reduction.       | None produced.             |
| In-duct Sorbent Injection:    | 50 - 70 %                 | No change.                | Dry pwdr. ok for landfill. |
| Advanced Coal Cleaning:       | 30 - 90 %                 | No change.                | Solids disposal.           |
| Int. Gas. Comb. Cycle (IGCC): | 95 - 99 %                 | Moderate reduction.       | Slag, S, min. addl solids  |
| Pressurized FBC:              | 90 - 95 %                 | Moderate reduction.       | Dry gran. nontox. solids   |
| Atmospheric FBC:              | 85 - 90 %                 | Moderate reduction.       | Dry gran. nontox. solids   |

This first solicitation was open to all market applications of CCTs that applied to any segment of the United States coal resource base; the solicitation also encompassed both "new" and "retrofit" applications. DOE issued a Program Opportunity Notice (PON) on February 17, 1986, and received of 51 proposals by the April 18, 1986, deadline.

The outcome was the selection, on July 25, 1986, of nine initial projects for negotiation of Cooperative Agreements, and the identification of 14 alternate projects to be considered should negotiations not be successfully completed with any of the initial candidates. As of this writing, 8 of the alternate projects eventually entered into negotiations. Seven Cooperative agreements have now been executed, while three additional projects are in various stages of negotiation. These ten CCT-I projects now in the Program, and their locations, are shown in Figure 1.

While CCT-I was directed at demonstrating technologies that could, through increased efficiency and flexibility, increase the role of coal as an energy option, CCT-II was more focused and directed specifically on demonstrating technologies that can address the environmental aspects of coal use associated with the issue of acid rain. The objectives were derived principally from the efforts and results of the Special Envoys on Acid Rain. (In March 1985, the President appointed Drew Lewis to be the United States Special Envoy on Acid Rain, and, at the same time, Prime Minister of Canada Brian Mulroney appointed William Davis as the Canadian Special Envoy. The Special Envoys were charged with the responsibility to assess the international environmental problems associated with transboundary air pollution, and then recommend actions that would solve them.)

In January 1986, the Envoys presented their findings, including their recommendation that the United States initiate a 5-year, \$5-billion, program for commercial demonstration of control technology projects recommended by industry and jointly funded by government and industry. In March 1986, the President endorsed the Special Envoys' recommendations, hence setting in motion the development of an expanded CCT Program that would build on the CCT-I effort, reflect ongoing State and privately funded initiatives, and be fashioned as fully as practicable from the guidelines recommended by the Special Envoys.

Accordingly, a second solicitation (CCT-II) was prepared and released on February 22, 1988, and, on September 28, 1988, 16 additional projects were selected for the Program; as of this writing, 9 of the projects have consummated Cooperative Agreements, while one project has withdrawn. The remaining 15 CCT-II projects and their locations are shown in Figure 2.

# Clean Coal Technology Round #1

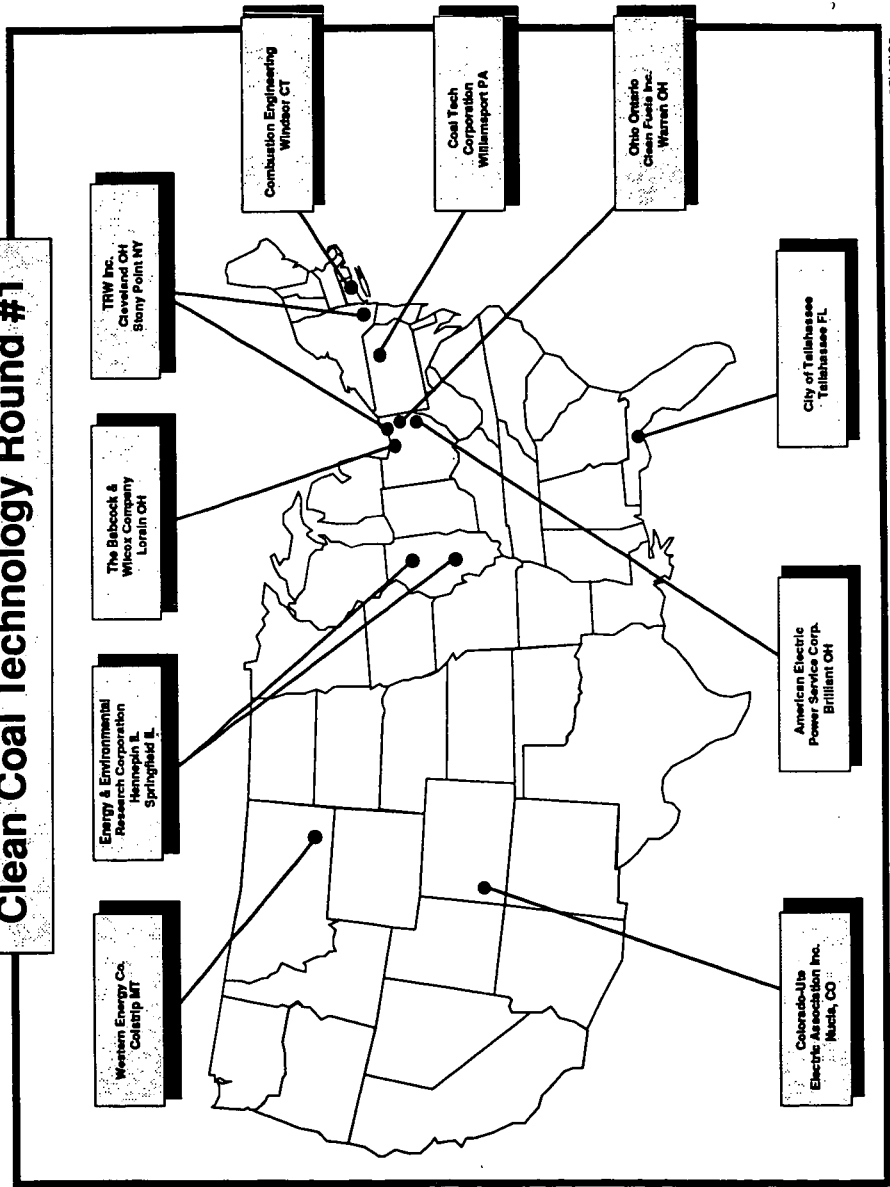


Figure 1

03/13/90

# Clean Coal Technology Round #2

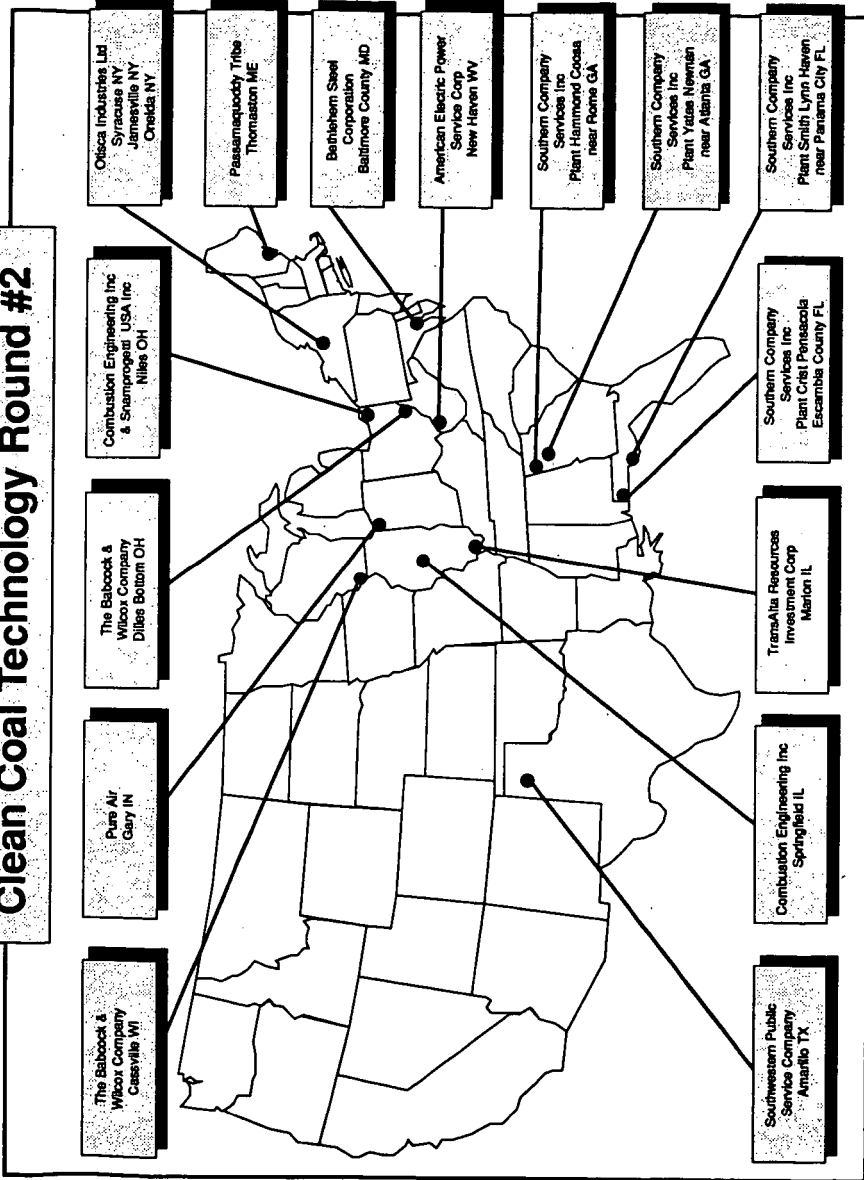


Figure 2

03/13/90

The cost-shared CCT-II projects will demonstrate technologies that are more cost-effective than existing technologies, and are capable of achieving significant reductions in SO<sub>2</sub> and/or NO<sub>x</sub> emissions from existing coal burning facilities, particularly those that contribute to transboundary and interstate pollution. Of the 15 projects, 12 technologies can be retrofitted to existing coal-burning plants, and three can be used to repower existing facilities. Analyses show that the generic technologies represented by the CCT-I and -II projects, if adopted by much of the market to which they are applicable, would result in significant National reductions in SO<sub>2</sub> and NO<sub>x</sub> emissions by the year 2010.

Language in Pub. L. No. 100-446, *Making Appropriations for the Department of the Interior and Related Agencies for the Fiscal Year Ending September 30, 1989, and for Other Purposes*, established the schedule for the third CCT Program solicitation (CCT-III). The PON was issued on May 1, 1989, and, on December 21, 1989, 13 additional projects were selected for the Program. Seven of the projects are advanced retrofit pollution control technologies, three are utility repowering technologies, and three are new coal-based fuel form technologies. The CCT-III projects and their locations are shown in Figure 3.

Regardless of the specific CCT technology, the Program can contribute to improving the world in which we live, as discussed below. As Secretary of Energy Watkins has noted, environmental issues transcend national, socioeconomic, ethnic, and cultural boundaries. We must curb emissions of pollutants that contribute to acid rain and urban smog. The past decade has also seen rising concerns over the potential for global climatic change, although, at present, our science is not conclusive regarding this threat. As a result, there is great uncertainty regarding the possible consequences of these changes.

## **Coal Use and Global Warming**

One of the critical environmental issues that has gained National attention is the possibility of global climatic change in response to increases in atmospheric concentrations of "greenhouse gases" — most notably carbon dioxide (CO<sub>2</sub>), methane (CH<sub>4</sub>), nitrous oxide (N<sub>2</sub>O), and chlorofluorocarbons (CFCs). The atmospheric concentration of CO<sub>2</sub> increased 9.5 percent between 1960 and 1986. It generally is recognized that combustion of fossil fuels is the primary contributor, although global deforestation is an important contributing factor. In 1986, the United States contributed 22 percent of the global CO<sub>2</sub> emissions from burning fossil fuels; of these 22 percent, electric power generation contributed 35 percent, transportation 30 percent, industrial sources 24 percent, and the remaining 11 percent was contributed by the residential and commercial sectors. Approximately 37 percent of the CO<sub>2</sub> emitted in the United States, which accounts for 8 percent of global CO<sub>2</sub> emissions, is attributable to the combustion of coal.

# Clean Coal Technology Round #3

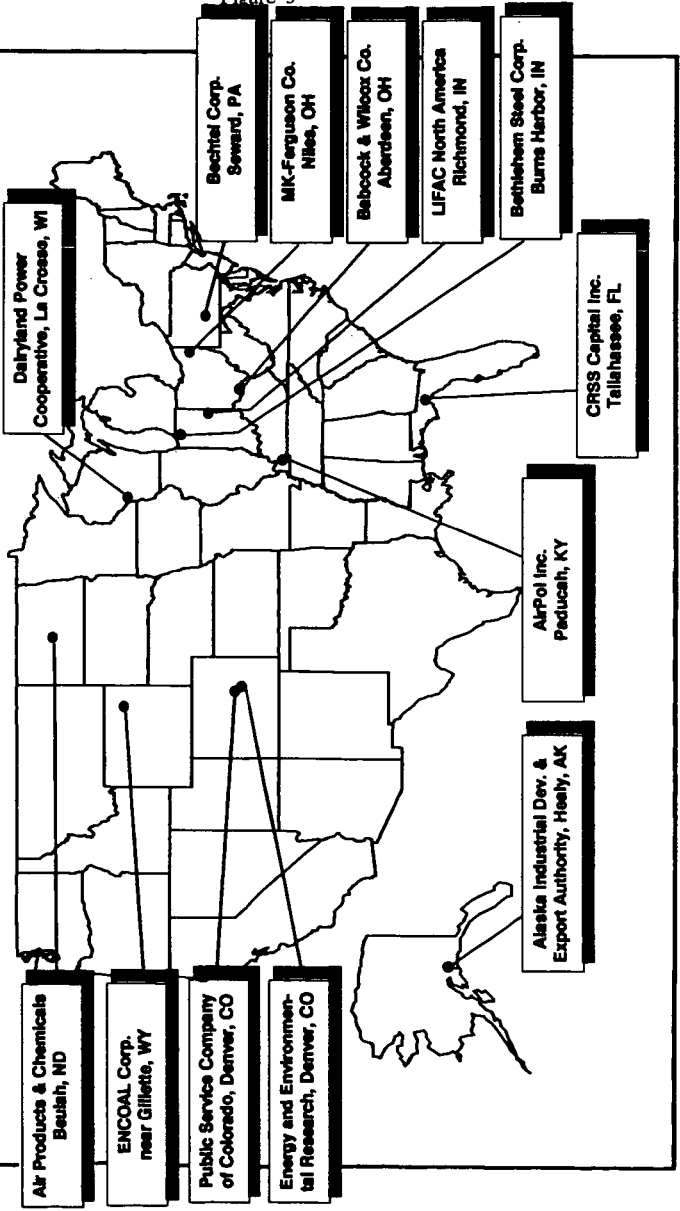


Figure 3

Another greenhouse gas produced by the combustion of fossil fuels is nitrous oxide ( $N_2O$ ), which is a product of both combustion conditions and fuel nitrogen content; recent data suggest that the  $N_2O$  production rate is correlated directly with  $NO_x$  production rates.

CCTs can impact the emissions of greenhouse gases in two fundamental ways: with respect to  $CO_2$ , many of the CCTs improve the efficiency of the conversion of coal to useful energy. Technologies such as pressurized fluidized bed combustion, integrated gasification combined cycle, and fuel cells consume less coal per unit of useful energy produced, thus lowering the amount of  $CO_2$  emitted. Furthermore, these repowering technologies in addition to low  $NO_x$  burners, selective catalytic reduction, and other  $NO_x$  reduction technologies, will reduce  $NO_x$  emissions, which should in turn result in  $N_2O$  emissions reductions. For example, gas reburning technology reduces  $NO_x$  emissions by up to 60 percent, and can reduce  $CO_2$  emissions from 5-10 percent since combustion of natural gas produces less  $CO_2$  than coal combustion.

It is not unexpected that reductions of greenhouse gases emissions will become more common as an international policy objective, and the worldwide commercial deployment of clean coal technologies will take on commensurately added significance.

### **The Clean Air Act Amendments of 1989**

On June 12, 1989, President Bush fulfilled a major campaign commitment by proposing a comprehensive program to provide clean air for all Americans. The President's plan, known as *The Clean Air Act Amendments of 1989* and formally proposed to the Congress on July 21, 1989, called for the first sweeping revisions to the Clean Air Act since 1977, and represented the first time an Administration had put forward a proposal since that time. The President's plan was designed to curb three major threats to the Nation's environment and to the health of millions of Americans: acid rain, urban air pollution, and toxic air emissions.

Five goals underlied the President's clean air proposals and the means for accomplishing them:

- ▶ **Protecting the Public's Health.** To prevent public exposure to cancer-causing agents and to protect those who live in cities with dirty air that does not conform to National health standards.
- ▶ **Improving the Quality of Life.** To improve the quality of life for all Americans by exercising responsible stewardship over the environment for future generations.
- ▶ **Achieving Early Reductions and Steady Progress.** Established realistic timetables to meet air quality standards, but cut substantial amounts of air pollution in the near term, while requiring steady reductions of harder to control emissions.

- ▶ **Harnessing the Power of the Marketplace.** The use of marketable permits to achieve acid rain reductions, and emissions trading to achieve reductions from automobile pollution, so as to clean the air to a definite standard while minimizing the burden on the American economy.
- ▶ **Employing Innovative Technologies.** Encouraged development of Clean Coal Technology, alternative fuel systems for automobiles, and other cost-effective means of using new technology to cut pollution.

The "Acid Deposition Control" (Title V) provisions of the President's bill, with emphasis on those aspects of greatest interest to the CCT Program, are highlighted below:

- A reduction of 10 million tons of SO<sub>2</sub> by the year 2000, using a baseline year of 1980 for tons of SO<sub>2</sub> emitted, primarily from coal-fired power plants.
- A two-phase program in order to ensure early reductions. A reduction of five million tons was required during the first phase, by the end of 1995. (All dates had assumed enactment of this legislation by December 31, 1989.)
- A 2 million ton reduction of NO<sub>x</sub> in Phase II. The plan would have allowed utilities to trade reductions of NO<sub>x</sub> for reductions of SO<sub>2</sub> and vice versa, and thus represented a call for a total reduction of 12 million tons in acid rain-causing pollutants.
- A 3-year extension of the Phase II deadline for plants adopting CCT repowering technologies, combined with regulatory incentives designed to smooth their transition into the marketplace. This would allow the United States to "make good" on the major investment in the CCT Program that the President has called for, and would ensure that coal continues to play an important role in America's energy future.
- Freedom of choice in cutting pollution. The plan required all plants above a certain size in affected States to meet the same emissions standard, but did not dictate to plant managers how the standard should be met. The plan required the largest polluting plants to make the greatest cuts in pollution. The emissions standard would be set at the rate necessary to achieve 5 million tons in the first phase. The plan envisioned a standard of 2.5 lb SO<sub>2</sub>/million Btu, which would affect 107 plants in 18 states. The standard would subsequently be tightened to approximately 1.2 lb/million Btu so as to achieve a 10 million ton reduction of SO<sub>2</sub> in Phase II.

- Maximum flexibility in obtaining reductions. The plan allowed utilities to trade required emissions reductions so that they would be achieved in the most optimal manner. In the first phase, trading would be allowed among electric plants within a State or within a utility system. In addition, full interstate trading would be allowed in Phase II.
- The estimated cost of the President's proposal would have been about \$700 million per year in the first phase, and \$3.8 billion annually in the second phase. While this represents an increase of over 2 percent by the year 2000 in the Nation's \$160 billion a year electricity bill, the flexibility built into the President's plan reduced, by up to half, the cost of various competing proposals mandating the use of specific technologies.

One important provision in the proposed bill, Section 508, "Repowered Sources," established the availability of a 3-year extension of the stage II compliance date (i.e., until the end of 2003, instead of 2000) for *any unit being repowered with one of the following CCTs:*

- ◆ Atmospheric (AFB) or Pressurized Fluidized Bed (PFB) Combustion
- ◆ Integrated Gasification Combined Cycle (IGCC)
- ◆ Magnetohydrodynamics
- ◆ Direct and indirect coal-fired turbines
- ◆ Integrated gasification fuel cells
- ◆ or a "derivative of one of these technologies, as determined by the Administrator of the Environmental Protection Agency (EPA), in consultation with the Secretary of Energy."

Such a repowered source would be exempt from meeting EPA New Source Performance Standards (NSPS) for SO<sub>2</sub>, and would benefit from streamlined New Source Review (NSR) procedures if their potential emissions were expected to increase.

Section 515 of the bill, entitled, "Clean Coal Technology Regulatory Incentives," also was very important to the CCT Program. Here, CCTs were defined as:

any technology, including technologies applied at the precombustion, combustion, or postcombustion stage, at a new or existing facility which will achieve significant reductions in air emissions of SO<sub>2</sub> or NO<sub>x</sub> associated with the utilization of coal in the generation of electricity, process steam, or industrial products, which is not in widespread use as of the date of enactment of this title.

In order to encourage the use of such CCTs, the Federal Energy Regulatory Commission (FERC) was required here to adopt regulations for a 5-year CCT demonstration program that would include establishment of an incentive rate of return and a 10- to 20-year amortization period. This proposal also required FERC to develop a process whereby it would negotiate a prudent level of investment for CCTs and other "innovative emission control technology."

This Section also exempted temporary and permanent CCT demonstration projects from NSR requirements under Section 111 (*Standards of Performance for New Stationary Sources*) and Parts C (*Prevention of Significant Deterioration of Air Quality*) and D (*[State Implementation] Plan Requirements for Nonattainment Areas*) of the current Clean Air Act, so long as the demonstration project would not increase the original facility's potential to emit any pollutant regulated under the Act.

Finally, States were encouraged to provide additional utility regulatory incentives for the promotion of CCTs, and several examples were provided.

### **The CCT Program and National Energy Strategy**

On July 26, 1989, the Secretary of Energy, Admiral James D. Watkins, appeared before the Senate Committee on Energy and Natural Resources to discuss the President's plan for development of a National Energy Strategy (NES). In his opening remarks, the Secretary noted that:

Environmental concerns are putting new pressures on our ability to use our most abundant domestic fuel, coal. Electricity reserve margins are shrinking across the country. Voltage reductions have already been required in the Northeast, and right here in Washington. Meanwhile, New York State officials are rushing to pull fuel rods from a completed, safe nuclear power plant. ... Our country needs a clear energy blueprint to take the United States into the next century — a National Energy Strategy.

The President has directed me to lead the development of this National Energy Strategy — an action plan essential to providing this Nation, in the years to come, with adequate supplies of competitively priced, clean energy. This strategy will serve as a blueprint for energy policy and government program decisions. It will contain specific short-term, mid-term,

and long-term recommendations. This strategy will chart our course, set our pace, and provide mileposts by which to evaluate our progress in providing the energy our economy needs, while protecting the Nation's health, safety, and environment.

... I have committed the Department to extensive consultations with the Governors and State officials of this Nation, with Congress, with industry, and with the American people.

The Secretary observed that, "If the National Energy Strategy is to gain the support of the American people, it must be built on a reliable foundation of data, analytical tools, and forecasting capability." Accordingly, he has instructed DOE to work closely with the Energy Information Administration to develop a National Energy Modeling System (NEMS); he has also asked the National Academy of Sciences "to examine our plans for the development of the NEMS and ensure that it will, to the maximum extent possible, address the critical energy issues before us. These include major environmental issues, strategic considerations and technology research and development."

The goals of the CCT Program are germane to and supportive of many of the recurring themes in the NES development process. For example, the National Laboratories were asked to assist DOE with the analyses of key issues and the preparation of special white papers, completed this past autumn, on such subjects as:

- The science of global climate change and the scope of uncertainty. This subject area encompasses CO<sub>2</sub> releases, and pertains to the increased efficiency of some of the CCTs, with attendant reduced emissions.
- Options available to enhance DOE technology transfer to the broader development community. Technology transfer is important not only to meet National energy and environmental objectives, but to assure that lesser developed nations — which are the fastest growing energy users — will do the same.

The subject of technology transfer is "near and dear" to the CCT Program, which considers this activity as vital to the promulgation and deployment of mature CCTs into the marketplace, both home and abroad. We believe that CCTs offer the opportunity for export of U.S. coal together with the know-how to consume it cleanly and cost-effectively to the mutual benefit of both the consumers and the vendors.

On April 2, 1990, the Secretary of Energy announced the completion of the first phase — information gathering — of the development of the NES, and released for public comment the *Interim Report on the Development of a National Energy Strategy, A Compilation of Public Comment*. The Secretary noted that the report "will provide a baseline for for development and analysis of energy options, and public comment on the report is invited." As was noted in the accompanying News Release, since August 1989, DOE has held 15 public hearings, received more than one thousand written submissions, and compiled twelve thousand pages of public hearing record. The *Interim Report* conveys the results of that public participation, presenting a compendium of public concern, and a series of publicly identified goals, obstacles to progress, and options for overcoming them.

This was followed almost immediately by the announcement on April 12, 1990, of the completion and release for review by the public of five National Laboratory "white papers" that had been commissioned by DOE to assist in the development of the NES:

- ▶ *Energy Efficiency: How Far Can We Go?*
- ▶ *The Potential of Renewable Energy.*
- ▶ *Energy and Climate Change.*
- ▶ *Energy Technology for Developing Countries.*
- ▶ *The Technology Transfer Process.*

Finally, some of the remarks about CCTs and the CCT Program, that were offered by panelists in the course of discussing the NES, are noteworthy, as follows:

Clean coal program of DOE is important for removing constraints to coal use, given current old technology and environmental concerns.

- **State government official**

Energy and environmental policy should be coordinated. Clean coal technology to reduce NO<sub>x</sub> and SO<sub>2</sub> emissions is good example.

- **Public utilities commissioner**

Coal is the largest domestic resource, however its viability as an energy source is seriously constrained by air quality regulations and cost of compliance; by the need for federal support of clean coal technology development; and proposed acid rain legislation capping SO<sub>2</sub> and NO<sub>x</sub> emissions.

- **Electric utility executive**

Coal is the most plentiful resource but is underutilized; energy research on effective and clean use of coal is needed ... Promotion of coal exports should be undertaken, and clean coal technology should be promoted.

- Energy company executive

Clean coal program R&D is now addressing containment of CO<sub>2</sub> emissions ... Progress being made in environmental protection is not being communicated to the public. Public information program is needed as part of the strategy of NES to inform public on environmental health and safety.

- Coal company executive

### **The Future; CCT-IV and -V**

On October 23, 1989, President Bush signed Public Law No. 101-121, "Department of the Interior and Related Agencies Appropriations, Fiscal Year 1990." Among other things, this Bill provided \$1.2 billion for the 4th and 5th rounds of CCT solicitations (\$600 million for each in FY 1991 and FY 1992), and specified dates for release of the solicitations, submittal of proposals, and selections of projects.

The language in the accompanying Conference Report (No. 101-264) included the guidance that the word "replacing" should be added to the definition of "clean coal technology," and noted that:

... the inclusion of "replacing" for clean coal IV and V is intended to cover the complete replacement of an existing facility if, because of design or site specific limitations, repowering or retrofitting of the plant is not a desirable option.

Although the original schedule called for release of the CCT-IV solicitation on or before June 1, 1990, on May 15, 1990, DOE announced that it intended to delay issuance of the solicitation "until uncertainties regarding Congressional action have been resolved." The News Release of that date noted that the Secretary of Energy had "informed Congress that unresolved issues in the pending Supplemental Appropriations Act and the Clean Air Act Amendments make it premature for the Energy Department to begin asking industry for new CCT proposals." The Release also pointed out that this delay will provide time for a draft of the solicitation to be issued for public comment prior to its official release. It is anticipated that, with the passage of the Clean Air Bill, PON-IV, revised as appropriate to accommodate the provisions of the Bill, will be released.

Er

## THERMOGRAVIMETRIC STUDY OF NOVEL SORBENTS FOR FLUE GAS CLEANUP\*

Sheila W. Hedges and R. A. Diffenbach  
Pittsburgh Energy Technology Center  
U. S. Department of Energy, Pittsburgh, PA 15236

**Keywords:** flue gas cleanup, regenerable sorbents, cerium oxide

### INTRODUCTION

Several promising new processes are being developed at the Pittsburgh Energy Technology Center (PETC) to remove the sulfur and nitrogen oxides from the flue gas of coal-fired utility boilers. The Fluidized-Bed Copper Oxide Process developed at PETC is one such new technology for the simultaneous removal of 90% of both  $\text{SO}_2$  and  $\text{NO}_x$  from the flue gas<sup>1</sup>. This process involves the absorption of  $\text{SO}_2$  by copper oxide on an alumina support in conjunction with sorbent catalyzed reduction of  $\text{NO}_x$  by ammonia addition. Alternate sorbents to  $\text{CuO}/\text{Al}_2\text{O}_3$  are also being considered at PETC for possible improvements in reactivity toward  $\text{SO}_2$ , regenerability, attrition resistance, and sorbent costs. A similar process concept based on a  $\text{CeO}_2/\text{Al}_2\text{O}_3$  sorbent<sup>2</sup> has been studied recently at PETC and is the subject of this report.

Cerium oxide is a particularly promising new sorbent because ceria imparts resistance to thermal loss of surface area to alumina<sup>3</sup>;  $\text{CeO}_2$  has potential for the uptake of two moles of sulfur per mole of metal to form  $\text{Ce}(\text{SO}_4)_2$ ;  $\text{CeO}_2$  sorbent reacts with  $\text{SO}_2$  over a fairly wide range of temperature; and when regenerated under the appropriate conditions,  $\text{CeO}_2/\text{Al}_2\text{O}_3$  sorbent produces an off-gas stream that can be used conveniently in a Claus plant for conversion into elemental sulfur<sup>2</sup>. The natural abundance of cerium is slightly higher than copper, and extensive deposits are located in the western United States, as well as in Australia, Brazil, India, and China. Rare earth minerals are mined both as a primary product and as a by-product of the mining of such metals as iron (in China), tin, titanium, and zirconium. Cerium is produced as a by-product of the isolation of other rare earths. The current price of cerium oxide is approximately \$1.50-\$2.00 per pound at 90-95% purity.<sup>4</sup>

The effects of sorbent preparation on the reactivity of  $\text{CeO}_2/\text{Al}_2\text{O}_3$  sorbents toward  $\text{SO}_2$  and on the regenerability of the sorbents have been examined using a thermogravimetric (TG) technique with simulated flue gas and hydrogen, respectively. Potassium-modified  $\text{CeO}_2/\text{Al}_2\text{O}_3$  and composite oxides of Co/Ce and Mn/Ce on alumina have also been investigated. Incorporation of potassium into  $\text{CeO}_2/\text{Al}_2\text{O}_3$  has been reported to decrease the  $\text{CeO}_2$  crystallite size and improve sorbent performance<sup>5</sup>. Several recent catalysis studies on Co/Ce and Mn/Ce composite oxide systems have described high redox properties<sup>6,7</sup> and catalytic activity for the  $\text{CO} + \text{SO}_2$  reaction<sup>8</sup> and the  $\text{CO} + \text{NO}$  reaction<sup>9</sup>. Both cobalt and manganese oxides have been previously identified as

---

\*Reference in this paper to any specific commercial product, process, or service is to facilitate understanding and does not imply endorsement or favoring by the United States Department of Energy.

promising supported sorbents (on alumina) for SO<sub>2</sub> absorption<sup>10</sup>. Manganese oxides have been investigated by several researchers for sulfur removal at a number of different conditions. Investigations of MnO<sub>x</sub>/Al<sub>2</sub>O<sub>3</sub> for flue gas desulfurization have been promising but problems have been identified with low manganese loading and some loss of capacity has been observed on repeated cycles of regeneration<sup>11,12</sup>.

## EXPERIMENTAL

Sorbent samples were prepared by aqueous impregnation of 1/16 inch alumina spheres. Reagent-grade, water-soluble cerium salts that can be decomposed thermally at moderate temperatures were selected for testing. The salts selected were ceric ammonium nitrate, cerous ammonium nitrate, cerous nitrate hexahydrate, and cerous acetate. The alumina spheres were obtained from three commercial catalyst manufacturers. After soaking in excess solution, the sorbent pellets were drained, dried in air overnight at 120°C, and calcined in N<sub>2</sub> at 650°C for 6 hours. Metal loadings on the sorbents were varied by changing the concentration of the impregnation solution and were determined by elemental analysis at Huffman Laboratories, Inc., using atomic absorption techniques. Surface areas were determined by the multipoint BET method using an automated Micromeritics Digisorb 2500 instrument with N<sub>2</sub> as adsorbate. Potassium nitrate was added to the K-modified CeO<sub>2</sub>/Al<sub>2</sub>O<sub>3</sub> sorbents by an incipient wetness technique prior to calcination of the sorbent. Composite oxide sorbents were prepared in the same manner as the Ce-only sorbents by simply combining cobalt or manganese nitrate with the cerium nitrate to form a mixed metal impregnation solution (eg. Co(NO<sub>3</sub>)<sub>2</sub> + Ce(NH<sub>4</sub>)<sub>4</sub>(NO<sub>3</sub>)<sub>6</sub> and Mn(NO<sub>3</sub>)<sub>2</sub> + Ce(NO<sub>3</sub>)<sub>3</sub>).

Reactivity of the various sorbent preparations toward SO<sub>2</sub> was measured in a modified Perkin-Elmer TGS-2 Thermogravimetric Analyzer that has been previously described<sup>13</sup>. For these tests, the sample-shielding tube was refabricated using quartz and a large external furnace was used for temperature control. Simulated flue gas was blended from certified gas mixtures and humidified using a sparger. The calculated typical gas composition was 2800-3000 ppm SO<sub>2</sub>; 480-500 ppm NO; 2.8-3.0 % O<sub>2</sub>; 13.7-14.7 % CO<sub>2</sub>; 4.0, 7.0, or 18 % (vol.) H<sub>2</sub>O; and N<sub>2</sub> as the balance. A sample size of 50 mg of sorbent was selected to just fill the quartz sample pan; this corresponds to about 18-20 pellets. A typical TG test sequence was composed of four steps: 1) the sample was heated to the desired reaction temperature at 10°C/minute in dry N<sub>2</sub>; 2) after allowing the sample to come to equilibrium at the test relative humidity a "dry" sample weight was obtained and the sample was exposed to humidified simulated flue gas for one hour; 3) the sample was regenerated by reduction in H<sub>2</sub> for 30 minutes followed by reoxidation in air for 10 minutes; and 4) the sample was re-exposed to flue gas for 60 minutes.

From the TG thermal curves, the sorbent capacity was calculated from the weight gain after 60 minutes of exposure to simulated flue gas which was sufficient to completely saturate most of the sorbents. For samples with high metal loadings, although the reaction had not completely stopped after 60 minutes, the rate of reaction had dropped to one percent or less of its initial value. The rate of SO<sub>2</sub> uptake was calculated from the weight gain averaged for the first 10 minutes of absorption. This somewhat long time interval was selected for comparison purposes to minimize the relative

uncertainty in measuring small weight gains. [Note: this estimated rate underestimates the true rate since the TG thermal curves show some deviation from linearity after about 5 to 8 minutes. The conversion of the solid is typically 30+ % after 10 minutes.]

## RESULTS AND DISCUSSION

The sorbent capacity for  $\text{SO}_2$  uptake as a function of temperature is shown in Figure 1 for several different metal loadings. Since cerium nitrates are thermally unstable above  $250^\circ\text{C}$  and hydrated ceric sulfate is completely dehydrated at approximately  $350^\circ\text{C}$ <sup>14</sup>, all of the weight gain observed during the TG test has been attributed to sulfate formation. X-ray diffraction results for several of the spent  $\text{CeO}_2/\text{Al}_2\text{O}_3$  sorbent samples showed weak lines not present in the fresh sorbent. However, these lines could not be assigned to known cerium sulfate compounds and suggested that the  $\text{CeO}_2$  is converted to an amorphous or highly dispersed sulfate on exposure to flue gas. Examination of fresh and spent sorbent by FTIR (Fourier transform infrared spectroscopy) clearly showed the presence of sulfate on the spent sorbents, but specific product compounds could not be identified.

As can be seen in Figure 1, at low metal loadings, the sorbent is essentially saturated at  $550^\circ\text{C}$  before 60 minutes of exposure to synthetic flue gas. For sorbents at moderate and high metal loading the capacity continues to increase up to  $600^\circ\text{C}$ . However, the TG curves are essentially flat for these sorbents after 60 minutes of exposure even though the sorbent has not reached the calculated, theoretical capacity (complete conversion of  $\text{CeO}_2$  to  $\text{Ce}(\text{SO}_4)_2$ ). The rate of  $\text{SO}_2$  uptake also decreases steadily below about  $600^\circ\text{C}$  as shown in Figure 2. Complete regeneration of these  $\text{CeO}_2/\text{Al}_2\text{O}_3$  sorbents occurred in 30 minutes or less in hydrogen at temperatures above  $550^\circ\text{C}$ . Figure 3 shows the weight loss after 30 minutes of exposure to  $\text{H}_2$  expressed as a percentage of the gain during absorption. Some of the sorbents show weight loss on reduction in excess of 100 %, which is probably due to the partial conversion of  $\text{CeO}_2$  to  $\text{Ce}_2\text{O}_3$  or  $\text{CeAlO}_3$ <sup>15,16</sup>. Based on these observations of the temperature dependence of absorption and regeneration, a temperature of  $600^\circ\text{C}$  was selected to compare the various methods of sorbent preparation.

Comparison of the various  $\text{CeO}_2/\text{Al}_2\text{O}_3$  sorbents prepared with differing precursor salts showed little or no difference in sorbent capacity between samples with comparable cerium loadings. A slightly higher rate of  $\text{SO}_2$  uptake was observed for sorbents prepared using  $\text{Ce}(\text{NH}_4)_4(\text{NO}_3)_6$  as the precursor salt. Although  $\text{Ce}(\text{NH}_4)_4(\text{NO}_3)_6$  has been shown to produce a highly porous  $\text{CeO}_2$  when decomposed at low temperature<sup>17</sup>,  $\text{Ce}(\text{NO}_3)_3 \cdot 6\text{H}_2\text{O}$  has been reported to produce  $\text{CeO}_2$  of smaller crystallite size when calcined at higher temperature<sup>14</sup>. The somewhat higher rate of  $\text{SO}_2$  uptake observed for sorbents prepared using  $\text{Ce}(\text{NH}_4)_4(\text{NO}_3)_6$  as the precursor salt suggests that the crystallite size of the  $\text{CeO}_2$  supported on alumina may not follow the same trends observed for pure, unsupported compounds<sup>14</sup>. X-ray diffraction results for several of the  $\text{CeO}_2/\text{Al}_2\text{O}_3$  sorbent samples were consistent with highly dispersed  $\text{CeO}_2$ , but no estimation of crystallite size was made. It should be pointed out that these differences in rate are small and, when experimental uncertainties are taken into consideration, the differences may not be statistically significant. All of the

precursor salts resulted in sorbents with high BET surface areas, 150 to 200 m<sup>2</sup>/g. However, no correlation was found between total surface area and sorbent capacity or rate of SO<sub>2</sub> uptake. The sorbent capacity and rate of SO<sub>2</sub> uptake were also found to be unaffected by increasing the water content of the simulated flue gas from 4 % to 18 % or by removing nitric oxide from the gas mixture.

Figure 4 shows the SO<sub>2</sub> to CeO<sub>2</sub> mole ratio (stoichiometry) after 60 minutes of exposure to simulated flue gas for sorbents prepared using various precursor salts on three different aluminas. For metal loading below about 5 %, the observed uptake is greater than the amount required to completely convert all the CeO<sub>2</sub> to Ce(SO<sub>4</sub>)<sub>2</sub>, indicating some uptake by the alumina support. For sorbents with loadings above about 15 %, the utilization drops to below one mole of SO<sub>2</sub> per mole CeO<sub>2</sub>. No difference was observed in the utilization of the CeO<sub>2</sub> on alumina from different suppliers. One of the aluminas did have a lower affinity for cerium uptake, that is, the metal retained on this support was significantly lower at a given impregnation solution concentration than for the other two aluminas. Figure 5 shows that the rate of SO<sub>2</sub> uptake was also lower on sorbents prepared using the third support. Simple grinding in a ball mill showed sorbent prepared on this support to be much less rugged than sorbents prepared on the other two supports and no further testing was done with this alumina. The small differences in the measured rate of SO<sub>2</sub> uptake for sorbents prepared on the same support material have been attributed to differences in sample preparation, i.e., the specific precursor cerium salt used.

As noted above, the CeO<sub>2</sub>/Al<sub>2</sub>O<sub>3</sub> sorbents undergo weight loss during hydrogen reduction at 600°C of 100+ % of the amount of SO<sub>2</sub> uptake. Since some reduction of Ce(IV) to Ce(III) also occurs, the sorbent samples were reoxidized in air prior to subsequent SO<sub>2</sub> absorption measurements. Following this regeneration procedure, the weight percent of any residual material remaining on the sorbent was recorded. The results of these measurements are summarized in Figure 6. For the CeO<sub>2</sub>/Al<sub>2</sub>O<sub>3</sub> sorbents, the residual was less than one percent of the total sorbent weight. The sorbent was pale yellow in color after regeneration. Ce<sub>2</sub>S<sub>3</sub> is reddish-purple or brown. However, there was not sufficient sample produced in these TG tests for a detailed characterization of the residual material. For the CuO/Al<sub>2</sub>O<sub>3</sub> sorbent with a 6-7 % Cu loading, a residual of 3-3.5 percent of the total sorbent weight was measured in the TGA test after a similar regeneration, however, both absorption and regeneration of the CuO/Al<sub>2</sub>O<sub>3</sub> sorbent were at 400°C. Following regeneration, the CeO<sub>2</sub> sorbent samples were exposed a second time to simulated flue gas. A small decrease in sorbent capacity was observed, but the rate of SO<sub>2</sub> uptake was the same as that measured for the freshly prepared sorbents as can be seen by comparing Figures 5 and 7. For laboratory prepared samples of the CuO/Al<sub>2</sub>O<sub>3</sub> sorbent with a 7 % Cu loading, the rate of SO<sub>2</sub> uptake measured in the TGA using the same gas compositions and reaction times but at 400°C, is 1.7 mg SO<sub>2</sub> per g sorbent per minute.

A series of K-modified CeO<sub>2</sub>/Al<sub>2</sub>O<sub>3</sub> sorbents was prepared with metal loadings of 4 to 12 % Ce and 0.8 % K to investigate reported<sup>5</sup> improvements in sorbent performance. The rate of SO<sub>2</sub> absorption measured for each of these sorbents at 600°C was the same as for the Ce-only sorbents. The K-modified sorbents have approximately 10-20 % higher mole ratio of SO<sub>2</sub> absorbed to CeO<sub>2</sub> present at comparable metal loadings than

the Ce-only sorbents. No increase in the residual material remaining on the sorbent after regeneration, as compared to the Ce-only sorbents, was observed for the K-modified  $\text{CeO}_2/\text{Al}_2\text{O}_3$  sorbents. Figure 8 compares the capacity of a K-modified  $\text{CeO}_2/\text{Al}_2\text{O}_3$  sorbent with a Ce-only sorbent, both with 4 % Ce loading. As pointed out above, at this low metal loading the observed sorbent capacity of  $\text{CeO}_2/\text{Al}_2\text{O}_3$  at temperatures above 550 °C corresponds to a sulfur to cerium stoichiometry of greater than 2 to 1. This effect is even more pronounced for the K- $\text{CeO}_2/\text{Al}_2\text{O}_3$  sorbent. At 600°C, the excess corresponds to a 115 % utilization of the  $\text{CeO}_2$  on the Ce-only sorbent and a 123 % utilization of the sum of  $\text{CeO}_2$  and  $\text{K}_2\text{O}$  on the K- $\text{CeO}_2/\text{Al}_2\text{O}_3$  sorbent. Both types of sorbent show the same temperature dependence of  $\text{SO}_2$  capacity and show evidence of a mechanism change below about 300°C.

Composite oxides of Co/Ce and Mn/Ce were prepared on the same alumina support to investigate whether the redox properties of these materials<sup>6-9</sup> would improve the  $\text{SO}_2$  reactivity or regenerability of the Ce-containing flue gas sorbent.  $\text{CeO}_2/\text{MnO}_x/\text{Al}_2\text{O}_3$  sorbents were prepared containing 8 and 13 percent cerium with manganese loadings ranging from 0.3 to 3.7 weight percent (mole fraction of manganese in the composite oxides ranged from 0.07 to 0.43). These sorbents had  $\text{SO}_2$  reactivities comparable to the Ce-only sorbents of similar Ce loading and maintained their reactivity after regeneration. (The test was carried out for only one regeneration cycle.) However, a substantial amount of residual material (1 to 4 % of the total sorbent weight) was observed to be left on these sorbents after regeneration. No advantage was found in the  $\text{CeO}_2/\text{MnO}_x/\text{Al}_2\text{O}_3$  sorbents as compared to the Ce-only sorbent.  $\text{CeO}_2/\text{CoO}_x/\text{Al}_2\text{O}_3$  sorbents were prepared containing 5, 10, and 14 percent cerium with cobalt loadings ranging from 0.2 to 2.0 percent (mole fraction of cobalt in the composite oxides ranged from 0.06 to 0.39). Reactivity measurements on these sorbents showed them to be essentially the same as the Ce-only sorbents. In this case no difference in residual material after regeneration in  $\text{H}_2$  was observed. The temperature dependence of the  $\text{SO}_2$  absorption by the  $\text{CeO}_2/\text{CoO}_x/\text{Al}_2\text{O}_3$  sorbent was also examined and found to be essentially the same as for the Ce-only sorbents.

A comparison of the  $\text{SO}_2$  reactivity measurements for all four types of sorbents is shown in Figures 9 and 10. The K-modified  $\text{CeO}_2/\text{Al}_2\text{O}_3$  and  $\text{CeO}_2/\text{Al}_2\text{O}_3$  prepared from  $\text{Ce}(\text{NH}_4)_4(\text{NO}_3)_6$  have slightly higher rates of absorption (Figure 9) but the differences are small. The K-modified  $\text{CeO}_2/\text{Al}_2\text{O}_3$  sorbents have somewhat higher capacities (Figure 10), but once again the improvement is modest. For laboratory prepared samples of the  $\text{CuO}/\text{Al}_2\text{O}_3$  sorbent with a 7 % Cu loading, the rate of  $\text{SO}_2$  uptake measured in the TGA using the same gas compositions and reaction times but at 400°C is 1.7 mg  $\text{SO}_2$  per g sorbent per minute and the sorbent capacity is 59 mg  $\text{SO}_2$  per g sorbent.

## CONCLUSIONS

$\text{CeO}_2/\text{Al}_2\text{O}_3$  sorbents have been prepared that have  $\text{SO}_2$  reactivity comparable to or slightly higher than the  $\text{CuO}/\text{Al}_2\text{O}_3$  sorbent, and can be regenerated in hydrogen with essentially complete removal of sulfur. Residual material remaining on the  $\text{CeO}_2/\text{Al}_2\text{O}_3$  sorbents was about one fifth the amount typically seen for the  $\text{CuO}/\text{Al}_2\text{O}_3$  sorbent with similar metal loading under similar experimental conditions (TG testing was performed using the same gas compositions and reaction times for both types of sorbents).

However, the temperature of operation is higher for the  $\text{CeO}_2$ , 600°C compared to 400°C for  $\text{CuO}$ .  $\text{CeO}_2/\text{MnO}_x/\text{Al}_2\text{O}_3$  and  $\text{CeO}_2/\text{CoO}_x/\text{Al}_2\text{O}_3$  sorbents were also prepared that gave quite comparable  $\text{SO}_2$  reactivity to the Ce-only sorbent. However, these composite oxide sorbents do not appear to offer an advantage to the Ce-only sorbent when  $\text{H}_2$  is the reducing gas. K-modified  $\text{CeO}_2/\text{Al}_2\text{O}_3$  sorbents exhibited approximately 10-20 % higher absorption capacity at comparable metal loadings than did the Ce-only sorbents, but the rate of  $\text{SO}_2$  uptake was essentially the same.

#### ACKNOWLEDGEMENTS

The authors would like to thank Dr. S.S. Pollack for providing the X-ray diffraction analysis and Michael Hilterman, Michael Ferrer, and Frank McCown for assistance in obtaining the TG data.

#### REFERENCES

1. Plantz, A.R.; Drummond, C.J.; Hedges, S.W.; Gromicko, F.N. "Performance of the Fluidized-Bed Copper Oxide Process in an Integrated Test Facility," presented at the 79th Annual Meeting and Exhibition of the Air Pollution Control Association, Minneapolis, Minnesota, June 1986.
2. Longo, J.M. U.S. Patent 4 001 375, 1977 and Longo, J.M.; Neville, L.C. U.S. Patent 4 251 496, 1981.
3. Yao, H.C.; Yao, Y.F. *Yu J. Catal.* 1984, 86, 254-65.
4. Hedrick, J.B. "Rare-Earth Minerals and Metals" in "Minerals Yearbook 1986"; Bureau of Mines; U.S. Government Printing Office: Washington, 1988; Vol. 1, pp. 771-782.
5. Lewis, P.H.; Dai, E.P.; Holst, E.H. U.S. Patents 4 600 898 and 4 626 419, 1986.
6. Imamura, S.; Doi, A.; Ishida, S. *Ind. Eng. Chem. Prod. Res. Dev.* 1985, 24(1), 75-80.
7. Imamura, S.; Nakamura, M.; Kawabata, N.; Yoshida, J.I.; Ishida, S. *Ind. Eng. Chem. Prod. Res. Dev.* 1986, 25(1), 34-37.
8. Bazes, J.G.I.; Caretto, L.S.; Nobe, K. *Ind. Eng. Chem. Prod. Res. Dev.* 1975, 14(4), 264-8.
9. Deremince-Mathieu, V.; Collette, H.; Nagy, J.B.; Deriyabem E.G.; Verbist, J.J. *Inorg. Chim. Acta* 1987, 140(1-2), 41-43.
10. Koballa, T.E.; Dudukovic, M.P. *AIChE Symp. Ser.* 1978, 73(165), 199-228.
11. Van den Bosch, P.J.W.M.; De Jong, W.A. *Adv. Chem. Ser.* 1974, 133, 571-87.
12. Van den Bosch, P.J.W.M.; De Jong, W.A. *Prep. Catal., Proc. Int. Symp.* 1975 (Pub. 1974), 651-62.
13. Duffenbach, R.A.; Hedges, S.W.; Friedman, S. *Thermochim. Acta* 1988, 127, 57-71.
14. El-Adham, K.A.; Gadalla, A.M.M. *Interceram* 1977, 26(3), 223-6.
15. Miki, T.; Ogawa, T.; Ueno, A.; Matsuura, S.; Sato, M. *Chem. Lett.* 1988, 565-568.
16. Shyu, J.Z.; Weber, W.H.; Gandhi, H.S. *J. Phys. Chem.* 1988, 92(17), 4964-70.
17. Zaki, M.I.; Baird, T. *React. Solids* 1986, 2, 107-23.

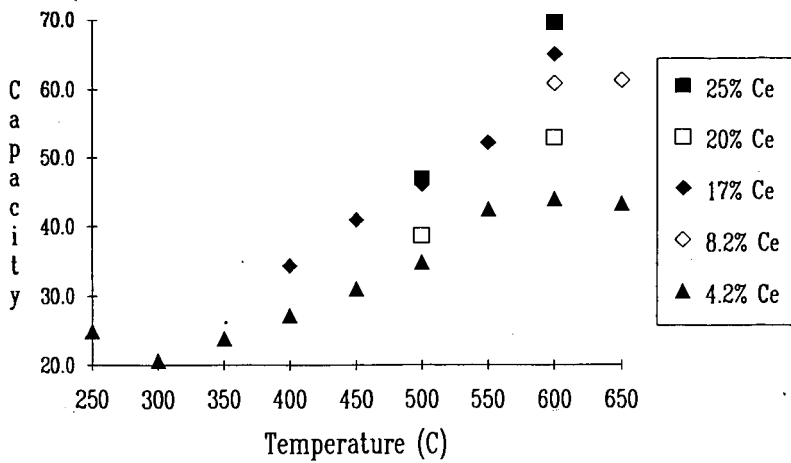


Figure 1. Capacity of  $\text{CeO}_2/\text{Al}_2\text{O}_3$  sorbents expressed in  $\text{mg SO}_2$  per g sorbent as a function of temperature.

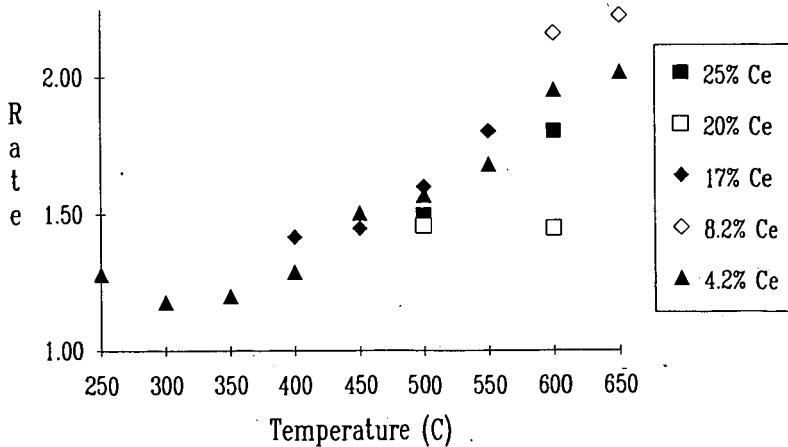


Figure 2. Rate of  $\text{SO}_2$  uptake by  $\text{CeO}_2/\text{Al}_2\text{O}_3$  sorbents expressed in  $\text{mg SO}_2$  per g sorbent per minute as a function of temperature. See text for discussion.

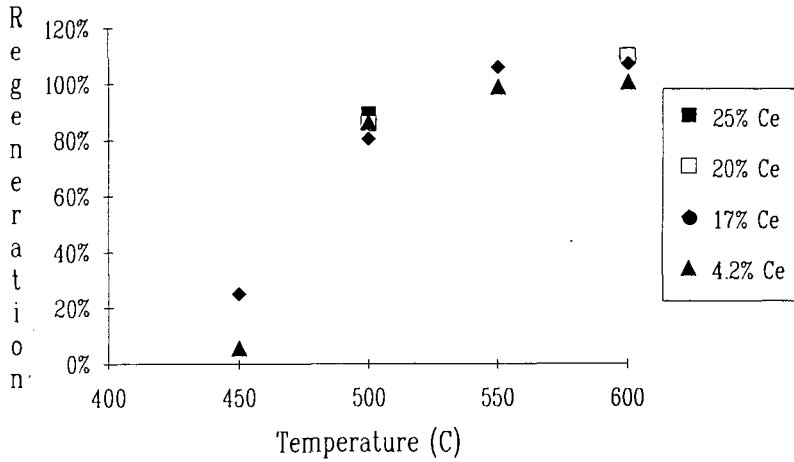


Figure 3. Reduction of spent  $\text{CeO}_2/\text{Al}_2\text{O}_3$  sorbents in hydrogen expressed as a percentage of the weight gain observed during  $\text{SO}_2$  absorption as a function of temperature.

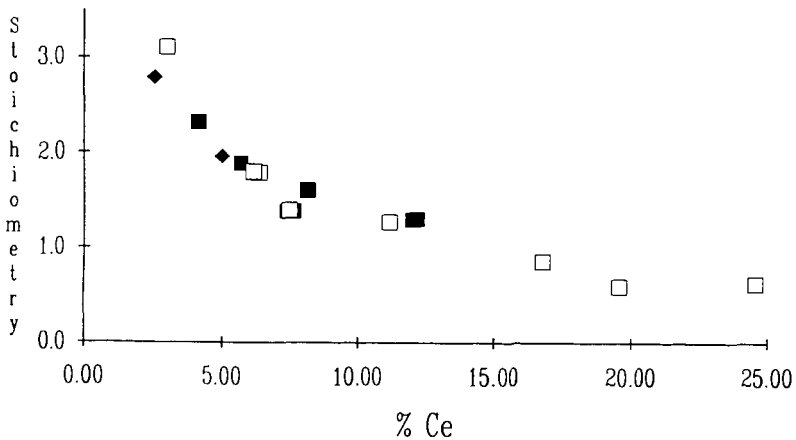


Figure 4. Mole ratio of  $\text{SO}_2$  absorbed at saturation at  $600^\circ\text{C}$  to  $\text{CeO}_2$  on the sorbent as a function of metal loading. Different point symbols represent aluminas from different commercial suppliers.

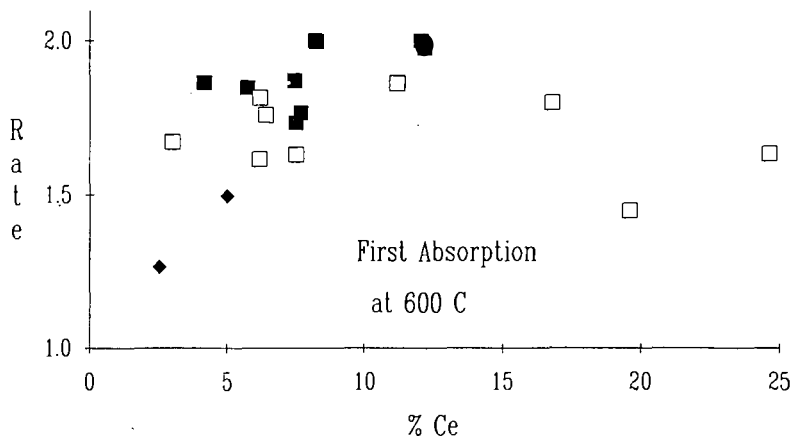


Figure 5. Rate of  $\text{SO}_2$  uptake by  $\text{CeO}_2/\text{Al}_2\text{O}_3$  sorbents expressed in mg  $\text{SO}_2$  per g sorbent per minute as a function of Ce loading. The standard deviation of the rates determined was 0.1 or less. Different point symbols represent aluminas from different commercial suppliers. See text for discussion.

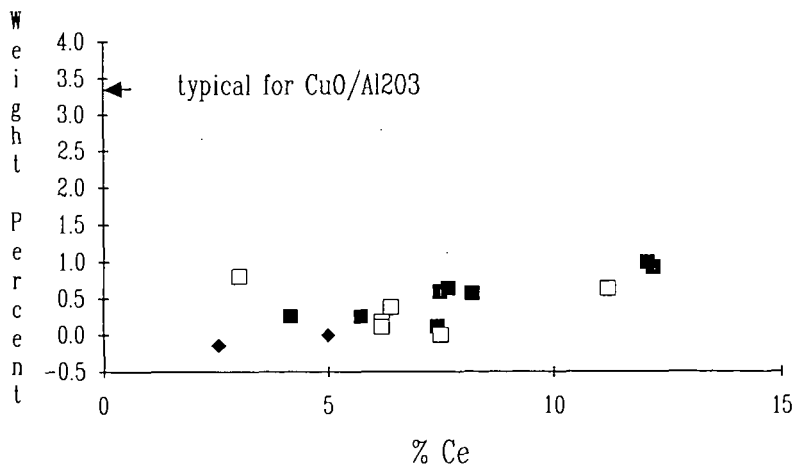


Figure 6. Residual remaining on  $\text{CeO}_2/\text{Al}_2\text{O}_3$  sorbents after regeneration in  $\text{H}_2$  in the TGA test unit. The value observed for  $\text{CuO}/\text{Al}_2\text{O}_3$  under similar conditions is shown for comparison.

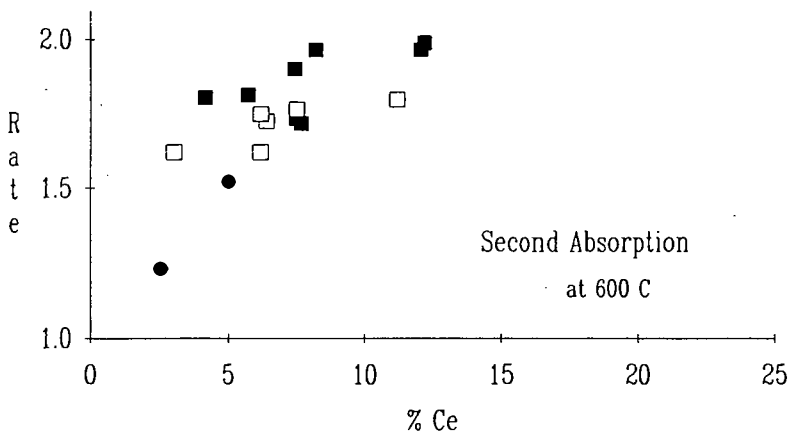


Figure 7. Rate of  $\text{SO}_2$  uptake by  $\text{CeO}_2/\text{Al}_2\text{O}_3$  sorbents during a second exposure to simulated flue gas after regeneration in  $\text{H}_2$  expressed in  $\text{mg SO}_2$  per g sorbent per minute as a function of Ce loading. The standard deviation of the rates determined was 0.1 or less. Point shapes represent aluminas from different commercial suppliers. See text for discussion.

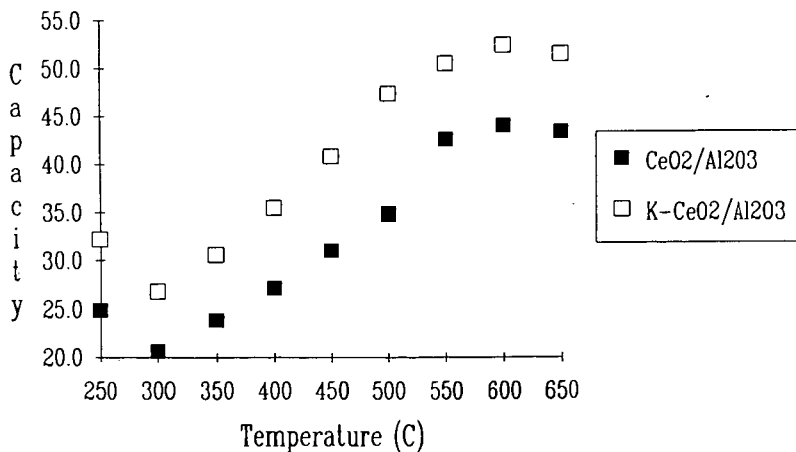


Figure 8. Comparison of  $\text{SO}_2$  capacity as a function of temperature of a K- modified and a Ce-only sorbent, both of which contain 4 % Ce. Capacity is expressed in  $\text{mg SO}_2$  per g sorbent.

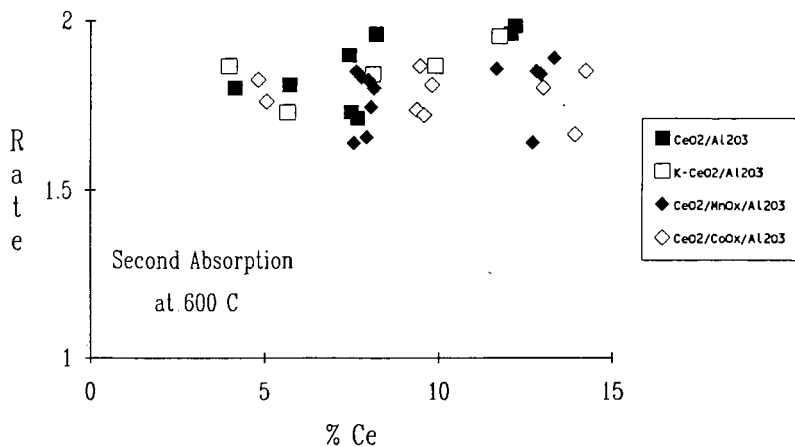


Figure 9. Rate of  $\text{SO}_2$  uptake by Ce-containing sorbents during a second exposure to simulated flue gas after regeneration in  $\text{H}_2$  expressed in  $\text{mg SO}_2$  per g sorbent per minute as a function of Ce loading. The standard deviation of the rates determined was 0.1 or less.

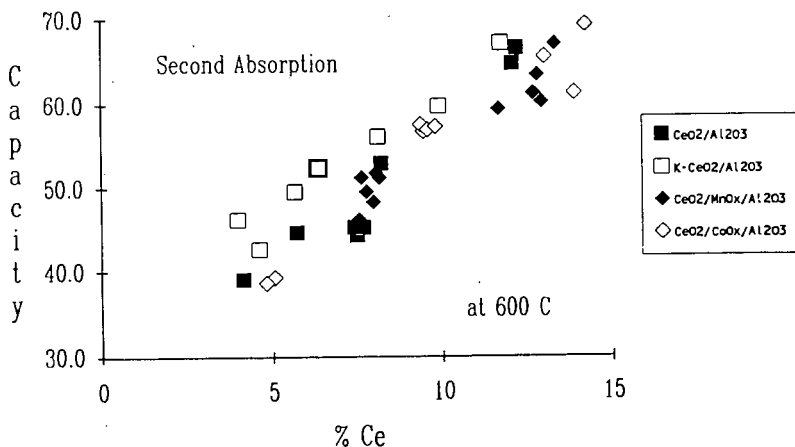


Figure 10. Comparison of  $\text{SO}_2$  capacity of Ce-containing sorbents during a second exposure to simulated flue gas after regeneration in  $\text{H}_2$  expressed in  $\text{mg SO}_2$  per g sorbent as a function of Ce loading. The standard deviation of the capacities determined was 2 or less.

?

**THE PHYSICAL NATURE AND THE CHEMICAL REACTIVITY  
OF A  
HETEROGENEOUS MgO/VERMICULITE FLUE-GAS SORBENT**

Richard J. Ruch, Carl J. Knauss, William E. Bacon, and Scott Miller  
Department of Chemistry  
Kent State University, Kent, OH 44242

Sidney G. Nelson, Brian W. Nelson, and Sidney G. Nelson, Jr.  
Sanitech, Inc.  
1935 East Aurora Road, Twinsburg, OH 44087

**INTRODUCTION**

Many advancing new technologies for removing SO<sub>2</sub> and NO<sub>x</sub> from flue gas emissions involve dry scrubbing, in contrast to wet scrubbing, the most widely used technology today [1]. These developments are being encouraged by a real need to reduce costs, to increase overall efficiency, and to avoid major problems relating to water pollution and to sludge handling and disposal. Cost reductions and increased efficiency can be achieved by using regenerable, high-capacity sorbents, and the water and waste-disposal problems can be alleviated by handling sorbents dry and by generating useful by-products from the wastes produced. Recently, a new family of dry, regenerable sorbents, called NelSorbents, has reached the stage of pilot-scale testing.

The reactivity of unsupported MgO for removal of flue-gas components has been studied extensively [2]. Studies have also been done on inert supports for MgO and other oxides [3]. In addition, the reactivity and catalytic activity of such support-type materials as aluminates, silicates, and zeolites, have been studied [4].

The present study was undertaken to determine the physical nature and the chemical reactivity of a promising NelSorbent material having vermiculite as a support for hydrated MgO. This patented sorbent has been shown to effectively remove SO<sub>2</sub> and NO<sub>x</sub> from flue gases in the laboratory and in pilot-scale operations. A fundamental scientific investigation of the material was performed to improve current methods of preparation, conditioning, utilization, and regeneration.

**EXPERIMENTAL**

NelSorbent Preparation

The NelSorbent used in the studies was prepared by Sanitech, Inc. using the techniques described in U.S. Patent Number 4,721,582. Vermiculite was variously coated with several grades of MgO, Mg(OH)<sub>2</sub>, or MgCO<sub>3</sub>. The samples were both bench- and batch-processed at 45% by weight MgO and conditioned at temperatures of 400, 550, and 800°C.

Sample Preparation

Sanitech exposed NelSorbents both in a dry and in a moistened condition to side-streams of flue-gas at the Gorge Power Plant of Ohio Edison in Akron, Ohio. In the laboratory, vermiculite and NelSorbents were exposed to synthetic flue-gas mixtures and to SO<sub>2</sub> or NO<sub>x</sub> under varying relative humidities.

### NelSorbent Regeneration

Flue-gas exposed samples were regenerated at 800°C in either air or in a 40% CH<sub>4</sub>/60% N<sub>2</sub> mixture.

### Gas Adsorption

Nitrogen adsorption and desorption measurements were made in a classical gas adsorption apparatus at liquid nitrogen temperature. Pressures were measured with a mercury manometer and masses were measured to ±0.01 milligrams with a Cahn electromagnetic balance. Adsorption and desorption for SO<sub>2</sub> and NO<sub>x</sub>, both in the presence and in the absence of added moisture, were measured to ±0.2 milligrams with a quartz spring balance.

Water adsorption isotherms were carried out over a period of weeks. Samples in desiccators were exposed to specific relative humidities achieved by various saturated salt solutions. Weight gains in these trials were determined with an analytical balance.

### Infrared Spectra

Fourier transform infrared spectra (FTIR) were measured with an IBM model 32 spectrophotometer. Both powder samples in a nitrogen atmosphere and solution spectra in silver chloride cells were measured. A Spectra-Tech high temperature environmental chamber was used to run series of spectra at elevated temperatures.

### X-Ray Diffraction

Samples were packed in Lindeman glass capillaries and exposed to Cu radiation at 35 kilovolts and 15 milliamps for about seven hours. The interlayer spacings were calculated from the resultant powder patterns.

### Electron Micrographs

Electron micrographs were made with several microscopes. Due to static charge phenomena, the best results were obtained at very low amperages and gave good resolution to the nanometer range.

## **RESULTS AND DISCUSSION**

### Nitrogen Isotherms

The classical BET theory was used to analyze adsorption isotherms such as those shown in Figures 1 and 3. Moisture variability is a problem in establishing a reliable mass baseline for minerals such as vermiculite. To minimize this variability, the samples were outgassed under a vacuum as the sample was heated to 200°C. Although this procedure reduced the baseline variability, it was necessary to plot the data in the form shown in Figures 2 and 4 to get reproducible results.

For the N(1-X) ordinate of Figures 2 and 4, N represents the mass reading in milligrams obtained from the Cahn balance. When X=P/Po=0, the intercept gives the correct baseline. Adding the baseline to the slope of the plot gives the mass in milligrams for a monolayer by the BET theory.

### Surface Areas

BET surface areas with N<sub>2</sub> are shown in Table 1. The value of 4 M<sup>2</sup>/gram represents the external surface area of vermiculite.

**TABLE 1**  
BET SURFACE AREAS - M<sup>2</sup>/gram Sample

| <u>SAMPLE</u>                         | <u>TEMPERATURE</u> | <u>NITROGEN</u> | <u>WATER</u> |
|---------------------------------------|--------------------|-----------------|--------------|
| Conditioned:                          |                    |                 |              |
| Vermiculite                           | 550°C              | 4               |              |
| MgO                                   | 550°C              | 50              |              |
| NelSorbent-Bench                      | 550°C              | 55              | 270          |
| NelSorbent-Bench                      | 800°C              | 11              |              |
| NelSorbent-Batch                      | 550°C              | 16              | 52           |
| Regenerated NelSorbenents:            |                    |                 |              |
| Batch-Air                             | 800°C              | 12              | 57           |
| Batch-CH <sub>4</sub> /N <sub>2</sub> | 800°C              | 8               |              |
| Previous Sample in Air                | 500°C              | 2               | 45           |

The surface area of MgO varies considerably depending on how it is prepared [7,8]. The NelSorbent bench-processed at 550°C had a surface area of 55 M<sup>2</sup>/gram of sample. Since this NelSorbent is only 45% MgO by weight, this corresponds to a surface area for this MgO of over 100 M<sup>2</sup>/gram or more than twice that of the original MgO. Special treatment of MgO has been shown to give areas in excess of 500 M<sup>2</sup>/gram [9].

Exposure to high temperatures caused surface areas to drop. Surface areas of NelSorbent conditioned at 800°C and NelSorbent batch-processed at 550°C, where hot-spots may exist, dropped below 20 M<sup>2</sup>/gram. After gas exposure, the batch-processed NelSorbenents were regenerated and the surface areas dropped even more, to 12 and 8 M<sup>2</sup>/gram. The sample regenerated in a CH<sub>4</sub>/N<sub>2</sub> atmosphere had a grey color which disappeared on heating in air to 500°C. However, the surface area then dropped even more to 2 M<sup>2</sup>/gram. The grey colored sample gave a positive sulfide test with lead acetate paper.

The 550°C bench-processed NelSorbent was sieved into fractions >1400, 500-1400, 250-500, and <250 microns. The surface areas ranged from 23-36 M<sup>2</sup>/gram sample, considerably below the 55 M<sup>2</sup>/gram for the unsieved sample. In the unsieved sample, the larger vermiculite particles may protect the MgO from being sintered.

### Water Isotherms

Table 1 also shows the surface areas determined by the adsorption of water on four selected samples. These water areas exceed the nitrogen areas by greater than three-fold. The most dramatic effect was for the regenerated sample which went from 2 to 45 M<sup>2</sup>/gram. This shows that the conditioning water can penetrate the interlayers of the vermiculite even if external surface area has been previously reduced.

### NO<sub>x</sub> Adsorption

Table 2 shows that a NelSorbent conditioned at 550°C and exposed to NO<sub>x</sub> under ambient conditions had an 11.2% weight gain which was retained on evacuating the system. After heating to 200°C in vacuum, the weight gain dropped to 7.0%. Vermiculite on the other hand, gained only 2.2%

by weight  $\text{NO}_x$  under similar conditions and lost almost all of the weight by pumping in a vacuum without the addition of heat. Hence, there is a much stronger interaction of  $\text{NO}_x$  with the NelSorbent than with the vermiculite, the former being akin to chemical adsorption and the latter to physical adsorption.

**TABLE 2**  
 $\text{NO}_x/\text{SO}_2$  ADSORPTION - PERCENTAGE WEIGHT GAIN

| SAMPLE                        | AMBIENT          |  | VACUUM |       |
|-------------------------------|------------------|--|--------|-------|
|                               | EQUILIBRIUM      |  | 20°C   | 200°C |
| $\text{NO}_x$ ADSORPTION      |                  |  |        |       |
| 550°C NelSorbent <sup>a</sup> | 11.4%            |  | 11.4%  | 7.0%  |
| Vermiculite <sup>a</sup>      | 2.2%             |  | 0.3%   | --    |
| $\text{SO}_2$ ADSORPTION      |                  |  |        |       |
| 550°C NelSorbent <sup>b</sup> | 4.0%             |  | --     | --    |
| Vermiculite <sup>a</sup>      | 1.0%             |  | 0.5%   | --    |
| 550°C NelSorbent <sup>a</sup> | 4.5%             |  | 3.4%   | --    |
| 550°C NelSorbent <sup>c</sup> | 94% <sup>d</sup> |  | 57%    | 30%   |
| Vermiculite <sup>c</sup>      | 24% <sup>e</sup> |  | 2%     | --    |

a. Prepared at ambient conditions b. Prepared by pumping to vacuum  
 c. Prepared at 100% relative humidity d. Weight gain includes 37% water e. Weight gain includes 12% water

#### SO<sub>2</sub> Adsorption

NelSorbent conditioned at 550°C gained nearly 5% by weight when exposed to  $\text{SO}_2$  under ambient conditions and dropped a few percent when pumped down in a vacuum. However, when the NelSorbent was pre-conditioned for a week in 100% relative humidity, there was over a 50% weight gain of  $\text{SO}_2$  which remained on evacuating the system under ambient conditions. Even on heating to 200°C in a vacuum, 30% by weight  $\text{SO}_2$  remained indicating a strong chemical interaction.

Vermiculite gained little weight under ambient conditions when exposed to  $\text{SO}_2$  and the weight gain dropped to near the original sample weight when pumped to a vacuum under ambient conditions. Although there was a larger weight gain when the vermiculite was first saturated with water vapor for a week at 100% relative humidity, most of the weight gain was lost on pumping to a vacuum. This suggests a very weak physical interaction between  $\text{SO}_2$  and vermiculite even in the presence of a large amount of pre-absorbed water.

#### FTIR Solid Spectra

Raw vermiculite and 550°C conditioned vermiculite gave bands at 3000-3500  $\text{cm}^{-1}$  and at 1650  $\text{cm}^{-1}$ . Silicon-oxygen absorption near 1000  $\text{cm}^{-1}$  interfered with sulfite and sulfate analyses.

Conditioned NelSorbent gave a strong  $\text{Mg}(\text{OH})_2$  band at 3700  $\text{cm}^{-1}$  which disappeared as the temperature of conditioning was increased.  $\text{MgCO}_3$  peaks at 1500  $\text{cm}^{-1}$  and 850  $\text{cm}^{-1}$  became evident on heating as well as 1400 and 400-700  $\text{cm}^{-1}$  peaks for  $\text{MgO}$ . Batch-processed material did not as effectively reduce the  $\text{Mg}(\text{OH})_2$  peaks as did bench-processing. When  $\text{MgCO}_3$  was used as the starting material, the carbonate peaks remained strong even after conditioning indicating that insufficient energy was added to the system to break down the carbonate.

When the NelSorbent was exposed to  $\text{SO}_2$ , a sulfite peak at  $950\text{ cm}^{-1}$ , a sulfate peak at  $1100\text{ cm}^{-1}$ , and bisulfite/bisulfate peaks at  $2250\text{ cm}^{-1}$  were noted in addition to the previously discussed peaks and bands.  $\text{MgCO}_3$  was particularly dominant when NelSorbents were run under dry conditions at the power plant suggesting that  $\text{CO}_2$  strongly competes in adsorption under these conditions.

In general, the concentration of  $\text{NO}_x$  was not high enough in the flue-gas streams to be absorbed to such an extent to be detected by FTIR. One NelSorbent sample exposed to NO and superheated steam showed the presence of nitrite at  $1250\text{ cm}^{-1}$ .

The spent NelSorbents regenerated in air showed MgO,  $\text{MgCO}_3$ , and  $\text{MgSO}_4$  peaks. The sample regenerated in  $\text{CH}_4/\text{N}_2$  suggested the presence of magnesium compounds not previously seen in other samples, perhaps Mg or MgS. Subsequent heating of the sample in air eliminated these compounds and peaks were observed for MgO and  $\text{MgSO}_4$ . Also, a particularly large  $\text{MgCO}_3$  peak appeared which may have been previously masked.

A NelSorbent well-spent with flue-gas was heated in situ in the FTIR environmental chamber. The sample was mixed with KBr and heated in a stream of nitrogen. Bisulfite/bisulfate peaks disappeared by  $200^\circ\text{C}$ , water peaks reached a minimum at  $300^\circ\text{C}$ , MgO and  $\text{MgCO}_3$  disappeared by  $500^\circ\text{C}$ , and  $\text{MgSO}_4$  increased in intensity at  $400^\circ\text{C}$  and remained constant up to  $660^\circ\text{C}$ , the maximum temperature of analysis.

#### FTIR Solution Spectra

Aqueous extracts of NelSorbents spent with flue-gas indicated the sulfate ion at  $1100\text{ cm}^{-1}$ . No sulfite was detected, perhaps due to its oxidation to sulfate.

A NelSorbent sample saturated in the laboratory with moisture and with  $\text{NO}_x$  gave a nitrite peak at  $1240\text{ cm}^{-1}$ . The nitrate peak was absent.

#### Basal Plane X-Ray Spacings

The raw and the  $550^\circ\text{C}$  processed vermiculite gave a 14 angstrom interlayer spacing expected for two layers of water. When conditioned at  $550^\circ\text{C}$  for 30 minutes in the NelSorbent preparation, the interlayer distance dropped to 12 angstroms expected for one interlayer of water. When conditioned at  $800^\circ\text{C}$  for 30 minutes, the interlayer collapsed to a 9 angstrom distance which indicates the complete loss of interlayer water.

The interlayer distance expanded back to 14 angstroms for the NelSorbent in the flue-gas stream indicating the presence of enough water to re-expand the lattice.

#### Interplanar X-Ray Spacings

Table 3 shows interlayer distances and compound assignments found for a NelSorbent which was used at the power plant during a week of heavy rains.

**TABLE 3**  
NELSORBENT EXPOSED TO FLUE GAS

| <u>COMPOUND</u>                      | <u>ANGSTROMS</u> | <u>COMPOUND</u>                      | <u>ANGSTROMS</u>       |
|--------------------------------------|------------------|--------------------------------------|------------------------|
| MgCO <sub>3</sub> ·3H <sub>2</sub> O | 6.49             | MgSO <sub>4</sub> ·2H <sub>2</sub> O | 2.03, 4.39             |
| MgSO <sub>4</sub> ·7H <sub>2</sub> O | 5.91             | MgSO <sub>3</sub> ·6H <sub>2</sub> O | 2.76                   |
| MgSO <sub>4</sub> ·6H <sub>2</sub> O | 2.89             | MgSO <sub>3</sub> ·3H <sub>2</sub> O | 4.19                   |
| MgSO <sub>4</sub> ·4H <sub>2</sub> O | 3.93, 5.41       | MgO                                  | 3.04                   |
| MgSO <sub>4</sub> ·3H <sub>2</sub> O | 2.49             | Mg(OH) <sub>2</sub>                  | 1.49, 1.57, 1.79, 2.39 |

The 2.10 angstrom spacing for MgO in the freshly processed NelSorbent disappears on flue-gas exposure but reappears on regeneration. Some residual MgSO<sub>4</sub> is present under all methods of regeneration. Several unidentified spacings were found when the NelSorbent was regenerated in CH<sub>4</sub>/N<sub>2</sub> but disappeared when the material was reheated in air. Any sulfides, for example, would be oxidized to the sulfate and/or the oxide in air.

NelSorbent exposed to superheated steam and NO<sub>x</sub> in the laboratory developed a red-orange color. X-Ray spacings showed MgO, Mg(OH)<sub>2</sub> and Mg(NO<sub>3</sub>)<sub>2</sub>. The nitrate occurred at 3.34 angstroms and was not found in any flue gas exposed samples of NelSorbent.

#### Electron Micrographs

At 100,000 magnifications of the NelSorbent, the MgO or Mg(OH)<sub>2</sub> patches were observed to be sparsely but uniformly distributed on the vermiculite. As the magnification increased, the patches appeared as crystalline clusters with a high degree of porosity. At the highest magnification, the clusters seemed to be composed of needles several hundred nanometers in length and about 50 nanometers in cross-section.

#### SUMMARY

The surface area of the NelSorbents is larger than would be expected from the collective surface areas of the constituent vermiculite and MgO suggesting that the vermiculite support is enhancing surface area development of the MgO. There is evidence of a mesoporous structure in the NelSorbent from the electron micrographs and by the hysteresis of some of the desorption isotherms. Difficulty in establishing baseline weights of the NelSorbents also suggests the existence of a microporous structure. MgO is a better starting material than either Mg(OH)<sub>2</sub> or MgCO<sub>3</sub> for preparation of the NelSorbent. The carbonate does not seem to completely decompose in the conditioning process.

There is a loss of surface area when the NelSorbents are subjected to too high a temperature. This can happen during conditioning or regeneration or when hot spots develop in batch conditioning or when sieved fractions tend to fuse. The vermiculite basal plane structure can also be collapsed by the higher temperatures.

Sulfites, sulfates, and sulfides are detected by FTIR, X-Ray, or qualitative tests. The sulfite tends to oxidize to the sulfate over longer periods of time. Some sulfate tends to remain even under fairly rigorous regeneration techniques. Any sulfides produced by a reducing regeneration atmosphere are reoxidized to sulfate or oxide by heating in air.

Nitrites or nitrates were not detected in pilot plant NelSorbent samples due to the small concentration of NO<sub>x</sub> in the flue-gas. They were variously detected in laboratory treated samples by FTIR, X-Ray, and qualitative tests.

Moisture plays an extremely important role in the adsorption process. Burning wet coal or adding moisture to the sorbent bed increased the adsorption efficiency of the NelSorbent for SO<sub>2</sub> and NO<sub>x</sub>. This observation is confirmed by laboratory studies under static conditions. X-Ray studies and adsorption studies with water substantiated the penetration of the vermiculite interlayers.

Dynamic studies have shown larger percentage utilizations of the NelSorbents than have static studies in the laboratory. Future studies will need to address what factors in the dynamic systems are responsible for this difference.

#### ACKNOWLEDGMENT

This work was funded by a Thomas Edison Seed Grant from the state of Ohio. The space for the pilot-plant operations was donated by the Ohio Edison Company.

#### REFERENCES

- [1] Chemical & Engineering News, 67, No. 20, 20(1989); 67, No. 50, 17(1989); 68, No. 3, 5(1990).
- [2] Egan, B.Z. and Felker, L.K., Ind. Eng. Chem. Process Des. Dev., 25, 558(1986).
- [3] Kocaefer, D., Karman, D., and Steward, F.R., Canadian J. Chem. Eng., 63, 971(1985).
- [4] Marier, P. and Ingraham, T.R., Mines Branch Information Circular IC 263, Department of Energy, Mines and Resources, Mines Branch, Ottawa, February, 1971.
- [5] Haggin, J., Chemical & Engineering News, 68, No. 3, 38(1990).
- [6] Marier, P. and Dibbs, H.P., Thermochemica Acta, 8, 155(1974).
- [7] De Vleeschauwer, W.F.N.M. in "Physical and Chemical Aspects of Adsorbents and Catalysts", B.G. Linsen, ed., Academic Press, N.Y., pp. 265-314, 1970.
- [8] Hartman, M. and Svoboda, K., Ind. Eng. Chem. Process Des. Dev., 24, No. 3, 613(1985).
- [9] Beruto, D., Rossi, P.F., and Searcy, A.W., J. Phys. Chem., 89, 1695(1985).

Key Words: sorption, flue-gas, vermiculite

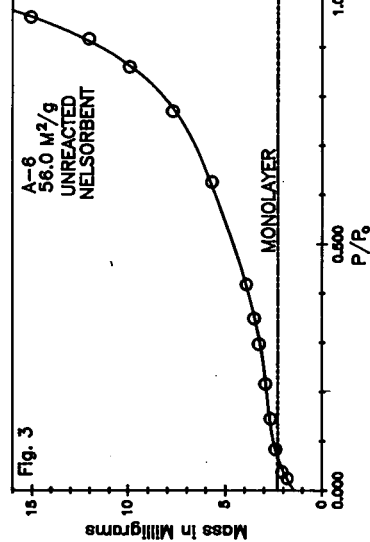
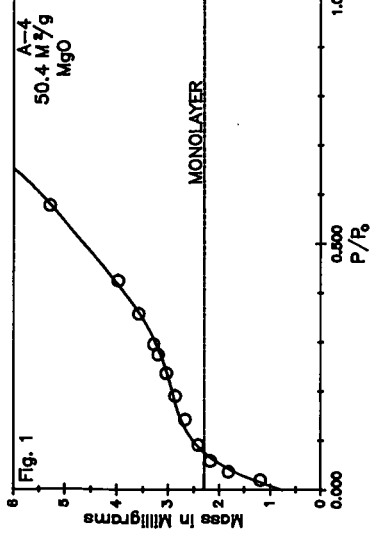
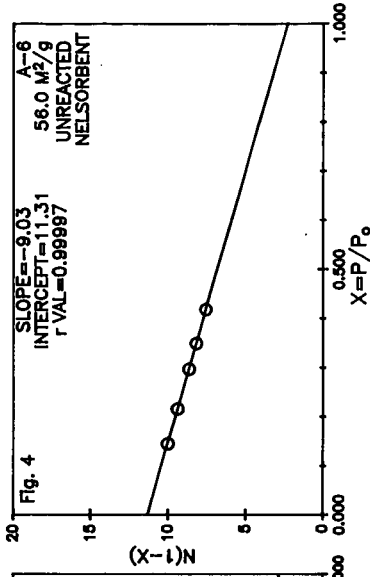
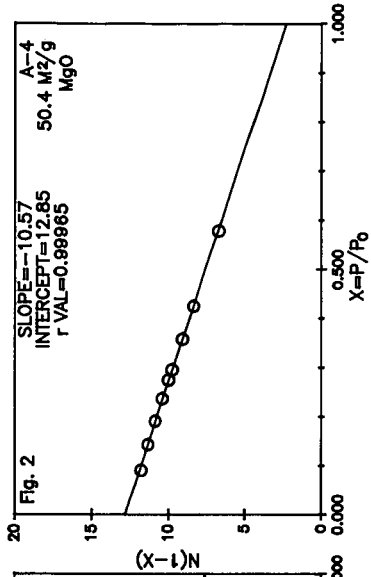


Figure 1 - Adsorption isotherm of MgO processed at 550°C.  
 Figure 2 - Variation of BET plot to determine mass of A-4 monolayer.  
 Figure 3 - Adsorption isotherm of Nelsorbent processed at 550°C.  
 Figure 4 - Variation of BET plot to determine mass of A-6 monolayer.

## PRODUCTION AND APPLICATION OF THIOSULFATE IN LIME-BASED WET FGD

Y. Joseph Lee<sup>a</sup>, Lewis B. Benson<sup>a</sup>, and Robert O. O'Hara<sup>b</sup>

a. Dravo Lime Company, Pittsburgh, PA 15225

b. Duquesne Light Company, Pittsburgh, PA 15279

Key Words: sulfur, alkaline hydrolysis, thiosulfate, oxidation inhibition, lime

### INTRODUCTION

Thiosulfate has been identified as a free radical scavenger which inhibits sulfite oxidation effectively (Owens and Rochelle, 1985). In flue gas scrubbers, excessive oxidation could cause some serious reliability problems such as scaling on scrubber internals and mist eliminators. Emulsified sulfur has been used in many limestone scrubbers (Moser et al., 1988) since it was found that sulfur could react with sulfite in scrubbing liquor to form thiosulfate feasibly (Rochelle et al., 1987). However, the reaction rate is very slow primarily because of the low solubility of sulfur in aqueous solution. Alkaline hydrolysis of sulfur is a potential alternative to synthesize thiosulfate by sulfur addition. At high pH and high temperature, sulfur can be converted to thiosulfate and polysulfides which react with sulfite readily to form thiosulfate. This paper is focused on the kinetics of the alkaline hydrolysis of sulfur and its effect on the overall performance of lime-based wet FGD.

### BACKGROUND

Several reactions related to the production of thiosulfate from sulfur are collectively listed in Table 1. Thiosulfate has been produced commercially by the reaction of sulfur and sulfite in neutral or alkaline media (rxn 1). Because of the equilibrium between sulfite and bisulfite (rxn 2), alkalinity is necessary to enhance reaction 1 by removing the proton released from bisulfite. The reaction rate is independent of pH or sulfite concentration and is first order in sulfur solids concentration when pH is above 5.0 and sulfite is greater than 1 mM (Donaldson and Johnston, 1969). At 55°C, typical for lime/limestone slurry scrubbers and recycle tanks, 0.04 hr<sup>-1</sup> was suggested for this first order kinetic constant (Rochelle et al., 1987).

One way to facilitate the production of thiosulfate is by using sulfide or polysulfides instead of sulfur (rxn 4). Polysulfides may be formed by dissolving sulfur in sulfide solutions (Gould, 1962). Reaction 4 is so fast that the proton released by reaction 2, in some instances, cannot be neutralized immediately. Besides, the pH at gas-liquid interface is low due to SO<sub>2</sub> dissolution. The consequence is the formation of "local" low pH spot despite the alkaline bulk solution and the generation of hydrogen sulfide that may cause serious odor problems. Because of this reason, polysulfide was abandoned in the EPA limestone scrubbing pilot plant at Research Triangle Park (Rochelle et al., 1987). However, if polysulfides are introduced to scrubbers together with lime slurries, the high pH of the feeding slurry and the scrubbing liquor as well as the fast dissolution of lime will neutralize the proton in reaction 2 effectively and therefore prevent the formation of H<sub>2</sub>S.

Boiling sulfur-lime slurry is a commercial process for polysulfide production.

Alkaline hydrolysis of sulfur is therefore a logical approach to synthesize thiosulfate in situ because of the highly exothermic reaction of lime slaking. The polysulfides will react readily with sulfite to form thiosulfates (rxn 7-9). The unreacted sulfur leaving the lime slurry storage tank will react with sulfite in the scrubbers and in the recycle tanks to produce additional thiosulfate (rxn 1). Another "reactor" for thiosulfate production is the thickener. Therefore, the conversion of sulfur to thiosulfate is expected to be substantially higher in lime-based FGD than in limestone-based FGD.

#### EXPERIMENTAL METHODS

Jacketed reactors were used to perform experiments at the desired temperature. The solutions were agitated by magnetic stirrers. When thiosulfate formation in slakers/lime tanks was studied, 500 ml of 3.3 wt% or 10 wt% lime slurry was used to react with sulfur. The slurry samples (25 ml) were quenched by adding 50 ml cold 0.2M sodium sulfite. The resulting mixtures were allowed to react 10 minutes to completely convert polysulfides to thiosulfate. Clarified filtrates were then analyzed for thiosulfate by iodometric titration after blocking sulfite with formaldehyde. The thiosulfate measured in this way was dubbed "available thiosulfate."

When the formation of thiosulfate by reacting sulfur with sulfite was studied, a calcium sulfite slurry available from a power station's (Elrama, PA) recycle tank was used as the source of sulfite. Fritted glass spargers were used to introduce gas containing SO<sub>2</sub> to the reacting solutions. Lime slurries (10 wt%) were used to neutralize the absorbed SO<sub>2</sub> and to keep the pH between 6.5 and 7.5. Both emulsified sulfur and powdered sulfur were used for this study. Emulsified sulfur had no problem getting into slurry solution while 2000X dilute Triton X-100 was needed to wet powdered sulfur first.

A schematic diagram of the flow system used for studying the impact of sulfur addition to a lime slurry scrubbing system is given in Figure 1. Nitrogen, air, and SO<sub>2</sub> were metered and mixed in a mixing chamber to simulate the flue gas. In most cases, both nitrogen and air were set at 1.0 scfm to give ~10% O<sub>2</sub> in the simulated flue gas. Sulfur dioxide was set at a rate slightly lower than necessary to neutralize the 5 wt% lime slurry fed at 12 ml/min. An auxiliary SO<sub>2</sub> flow was activated by a pH controller when the pH value of the scrubbing liquor was higher than 7.2. The scrubber pH was thus maintained between 7.0 and 7.2 throughout all experiments. The temperature of the scrubbing liquor was maintained at 55°C by circulating the liquor through a heat exchanger. The simulated thickener overflow (TOF) was fed to the scrubber at 100 ml/min. The composition of the simulated TOF is also given in Figure 1. Sodium thiosulfate or available thiosulfate was fed to the scrubber at 16 ml/min. The volume of the absorber was maintained at 5.5 liters by a level controller. Samples were taken once an hour and analyzed for both sulfite and thiosulfate by iodometric titration.

#### RESULTS AND DISCUSSIONS

##### Sulfur to Thiosulfate and Polysulfides in Slakers and Lime Tanks

Boiling a slurry mixture of lime and sulfur is a general practice to

manufacture polysulfides commercially. This process prompted the testing of thiosulfate production by feeding sulfur to the slaker or the lime slurry storage tank because of the fast conversion of polysulfides to thiosulfate and the highly exothermic reaction of lime slaking. According to the reactions 6-9 listed in Table I, one mole of sulfur will generate one mole of thiosulfate stoichiometrically. The calculation of sulfur conversion is based on the formation of the available thiosulfate.

Both powdered sulfur and emulsified sulfur were tested for the production of available thiosulfate. It is very clear that the conversions of powdered sulfur (Figure 2) and emulsified sulfur (Figure 3) to available thiosulfate are strongly dependent on reaction temperature. The dramatic difference between 70°C and 80°C in converting powdered sulfur to available thiosulfate is probably not exclusively due to the activation energy of reaction 6. A possible contribution is the dissolution of powdered sulfur in sulfide or polysulfide solutions. As a matter of fact, one way to produce polysulfide is dissolving powdered sulfur in sodium sulfide solution (Hartler et al., 1967; Arntson et al., 1958). Therefore, when the concentration of sulfide or polysulfide is high, the conversion of sulfur to available thiosulfate will be accelerated. The ceiling conversion is probably controlled by the thermodynamic equilibrium and the coprecipitation with lime solids.

Figure 2 indicates that higher concentrations (1.0 g S/500 ml lime slurry) of sulfur are subjected to lower conversion rates. Probably the agglomeration of sulfur particles, that reduces the available surface area for reactions, is more severe at higher concentrations. Emulsified sulfur is a lot more reactive than powdered sulfur for alkaline hydrolysis. Compared to powdered sulfur (>30 $\mu$ ), emulsified sulfur (<5 $\mu$ ) is at least 100 times more reactive at 70°C primarily due to its smaller particle size.

It is well known that thiosulfate is not stable in acidic solution (rxn 3). It is also known that thiosulfate decomposes to sulfate and sulfide in alkaline media (Kirk-Othmer, 1969). To investigate the stability of thiosulfate in lime slurry, sodium thiosulfate was added to 3.3 wt.% lime slurry. The samples at different "seasoning" time were analyzed for thiosulfate. The results indicate that 20% and 30% of the sodium thiosulfate are not accounted for in the filtrate for 12.5 mM and 25 mM sodium thiosulfite solutions respectively, however the thiosulfate concentrations did not change with time. Another study, mixing lime slurry (3.3 and 10 wt%) with varying amounts of sodium thiosulfate (up to 25.3 mM) for one hour at 80°C, indicated that the unaccounted for fraction was larger when using more concentrated lime slurry. These results imply that the major source of unaccounted thiosulfate is the "coprecipitation" with lime, while the decomposition of thiosulfate in lime saturated solutions is probably not significant. This was verified by analyzing the available thiosulfate in the filtered lime solids. Nevertheless, thiosulfate incorporation into lime solids should not cause any problems in lime slurry scrubbing systems because as the lime dissolves the coprecipitated "available thiosulfate" will be released.

#### Sulfur to Thiosulfate in Scrubbers and Recycle Tanks

Scrubbers and recycle tanks are the major reactors for the conversion of sulfur to thiosulfate (rxn 1) in limestone slurry scrubbing systems. For lime slurry scrubbing systems, the unreacted sulfur leaving from lime slurry storage tank

will contribute additional thiosulfate generation in scrubbers and recycle tanks. The reaction rate can be expressed empirically as first order in sulfur solids concentration (eq. 10)

$$\frac{d[S]}{dt} = -k[S] \quad (10)$$

Based on reaction 1 and equation 10, equation 11 can be derived.

$$\ln \left( 1 - \frac{[S_2O_3]_t - [S_2O_3]_0}{[S]_0} \right) = -kt \quad (11)$$

Where subscripts t and o denote time t and time zero respectively. Plotting the experimental data as  $\ln \left( 1 - \frac{[S_2O_3]_t - [S_2O_3]_0}{[S]_0} \right)$  versus time should then give a straight line of slope -k. The results are summarized in Table 2.

The conversion of sulfur to thiosulfate by reacting with sulfite decreased with increasing sulfur loading just like what was observed in the study of alkaline hydrolysis of sulfur. When sulfur solid concentration increased from 0.4 g to 1.2 g per 500 ml slurry, the empirical reaction rate constant decreased from 0.072 hr<sup>-1</sup> to 0.040 hr<sup>-1</sup> when N<sub>2</sub> blanket was applied above the reaction solutions. Similar results were reported by Rochelle et al. (1987). However, no significant differences were observed with different sulfur loadings (0.17-1.2 g) when gases were sparged through the solutions. Probably, the gas sparging helps the dispersion of sulfur solids and enhances the solid-liquid reactions.

In reacting with sulfite to form thiosulfate, emulsified sulfur has significantly larger initial conversion rate while powdered sulfur has an "incubation" period. The latter was also observed by Rochelle et al. (1987). The reaction rate constant measured after incubation period is 0.087 hr<sup>-1</sup> for powdered sulfur. The corresponding kinetic constant for emulsified sulfur is 0.090 hr<sup>-1</sup>. In other words, there is no significant difference between emulsified sulfur and powdered sulfur except for the much faster initial rates of emulsified sulfur and the long incubation time of powdered sulfur.

Previous studies suggested a kinetic constant of 0.04 hr<sup>-1</sup> at 55°C in the absence of sulfite oxidation (Rochelle et al., 1987). Thiosulfate decomposition is coupled with sulfite oxidation. Table 2 indicates that the kinetic constants are well above that value even in the presence of significant sulfite oxidation caused by 15% O<sub>2</sub>. Perhaps some unidentified chemistry facilitated the conversion of sulfur to thiosulfate in Elrama slurries more effectively.

#### Impact of Available Thiosulfate on the Performance of Wet Scrubber

In a laboratory scale slaker, elemental sulfur (32 g powdered sulfur or 45.7 g 70 wt% emulsified sulfur was mixed with 10 liter preheated water (46°C) first and 2 kg pebble lime was then fed to the water-sulfur mixture. The slurry temperature rose and then dropped from 81.5°C to 72°C over 25 minutes. The slurry was then diluted with water make 8.4 wt% solids. The temperature was maintained at 44°C by a heating tape and the slurry was gently stirred for one hour. The slurry was then quenched with water to make 5.0 wt% slurry. The conversions of sulfur to available thiosulfate were 78% and 21% for emulsified sulfur and powdered sulfur, respectively.

A bench scale absorber was used to evaluate the effect of the available thiosulfate on the general performance of magnesium-enhanced lime slurry scrubber. During the experiments, lime slurry and available thiosulfate were fed to the absorber separately. Separate feeding made the control of thiosulfate concentration independent of the lime slurry feed rate. A very light odor of emulsified sulfur was detected during the process of conducting experiments, but no H<sub>2</sub>S odor problem was encountered.

The result indicated that the oxidation of sulfite could be suppressed by thiosulfate when thiosulfate concentration was higher than a certain level, the so-called threshold concentration. For example, 0.63 mM thiosulfate gave a calcium sulfite/sulfate solid with 87% oxidation, which was essentially the same as the solid oxidation in the absence of thiosulfate. As low as 15% solid oxidation was achieved when 1.8 mM thiosulfate was present.

Two experiments were performed under similar conditions except one used Na<sub>2</sub>S<sub>2</sub>O<sub>3</sub> directly and the other used polysulfides, which were produced by alkaline hydrolysis of sulfur, as the source of thiosulfate. The results show practically no difference between these two experiments except polysulfides slightly decreased calcium and increased sulfate but kept the oxidation level in the solids (15%) essentially the same.

It seemed that polysulfides reacted with sulfite fast enough to provide thiosulfate reliably. Fortunately, the absorption of SO<sub>2</sub> into lime slurry to supply sulfite for thiosulfate production was even faster. Therefore, the concentration of sulfite in the solution was maintained nearly constant. Sulfite is important because SO<sub>3</sub><sup>2-</sup> is the major source of alkalinity used to absorb SO<sub>2</sub>.

Figure 4 shows the effect of thiosulfate concentration on its utilization. The utilization here is defined as the ratio of the measured thiosulfate concentration to the "maximal" thiosulfate concentration, which is obtained by assuming no decomposition and no coprecipitation. The results imply that the major loss of thiosulfate is due to coprecipitation with calcium sulfite hemihydrate when thiosulfate concentration is higher than 1.9 mM. (Because thiosulfate utilization in the absence of oxygen is 92%, which is not significantly higher than 85-88% utilization with 1.9-3.8 mM thiosulfate in the scrubbing liquor and 10.5% O<sub>2</sub> in the flue gas. And the thiosulfate degradation is supposed to be coupled with sulfite oxidation). Thiosulfate utilization increases with its concentration up to 1.9 mM thiosulfate. This trend implies that thiosulfate, at lower concentration, is subjected to more severe chemical degradation. It seems consistent with previous study (Maller et al. 1988), which correlated thiosulfate degradation rate (R<sub>d<sub>eg</sub></sub>) and sulfite oxidation rate (R<sub>o<sub>x</sub></sub>) as:

$$R_{d_{eg}} = a(R_{o_x} \times [S_2O_3^{2-}])^{0.5} \quad (12)$$

$$R_{o_x} = b\{[SO_3^{2-}]/[S_2O_3^{2-}]\} \quad (13)$$

Equations (12) and (13) can be combined to give equation (14):

$$R_{d_{eg}} = c[SO_3^{2-}]^{0.5} \quad (14)$$

Where a, b, and c are constants. In other words, the degradation of thiosulfate was predicted to be half order in sulfite but was independent of thiosulfate concentration. Equation (15) can be derived from equation (14) if the sulfite concentration is maintained constant:

$$\frac{[S_2O_3^{2-}]}{[S_2O_3^{2-}]_0} = 1 - \frac{[SO_3^{2-}]^{0.5}}{d[S_2O_3^{2-}]_0} \quad (15)$$

Where d is a constant. Equation (15) indicates qualitatively that the utilization of thiosulfate increases with thiosulfate and decreases with sulfite. More research is needed to better understand the degradation and coprecipitation of thiosulfate in lime slurry scrubbing systems.

#### ACKNOWLEDGMENT

This research project was financially supported by Duquesne Light Company. Special appreciation is extended to Mr. John College, who helped initiate this research project. The authors would like to thank Mr. James Zahorchak, Ms. Pat Kerr, and Mr. Jerry Hoffman for their help in performing the experiments, typing the paper, and preparing the figures, respectively.

#### REFERENCES

- Arntson, R. H., F. W. Dickson, and G. Tunell, "Saturation Curves of Orthorhombic Sulfur in the System S-Na<sub>2</sub>S-H<sub>2</sub>O at 25°C and 50°C," *Science*, Vol. 128, 716-718 (1958)
- Donalson, G. W. and F. J. Johnston, "The Reaction of Colloidal Sulfur with Sulfite," *J. Phys. Chem.* Vol. 73, 2064-2068 (1969)
- Gould, E. S., "Inorganic Reactions and Structure," Revised Ed. 291-292 (1962)
- Hartler, N., J. Libert, and A. Teder, "Rate of Sulfur Dissolution in Aqueous Sodium Sulfide Solution," *Ind. Eng. Chem. Proc. Dea. Dev.* Vol. 6, 398-406 (1967)
- Kirk-Othmer, "Encyclopedia of Chemical Technology," 2nd Ed. Vol. 20, 227-247 (1969)
- Moser, R. E., J. D. Colley, J. G. Noblett, and A. F. Jones. "Control and Reduction of Gypsum Scale in Wet Lime/Limestone FGD Systems by Addition of Thiosulfate: Summary of Field Experiences," Presented at the First Combined FGD and Dry SO<sub>2</sub> Control Symposium, St. Louis, MO, October (1988)
- Rochelle, G. T., Y. J. Lee, R. N. Ruiz-Alsop, J. C. S. Chang, and T. G. Brna, "Thiosulfate Additives for Lime/Limestone Scrubbing," EPA - 600/9-87-004b, February (1987)

TABLE I  
THIOSULFATE FORMATIONS IN LIME SLURRY SCRUBBING SYSTEMS

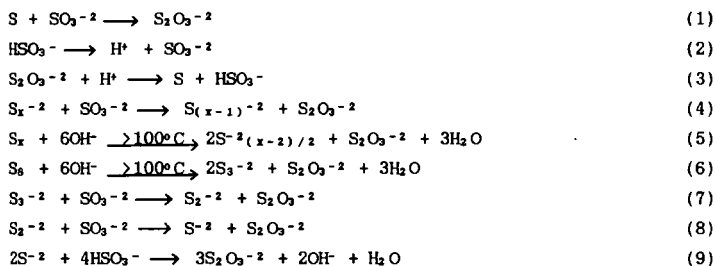


TABLE 2  
SUMMARY OF KINETIC CONSTANTS OF THIOSULFATE  
FORMATION BY REACTING SULFUR WITH SULFITE AT 55°C

| Sulfur (powdered)<br>(g/500 ml slurry) | Reaction Rate Constant (hour <sup>-1</sup> ) |                                  |   |
|--|--|----------------------------------|---|
|  | N <sub>2</sub> Blanket                       | 1% SO <sub>2</sub><br>200 ml/min | 2000 ppm SO <sub>2</sub><br>15% O <sub>2</sub><br>1 l/min |
| 0.1668                                 |  | 0.081                            | 0.042   |
| 0.336                                  |  | 0.087                            | 0.049   |
|  |  | 0.090*                           | 0.052   |
| 0.40                                   | 0.072  | 0.059                            |   |
| 1.20                                   | 0.040  | 0.062                            |   |

\*0.4766 g 70 wt% emulsified sulfur

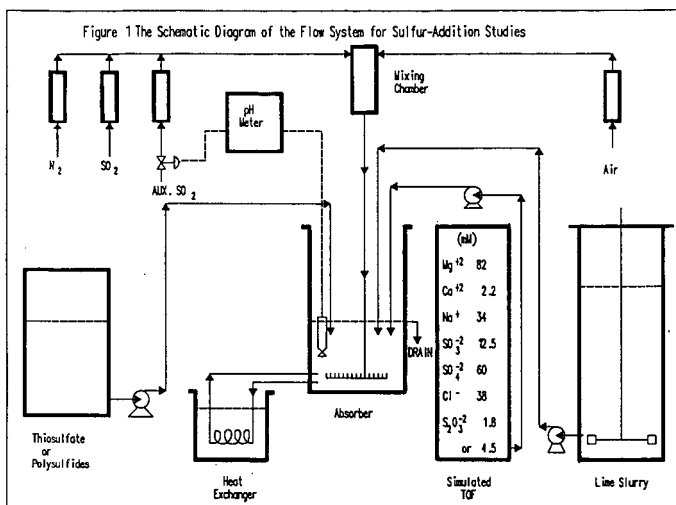
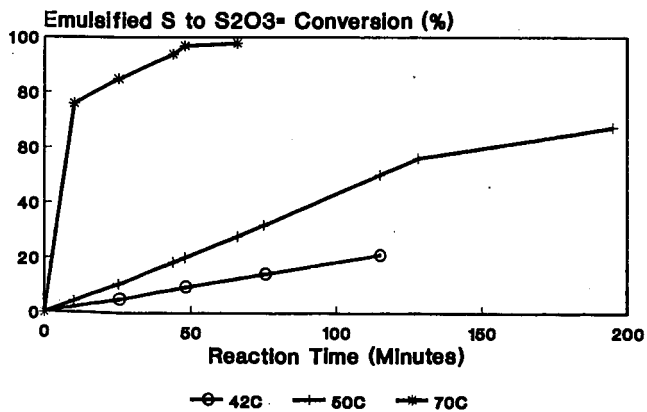
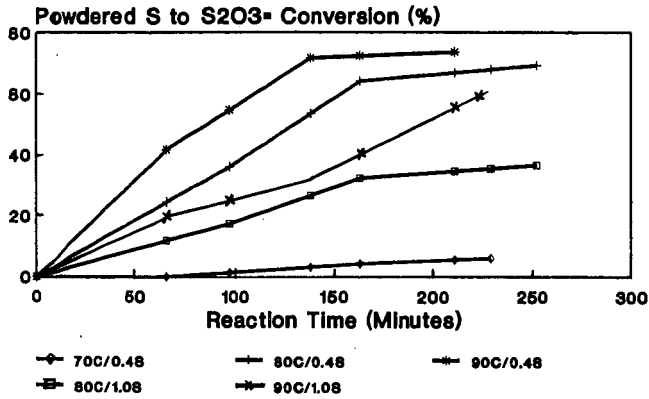


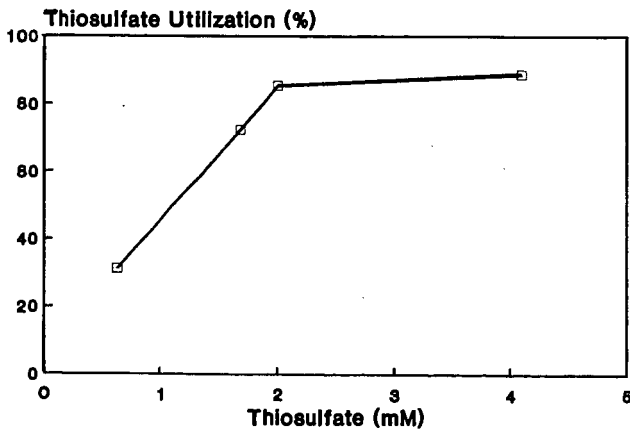
Figure 2 Temperature Effects on Alkaline Hydrolysis of Sulfur



**Figure 3 Temperature and Sulfur Loading Effects on Alkaline Hydrolysis of Sulfur**



**Figure 4 Utilization of Thiosulfate in Thiosorbic Lime Slurry Scrubbers**



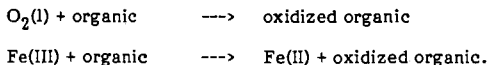
**Enhanced Flue Gas Denitrification  
Using Ferrous\*EDTA and a Polyphenolic Compound  
Having Combined Antioxidant and Reducing Properties**

M. H. Mendelsohn and J. B. L. Harkness  
Energy Systems Division  
Argonne National Laboratory, Argonne, IL 60439

Keywords: NO<sub>x</sub>-control, ferrous\*EDTA, antioxidant/reducing agents

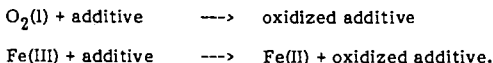
**ABSTRACT**

Previous work in this laboratory has involved studying the possibility of combined NO<sub>x</sub>/SO<sub>x</sub> scrubbing using various aqueous chemistries with a metal chelate additive. Recently, we have focused our work on the metal chelate ferrous\*EDTA. A major problem encountered in the practical application of ferrous\*EDTA is that the ferrous ion has been found to oxidize to the corresponding ferric species leading to a decrease of the NO<sub>x</sub> removal for the scrubbing solution containing the additive. We have found that addition of a polyphenolic compound leads to a sustained high NO<sub>x</sub> removal under various oxidizing conditions. We believe that the improved performance of ferrous\*EDTA is due to the known capabilities of these organic compounds to both inhibit oxidation of ferrous chelates by dissolved oxygen and to rapidly reduce any ferric ions back to the original ferrous species. These effects are illustrated by the chemical reactions shown below:



**INTRODUCTION**

The use of metal chelate additives in an aqueous scrubbing environment for combined NO<sub>x</sub>/SO<sub>2</sub> removal from oxygen-containing flue gases has been investigated in this laboratory for several years (1,2,3). Recent work with the metal chelate Fe(II)\*EDTA has shown initially high NO<sub>x</sub> removals which, however, decline with time as a function of the amount of oxygen gas in the feed gas stream. Because of this dependence on oxygen concentration in the feed gas, we have attributed the decline in NO<sub>x</sub> removal to the oxidation of the Fe(II)\*EDTA additive to the ferric form. One possible solution to this problem would be to add a secondary additive to the system which is either capable of preferentially reacting with any dissolved oxygen or capable of reducing any oxidized ferric species back to the ferrous form. These chemical reactions may be summarized simply as follows:



From an examination of previous work in the literature, we have found one class of compounds which is capable of performing both of the above stated reactions. Theis and Singer (4) found that certain polyphenolic compounds, which are products of natural vegetative decay, are capable of significantly affecting the rate of oxidation of ferrous iron. This study showed, for example, that an equimolar amount of tannic acid was able to maintain a ferrous iron concentration of  $5 \times 10^{-5}$  M unchanged for 7 days in the presence of 0.5 atm O<sub>2</sub>. Also phenols, such as gallic acid, are well-known antioxidants (5).

Because of the above stated properties of polyphenolic compounds, we have investigated the effect of tannic acid, pyrogallol, and gallic acid as secondary additives in aqueous scrubbing

systems containing the primary additive Fe(II)\*EDTA. Using these secondary additives, we have been able to maintain NO<sub>x</sub> removals as high as 60-65% for up to 2 hours.

#### EXPERIMENTAL SETUP

The complete experimental setup has been described previously (1,2). Some recent modifications to the scrubbing section have been made and are described herein. Figure 1 shows a flow diagram of the aqueous scrubber system that was used. One major modification is that a disk and donut scrubber having four (4) stages was used instead of the previously described flooded column. A sieve plate having 3/16" diameter holes with a total open area of 10.3% was placed at the bottom of the scrubber in order to provide the capability of having some liquid holdup in the column. Also, an approximately 10 liter holding tank was added to the system and connected to the bottom of the scrubber column. Circulation rates from the holding tank to the top of the scrubber could be varied from about 330-1420 ml/min. For the experiments described below, an average circulation rate of 890 ml/min was used. However, the circulation rate was varied in the range of 790-985 ml/min in order to maintain a fixed liquid level in the scrubber. All of the experiments discussed below were performed in a sodium, double-alkali chemistry by using a 0.31 M sodium carbonate solution.

Although the feed gas system is basically unchanged from that reported earlier (1,2), we have modified the procedure for preparing the simulated feed gas mixture. For the experiments to be reported, simulated feed gas was prepared by first setting the NO level at 450 ppm in the presence of carbon dioxide, oxygen, and nitrogen gases only. In all runs, the feed gas mixture contained 14.5% CO<sub>2</sub>, 5.4% O<sub>2</sub>, and N<sub>2</sub> as the balance. After the metering valve for the NO gas was set to give 450 ppm, a shut-off valve was closed and nitrogen dioxide was then set in the same CO<sub>2</sub>, O<sub>2</sub>, and N<sub>2</sub> mixture. Nitrogen dioxide is calculated as a difference between measured NO<sub>x</sub> and measured NO and except where noted below was set around 75 ppm. The preset amount of NO was then added to the nitrogen dioxide. Finally, sulfur dioxide was added to the feed gas mixture and adjusted to the desired level. This new feed gas preparation procedure has improved the reproducibility and reliability of our removal measurements compared to the previously used method (1,2). Except where noted, approximately 8% water vapor was also added to the simulated feed gas mixture.

#### RESULTS AND CONCLUSIONS

We note that all experimental comparisons in this paper are made using total NO<sub>x</sub> removal data. This is because we have observed that the presence (as in the feed stream) or absence (as in the effluent stream) of sulfur dioxide can alter the NO or (NO<sub>x</sub> - NO) value, but has little effect on the total NO<sub>x</sub> value. This "SO<sub>2</sub> effect" depends on the amount of unmixed nitrogen dioxide in the feed gas mixture and most likely arises from a gas phase reaction between SO<sub>2</sub> and NO<sub>2</sub>. Because of the relatively small amount of NO<sub>2</sub> that we are adding in our new feed gas preparation procedure, as described above, this effect is small. In fact, although we still consider NO<sub>x</sub> removals more reliable, in all cases discussed below, NO removals were never more than a few percent different from the reported NO<sub>x</sub> removals.

We first present our initial experiment which was performed with tannic acid as the secondary additive using the previously described flooded column scrubber (1,2). Figure 2 shows NO<sub>x</sub> removal for a baseline run with 0.24 moles of Fe(II)\*EDTA alone versus that of an identical run with the addition of 0.04 moles of tannic acid. This first try experiment showed a significant improvement in NO<sub>x</sub> removal from about 14% to about 40% in the stable portions of both curves. After this experiment, the scrubber column was changed from the flooded type to the disk and donut type described above.

Because of several problems with tannic acid, including the viscosity changes it caused, its high molecular weight, and its relatively high cost; we performed the remaining experiments with the polyphenolics pyrogallol and gallic acid. After trying several ferrous;polyphenolic

ratios, the most effective ratio was found to be approximately 1:1. This ratio of primary additive to secondary additive was used in all the experiments which follow.

Figure 3 compares  $\text{NO}_x$  removal for  $\text{Fe(II)*EDTA}$  alone versus that with pyrogallol as a secondary additive. This figure clearly demonstrates the declining  $\text{NO}_x$  removal with  $\text{Fe(II)*EDTA}$  alone versus the slightly increasing removal with pyrogallol. After 90 minutes,  $\text{NO}_x$  removal with pyrogallol was about twice that of  $\text{Fe(II)*EDTA}$  alone (64% vs 32%). The tests represented by this figure are the only ones in this paper which did not have moisture added to the feed gas stream. Figure 4 compares  $\text{NO}_x$  removals with pyrogallol for feed gas mixtures with and without added moisture.  $\text{NO}_x$  removal with added moisture was consistently about 6% greater than without added moisture. This effect is probably indicative of gas phase interactions of  $\text{NO}$  and/or  $\text{NO}_2$  with water vapor as discussed earlier (1).

The next three figures illustrate the effect on  $\text{NO}_x$  removal of various changes in the feed gas stream composition. Figure 5 compares  $\text{NO}_x$  removals with pyrogallol for feed gas mixtures containing 1500 ppm and 3000 ppm sulfur dioxide. Although  $\text{NO}_x$  removal was 9% higher, on average, with 3000 ppm sulfur dioxide; it is interesting to note that after two hours of scrubbing with 1500 ppm  $\text{SO}_2$ , the  $\text{NO}_x$  removal had increased to about 56% with no apparent peak. Figure 6 compares  $\text{NO}_x$  removals for feed gas mixtures with 0 ppm versus 75 ppm  $\text{NO}_2$  and 0 ppm versus 150 ppm  $\text{NO}_2$ , respectively. Figure 6a shows the removals were virtually identical for the first 90 minutes of each test; but for the last 30 minutes, the run with no  $\text{NO}_2$  showed removal about 4% higher than the test with 75 ppm  $\text{NO}_2$ . Figure 6b shows that the test with 150 ppm  $\text{NO}_2$  had slightly improved  $\text{NO}_x$  removal for the 10 - 90 minute interval (about 3%); but, again as in Figure 6a, the run with no  $\text{NO}_2$  had a removal about 3% higher for the last 30 minutes. The point to be stressed here is that  $\text{NO}_2$  levels of 0-150 ppm make relatively little difference on total  $\text{NO}_x$  removal.

Finally, Figure 7 compares  $\text{NO}_x$  removals for the secondary additives gallic acid and pyrogallol under identical conditions. While  $\text{NO}_x$  removal with pyrogallol was slightly better in the 20 to 80 minute interval (3% higher on average), after 80 minutes their performances were comparable.

#### ACKNOWLEDGMENT

This work is supported by the U.S. Department of Energy, Assistant Secretary for Fossil Energy, under contract W-31-109-ENG-38, through the Pittsburgh Energy Technology Center (PETC). The authors wish to acknowledge the support provided by Perry Bergman and Charles Drummond of the PETC. In addition, the authors express their deep appreciation and gratitude to Sherman Smith for his invaluable contributions on the modifications and maintenance of the experimental apparatus as well as on the performance of the tests described herein.

#### REFERENCES

1. Harkness, J.B.L. and Doctor, R.D., Development of Combined Nitrogen Oxide/Sulfur Oxide Environmental-Control Technology, Argonne National Laboratory Report ANL/ECT-14, Argonne, Ill. (Aug. 1985) (also available through NTIS).
2. Harkness, J.B.L. and Doctor, R.D., Simultaneous  $\text{NO}_x/\text{SO}_x$  Removal In Aqueous Scrubber Chemistries, American Institute of Chemical Engineers National Meeting, New Orleans, La., April 1986.
3. Harkness, J.B.L., Doctor, R.D., and Wingender, R.J., U.S. Patent No. 4,612,175 (1986).
4. Theis, T.L. and Singer, P.C., Environ. Sci. Technol., 8, 569 (1974).
5. Loginova, L.F., Medyntsev, V.V., and Khomutov, B.I., Zh. Obsh. Khim., 42, 739 (1972).



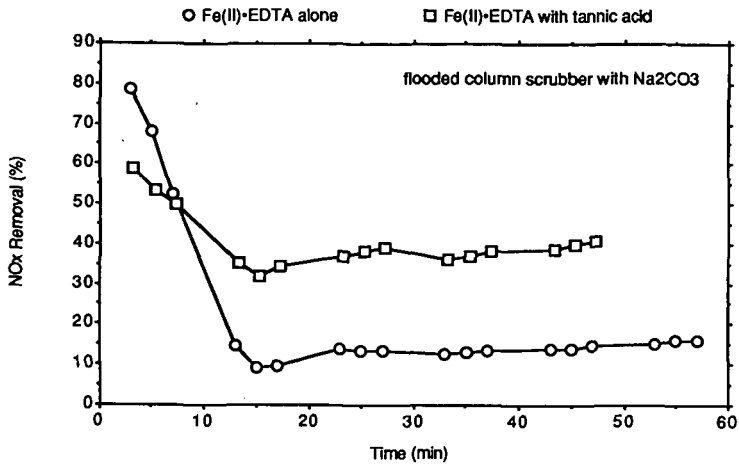


Figure 2. NO<sub>x</sub> removal for Fe(II)-EDTA alone vs Fe(II)-EDTA with tannic acid

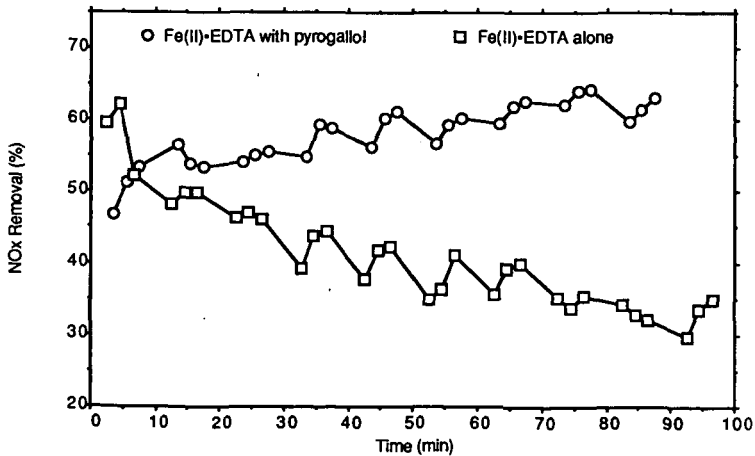


Figure 3. Comparison of NO<sub>x</sub> removals with or without the secondary additive pyrogallol

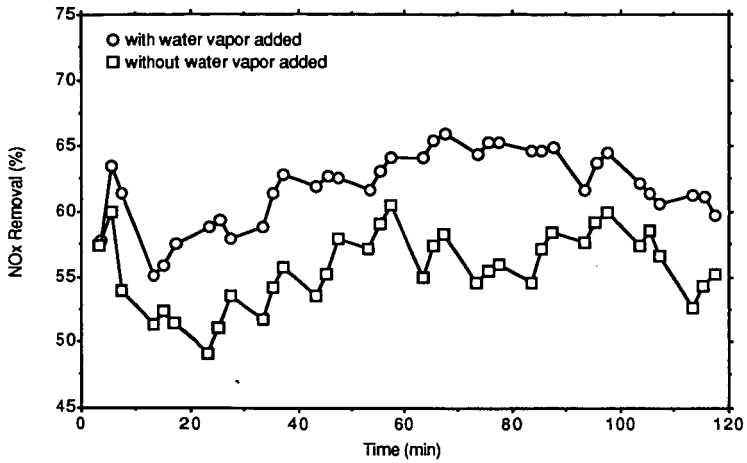


Figure 4. Comparison of NOx removal for Fe(II)-EDTA and pyrogallol with or without moisture

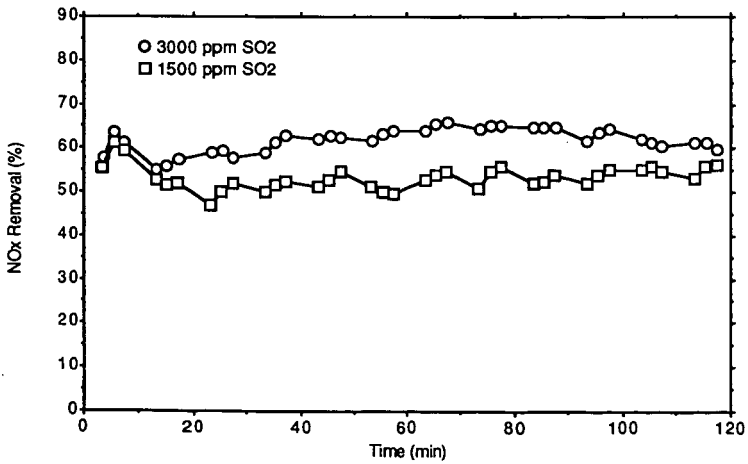
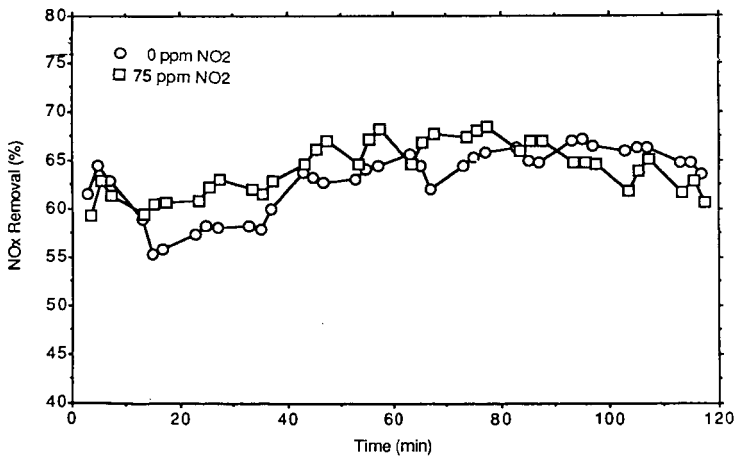
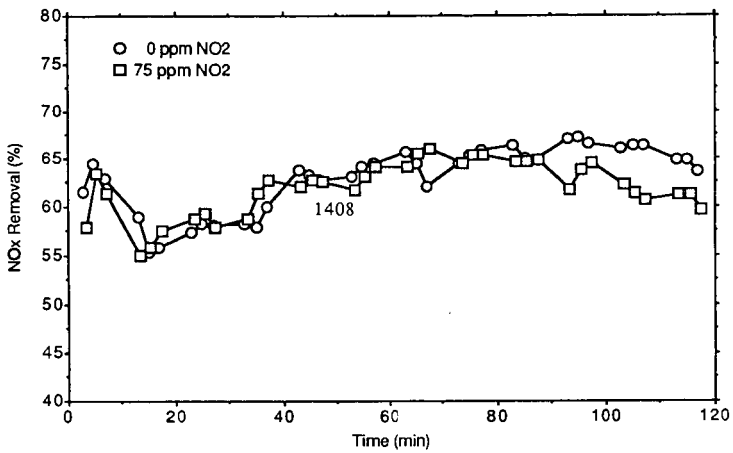


Figure 5. Comparison of NOx removal for Fe(II)-EDTA and pyrogallol with different SO2 levels



Figures 6a. and b. Comparison of NOx removals for three different NO2 levels

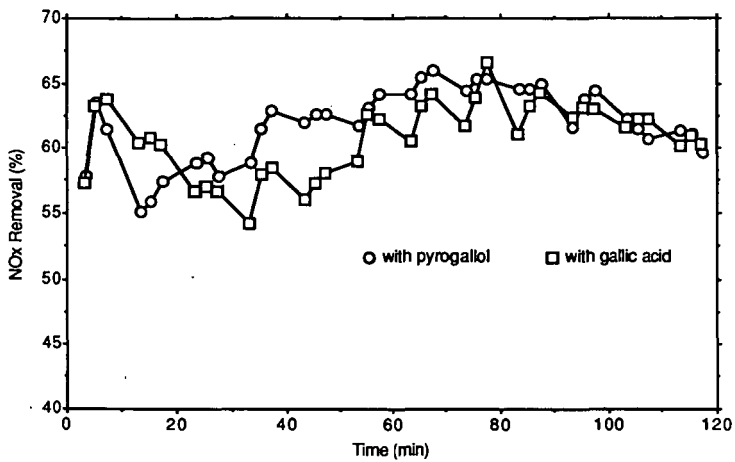


Figure 7. NOx removal comparison for secondary additives pyrogallol and gallic acid

## IN-SITU X-RAY ABSORPTION STUDIES OF A $\text{CuO}/\text{Al}_2\text{O}_3$ SORBENT DURING $\text{SO}_2$ REMOVAL FROM COAL FLUE GASES

Yuqun Cao<sup>1</sup> and Pedro A. Montano<sup>1,2</sup>

1) Department of Physics, Brooklyn College of CUNY, Brooklyn, NY 11210

2) Department of Physics, West Virginia University, Morgantown, WV 26506

**Keywords:** X-ray absorption, copper oxide sorbent, coal cleaning

### ABSTRACT

We have studied the local structure around the Cu ion in a  $\text{CuO}/\text{Al}_2\text{O}_3$  sorbent using X-ray absorption (XAS). This sorbent is commercially used for the removal of sulfur dioxide from flue gases. Pure oxides of CuO and  $\text{Cu}_2\text{O}$  were also studied as a function of temperature and in the presence of flue gases. The pure oxides were used as standards. The XANES and EXAFS spectra for the sorbent in nitrogen gas at the same temperatures did not show any significant changes. By contrast, we observed the appearance of a new near edge feature in the XANES spectra of the sorbent in the presence of flue gases. A strong peak appears at an energy characteristic of monovalent copper. The amount of  $\text{Cu}^+$  reaches a maximum at about 200C and then decreases at higher temperatures. It is noted that the EXAFS spectra do not show any significant change in the nearest neighbors distance during reaction with the flue gases.

### INTRODUCTION

The removal of sulfur dioxide from the coal flue gases is one of the major tasks in the electrical power industry. The deleterious effect of the pollutants resulting from the combustion of coal is a great concern in contemporary society. A common industrial practice is the use of a sorbent for the capture of the flue gas pollutants [1,2]. Copper oxide supported on alumina is commonly used as a commercial sorbent. This sorbent is used to remove  $\text{SO}_2$  from the coal flue gases. Our major interest in this study is to investigate the Cu local environment in the presence of the flue gases. It is important to understand the undergoing processes in order to facilitate a most efficient use of the sorbent. The chemical environment at the transition metal site can be better studied using XAS, because of the penetration capabilities of X-ray in-situ studies become possible. X-ray Absorption Fine Structure (EXAFS) and X-ray Absorption Near Edge Structure (XANES) have been used in recent years to study local structures [3,4,5]. We report here a series of in situ EXAFS and XANES measurements of a  $\text{CuO}/\text{Al}_2\text{O}_3$  sorbent and model compounds. We investigated the evolution of the structure at the Cu site as a function of temperature in the presence or absence of flue gases. In the following paragraphs we describe the methodology employed and summarize the results of our measurements.

### EXPERIMENTAL

The measurements were carried out at beamline X-18B at the National Synchrotron Light Source. The beamline is equipped with a double crystal monochromator. The two crystal monochromator has the advantage that the exit beam path is fixed [6]. Two ion chambers are used to measure the incident and transmitted beam intensities. They were

filled with 30 KPa of Ar. A third ion chamber is placed at the end of the second ion chamber with a thin Cu foil to obtain accurate energy calibrations. The data collecting procedure is automatic and controlled by a PDP 11/24 computer. The energy range covered in these measurements was 200 eV below and 1200 eV above the Cu K-edge ( $E=8.979$  KeV). The experimental setup is schematically shown in Fig. 1. The sample chamber has two windows sealed with thin Capton films to let the X-ray beam go through. The flue gas passes through the sorbent in the chamber. A Chromel/Alumel thermocouple is attached to the sample holder for temperature monitoring. A variable transformer and a temperature controller are used for setting up the desired sorbent temperature. The coal is burned in a separate combustion chamber. It has an inlet for air and an outlet for the flue gas. A thermocouple is used here to measure the combustion temperature. We burned a West Virginia Blacksville #2 coal. This coal sample has 3.4% by weight of total sulfur (organic and inorganic). The sorbent sample used in this measurement is  $\text{CuO}/\text{Al}_2\text{O}_3$ . The fresh sample is in the form of small sphere of 2mm in diameter. The sample is made into powder right before the measurement and put into the sample cell. The sample cell is a 0.5mm aluminum plate with a 5mmx15mm hole in the center. The powder is sandwiched between two thin aluminum foils. On the aluminum foils a matrix of tiny pinholes are punched to allow the flue gases to go through the sorbent. Careful measurements on the effects of the aluminum foils were conducted before we began collecting data. It is found out that the aluminum foil we used here does not have side effects to the XANES. However, it contains a very small amount of zinc impurities which can be seen on the EXAFS spectrum 680 eV above the Cu K-edge. In figure 2 we show the raw EXAFS data for the sorbent at room temperature. The measurements were performed from room temperature to 400C. The sample were measured in nitrogen gas flow and in the presence of flue gases. The measurements were repeated several times in order to evaluate their reproducibility. The same set of measurements were performed using model compounds, pure copper oxides ( $\text{Cu}_2\text{O}$  and  $\text{CuO}$ ) and  $\text{CuSO}_4$  and is shown in Fig. 3. The data was analyzed using the conventional methods described in the literatures [3,4].

## RESULTS AND DISCUSSION

We choose the maximum of the 1st derivative of Cu metal foil at the K absorption edge as  $E_0$ . All the energy values are given with respect to this  $E_0$ . The most prominent energy peaks of the samples are given in Table 1. The XANES of the copper compounds consists two parts: (1) the discrete part below the continuum threshold, where the weak features are usually called pre-edge peaks, due to transitions to unoccupied bound antibonding orbitals and (2) the continuum part where the peaks are due to multiple-scattering of the photoelectron, which are sensitive to both coordination geometry and interatomic distances [4,7,8,9]. The K-edge XANES of Cu primarily represents electric dipole transitions ( $E1$ ) from the 1s core level to final states with nonzero np components, which are governed by the electronic structure of the material [8,9,10]. Peak P corresponds to the 1s  $\rightarrow$  3d transition and peak A corresponding to the 1s  $\rightarrow$  4p transition. The absence of peak P for Cu metal and  $\text{Cu}_2\text{O}$  is attributed absence of vacancies in the 3d orbitals.

The XANES spectra and its 1st derivative for the sorbent at various temperatures before reaction with flue gases are shown in Fig. 4. There is no noticeable change when the temperature is raised to 300C from RT and then back to RT. Comparing the peak positions

with that of the CuO standard, the first major peak A shifts from 5.0 eV to 6.0 eV, the second one, B at 12.0 eV does no change and the third peak C at 17.5 eV does not exist. The EXAFS of the sorbent is significantly different from that of the CuO standard. We identify the first shell as due to Cu-O bond. The higher order shells ( 2nd, 3rd and 4th ) are not clearly seen in the Fourier transform of the  $k^3X(k)$  ( Fig. 5 ). This makes us believe that the CuO in the sorbent is in highly dispersed form, very small clusters. The Cu-O interatomic distance is almost the same as that in bulk CuO. The magnitude of the Fourier transform of the 1st shell decreases with temperature (Fig. 6 ). This is understood to be related to thermal effects on the interatomic vibrations.

The most significant change happens when the sorbent is exposed to the flue gases (Fig. 7 ). A peak S at 1.5 eV characteristic of  $Cu^+$  begins to appear. It reaches a maximum at about 200C. This feature disappears when the sample is returned to RT. For temperatures in excess of 300C there is a remnant small peak at about 1.5 eV. The remaining XANES features are the same as those before reaction with the flue gases. The new peak indicates that  $Cu^+$  is formed during the  $SO_2$  removal process. 200C seems to be an optimal temperature for the formation of this intermediate species. At this stage the reaction product is unlikely to be  $CuSO_4$ . The XANES spectrum of  $CuSO_4$  is different from the sorbent. We suggest that the following process is taking place,



The  $SO_2$  molecules are chemically absorbed by the CuO clusters. The Cu is in a mixed state of  $Cu^{++}$  and  $Cu^+$ . The EXAFS amplitudes also have a consistent change. It decreases with the increasing temperature until 200C then increases at higher temperature ( Fig. 6 ). The magnitude also recovers at RT after the reaction. Table 2 shows the ratio of the oxygen coordination number surrounding Cu ion,  $N_{CuO}/N_{Sorbent}$ , and the deviation of the sorbent Debye-Waller factor from that of CuO. This gives us information on how the average oxygen coordination number around the Cu ion changes with temperature. The average oxygen coordination number for the sorbent becomes minimum at 200C. Our XANES measurements show strong evidence of mixed charge states (  $Cu^{++}$  and  $Cu^+$  ).

## CONCLUSIONS

We have measured XANES and EXAFS spectra of a commercial sorbent ( $CuO/Al_2O_3$ ) used for the removal of  $SO_2$  from coal flue gases. The studies shows that CuO in the sorbent is in the form of very small disordered clusters. The sorbent is thermally stable from RT to 400C in the nitrogen atmosphere. We observed a partial transformation of  $Cu^{++}$  to  $Cu^+$  at 200C This happens only when the flue gases are present. The observed transformation is reversible if the temperature of the sorbent does not exceed 300C. Our result suggests that at 200C optimum conditions exist for the formation of this intermediate species.

## ACKNOWLEDGMENT

We would like to express our appreciations to A. Bommannavar and M. Ramanathan for their help. This work was supported by the US DOE and Y. Cao acknowledge the financial support of the Division of Educational Program at Argonne National Laboratory .

## REFERENCE

1. D.H. McCrea, A.J. Forney, J.G. Myers, J. Air Pollut. Control Assoc. 20, 819 (1970)
2. Sidney S. Pollack, William P. Chisholm Richard T. Obermyer, Sheila W. Hedges, Mohan Ramanathan, and Pedro A. Montano, I&EC Research, 27, 2276 (1988).
3. B.K. Teo, *EXAFS : Basic Principles and Data Analysis* (Springer, 1986).
4. *X-ray Absorption : Principles, Applications, Techniques of EXAFS, SEXAFS, and XANES*. edited by D.C. Konigsberger and R. Prinz, Chemical Analysis, Vol. 92 (1988).
5. R.B. Greeger, F.W. Lytle, E.C. Marques, E.M. Larson, A.J. Panson, and J. Stohr in *Electronic Materials and Processes*, edited by J.T. Hoggatt, W. Jensen, M. Kushner, and S. McCollough, 2nd international Sample Electronics Conference Series, Vol 2, P.179 (June 1988).
6. M. Ramanathan, PhD thesis, *X-ray Absorption Study of the Interaction of Coal Combustion Gases with Calcium Oxide*, 1988.
7. A. Bianconi, E. Fritsch, G. Calas, and J. Petiau, Phys. Rev. B32, P.4292 (1985).
8. L.S. Kau, D.J. Spira-Solomon, J.E. Penner-Hahn, K.O. Hodgson, and E.I. Solomon, J. Am. Chem. Soc. 109, 6433 (1989).
9. F.W. Lytle, R.B. Greeger, and A.J. Panson, Phys. Rev. B37, P.1550 (1988).
10. E.E. Alp, G.K. Shenoy, D.W. Capone II, L. Soderholm, H.B. Schuttler, J. Guo, D.E. Ellis, P.A. Montano, and M. Ramanathan, Phys. Rev. B35, P.7199 (1987).

Table 1 Characteristic Energies of the XANES (Unit is in eV)

|                   | P    | A   | B    | C    | D    |
|-------------------|------|-----|------|------|------|
| Cu                | —    | 0.0 | 6.0  | 11.0 | 22.0 |
| Cu <sub>2</sub> O | —    | 1.5 | 6.0  | —    | —    |
| CuO               | -1.5 | 5.0 | 12.0 | 17.5 | —    |
| CuSO <sub>4</sub> | -2.5 | 9.0 | 14.5 | —    | —    |
| Sorbent           | -3.5 | 6.0 | 12.0 | —    | —    |

Table 1. Characteristic XANES energies for the samples in this experiment.

Table 2

|                     | Temp | N <sub>CuO</sub> /N <sub>Sorbent</sub> | ΔDW (Å) |
|---------------------|------|--|---------|
| Sorbent<br>Only     | RT   | 0.62                                   | 0.058   |
|                     | 100C | 0.59                                   | 0.060   |
|                     | 200C | 0.68                                   | 0.062   |
|                     | 300C | 0.68                                   | 0.067   |
|                     | RT   | 0.62                                   | 0.058   |
| Sorbent<br>Flue Gas | RT   | 0.72                                   | 0.063   |
|                     | 100C | 0.82                                   | 0.065   |
|                     | 200C | 0.89                                   | 0.064   |
|                     | 300C | 0.77                                   | 0.064   |
|                     | RT   | 0.70                                   | 0.061   |

Table 2. The ratio of the average oxygen coordination number surrounding the Cu ion, N<sub>CuO</sub>/N<sub>Sorbent</sub>, and the deviation of the Debye-Waller factor from that of CuO, ΔDW, obtained by the ratio method of EXAFS.

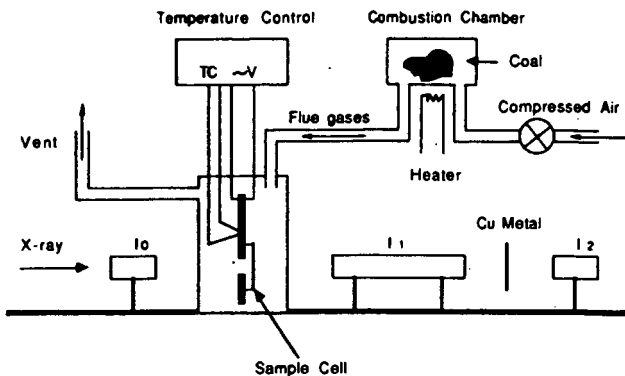


Fig. 1. Schematic drawing of the experimental setup inside the experiment hutch.

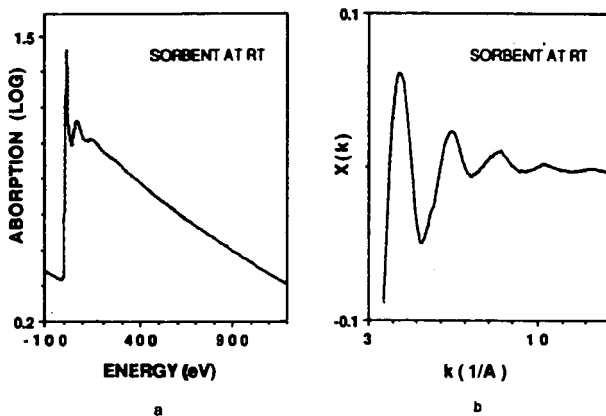


Fig. 2. a. EXAFS of the Sorbent at RT before the reaction.  
 b.  $X(k)$  after the EXAFS background subtraction and step height normalization.

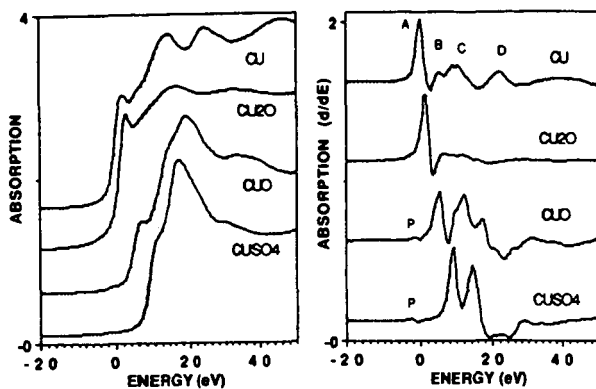


Fig. 3. XANES and 1st derivatives of pure  $\text{Cu}_2\text{O}$ ,  $\text{CuO}$  and  $\text{CuSO}_4$ .

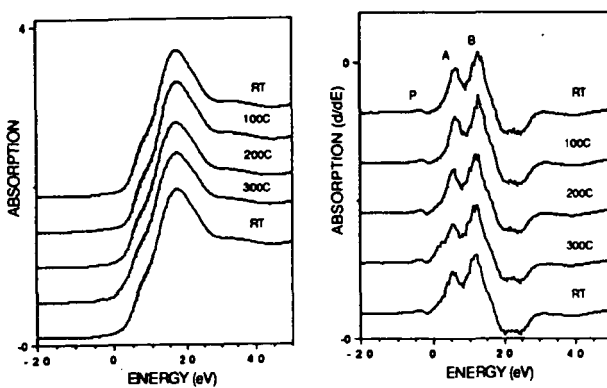


Fig. 4. XANES and 1st derivatives of the Sorbent at various temperatures under the  $\text{N}_2$  environment.

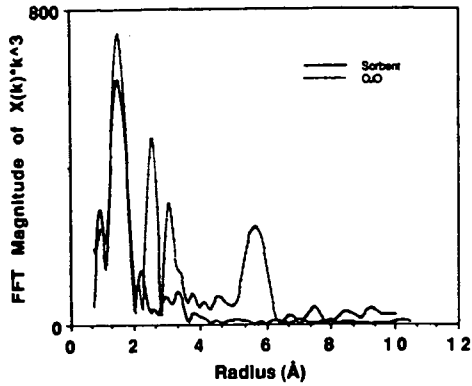


Fig. 5. Fourier transforms of the  $k^3X(k)$  for the pure CuO and the sorbent at RT.

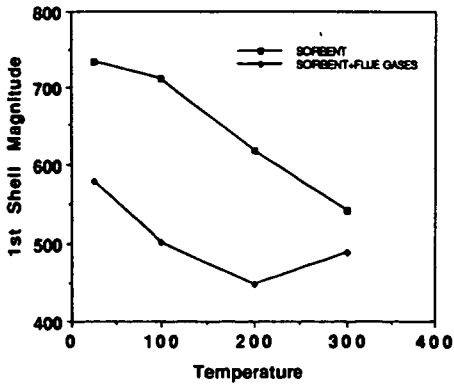


Fig. 6. Comparison of the 1st shell magnitude changes with the temperature for the sorbent with and without the flue gases.

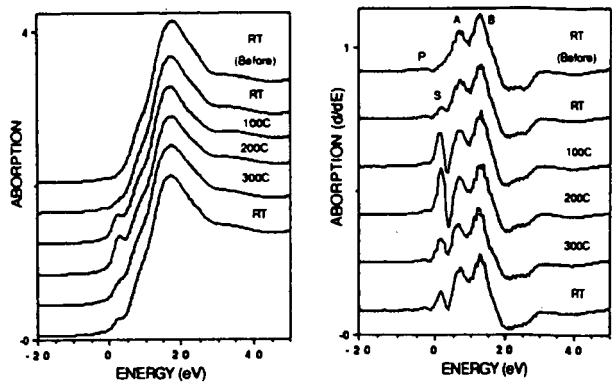


Fig. 7. XANES and 1st derivatives of the Sorbent at various temperatures in the presence of flue gases.

## HIGH-SURFACE-AREA HYDRATED LIME FOR SO<sub>2</sub> CONTROL

M. Rostam-Abadi, D. L. Moran, Illinois State Geological Survey, Champaign, IL  
V. P. Roman, R-C Environmental Services and Technologies, Irvine, CA  
H. Yoon and J. A. Withum, Consolidation Coal Company, Library, PA

**KEYWORDS:** SO<sub>2</sub> removal, hydrated lime, dry sorbent injection

### INTRODUCTION

For many site specific applications, dry sorbent injection technologies offer advantages over the wet flue gas desulfurization systems for controlling the emissions of SO<sub>2</sub> produced during combustion of high sulfur coal. These potential advantages include ease of retrofit, dry waste, and lower capital investment. The technologies that have been researched considerably in recent years include furnace sorbent injection (FSI), boiler economizer injection, and post furnace duct-injection/humidification (Coolside). The main factor which distinguishes the dry processes is that a calcium-based sorbent is injected into different locations within a pulverized coal boiler unit. In the FSI, limestone (CaCO<sub>3</sub>) or hydrated lime (Ca(OH)<sub>2</sub>) is injected into the upper furnace cavity where temperatures range from 1800-2200°F. The sorbent is rapidly calcined forming CaO which reacts with SO<sub>2</sub> to form CaSO<sub>4</sub>. In the boiler economizer process, Ca(OH)<sub>2</sub> is injected in a location between the superheater and air preheater where the temperature is in the range of 800-1200°F.<sup>1</sup> Coolside desulfurization involves Ca(OH)<sub>2</sub> injection in the duct work downstream of the air preheater at about 300°F followed by flue gas humidification with a water spray.<sup>2</sup> SO<sub>2</sub> is removed by the entrained sorbent particles in the duct work and by the dense sorbent bed collected in the particulate removal system. Unlike the FSI where CaSO<sub>4</sub> is formed, under boiler economizer and Coolside conditions CaSO<sub>3</sub> is the major product.

Bench- and pilot-scale tests have shown that typical SO<sub>2</sub> capture efficiencies under FSI conditions are about 35 and 55% for CaCO<sub>3</sub> and commercial Ca(OH)<sub>2</sub>, respectively,<sup>3,4</sup> and 30-50% with commercial Ca(OH)<sub>2</sub> under boiler economizer and Coolside conditions<sup>6</sup> (all at Ca/S ratio of 2). In some Coolside process pilot tests, an additive such as sodium hydroxide or sodium carbonate has been injected with the humidification water resulting in SO<sub>2</sub> removal of about 70 to 80%.<sup>6, 11</sup> Because these SO<sub>2</sub> removal levels correspond to less than 50% of the theoretical saturation capacity for the sorbents, a major objective of research in the recent years has been to identify sorbent properties that result in enhanced SO<sub>2</sub> capture in order to reduce operating costs and the amount of waste products. In FSI studies, the superiority of Ca(OH)<sub>2</sub> over CaCO<sub>3</sub> has been attributed to the smaller mean particle size,<sup>5</sup> higher surface area and porosity,<sup>8</sup> larger pores<sup>9</sup> and plate-like grain structure<sup>10</sup> (vs. sphere-like) of the CaO derived from Ca(OH)<sub>2</sub> compared to that derived from CaCO<sub>3</sub>. In boiler economizer and Coolside studies, improved SO<sub>2</sub> removal performance has also been reported for Ca(OH)<sub>2</sub> with high porosity, high surface area, and small particle size.<sup>1,5,11</sup>

This paper reviews recent work comparing the SO<sub>2</sub> removal performance of two commercial hydrated limes and a high-surface-area (HSA) hydrated lime under FSI, boiler economizer, and Coolside conditions. The properties of the sorbents and a discussion of the results are presented.

### EXPERIMENTAL

#### Test Sorbents

The sorbents tested included a HSA hydrate and two commercial hydrated limes designated as A and B. The HSA hydrate and commercial hydrate A were made from the same lime. The HSA hydrated lime was prepared by a proprietary hydration process developed at the

Illinois State Geological Survey. Three hundred pounds of the sorbent was prepared using a bench-scale hydrator capable of producing seven pounds of products per batch. The HSA hydrate was not subjected to air classification or milling prior to being tested for sulfur removal efficiency.

Chemical compositions of sorbents were determined by X-ray fluorescence. Surface areas were obtained by  $N_2$ -adsorption in conjunction with the one point BET method. Pore volumes and pore size distributions (pores smaller than 0.25 micrometers) were determined by nitrogen porosimetry. Sorbent particle size analyses were performed on a Micromeritics sedigraph 5100 using Micromeritics dispersant. Hydrate A and the HSA hydrate were examined by X-ray diffraction (XRD) and the data were used for determination of crystallite size using the Scherrer equation.<sup>12</sup>

#### Pilot-Scale $SO_2$ Removal Tests

FSI tests - These experiments were performed in the Innovative Furnace Reactor (IFR) located at the U. S. Environmental Protection Agency, Research Triangle Park, North Carolina.<sup>13</sup> FSI tests were performed burning four Illinois coals from the Illinois Basin Coal (IBC) Sample Program. The analyses of the coals identified as IBC-101, -102, -106 and -109 are presented in table 1.

Testing in the IFR consisted of determining the  $SO_2$  concentration in the flue gas during sorbent injection while burning each of the coals at feed rates sufficient to yield a thermal rating of approximately 14 kW. The tests were conducted with HSA hydrate and hydrate A at Ca/S ratios of approximately 1:1 and 2:1 and at a temperature of 2192°F. The details of test procedures and a description of the IFR are given elsewhere.<sup>13</sup>

Boiler economizer tests - The Research-Cottrell Environmental Services and Technologies (R-C EST) 150 kw pilot-scale furnace located in Irvine, California was used for boiler economizer tests. The experiments were conducted at a nominal input rate of 75 kw. A detailed description of the unit is given elsewhere.<sup>5</sup> The furnace is fired on natural gas and  $SO_2$  is added at the proper concentration. A time-temperature history representative of a utility boiler backpass is generated by using the upper section of the furnace to reduce the flue gas temperature to approximately 1300°F. The gas temperature is then decreased from 1300 to 800°F in approximately 0.5 seconds in the section of the furnace where convective tube banks are located. The flue gas is continuously analyzed for oxygen, sulfur dioxide and carbon dioxide using the R-C EST continuous emissions monitor (CEM).

The test program involved testing HSA hydrate and hydrate A at injection temperatures of 900, 1000 and 1100°F, a Ca/S ratio of 2, and  $SO_2$  concentrations of 500 and 3000 ppm. The flue gas composition was typically 4.0%  $O_2$ , 9.8%  $CO_2$ , and 50 ppm CO.

Coolside tests - These tests were conducted in a 100 kW pilot unit located in the Research and Development Department of the Consolidation Coal Company, Liberty, Pennsylvania. The Coolside pilot plant is described elsewhere.<sup>2</sup> Briefly, the exhaust from a natural gas burner is mixed with recycle gas, into which  $CO_2$ ,  $SO_2$ ,  $N_2$ , steam and fly ash are injected to produce the simulated flue gas from a coal-fired boiler. The humidifier is an 8.3-inch ID down-flow duct installed with a water-spray nozzle, and is 20 feet long from the nozzle location to the exit. The gas exiting the humidifier enters a baghouse which separates the solids from the gas. The gas is further cooled and dehumidified in a condenser, and the process fan recycles most of the flue gas for reuse.  $SO_2$  removal is calculated from measurements of  $SO_2$  and  $O_2$  analyzers at the humidifier inlet and exit, and the baghouse exit.

HSA hydrated lime and hydrate B were tested at Ca/S ratios of 0.5 to 2.0 and 25°F approach to adiabatic saturation temperature. The conditions selected represent standard pilot plant tests for evaluating a new sorbent to provide SO<sub>2</sub> removal data at typical Coolside in-duct injection operating conditions. The common conditions were 300°F inlet flue gas temperature, 1500 ppm inlet SO<sub>2</sub> content (dry basis), and 125°F adiabatic saturation temperature. The flue gas flow rate was set at 175 scfm, which provided a 2.0 sec humidifier residence time.

## RESULTS AND DISCUSSION

### Test Sorbents

The chemical and physical properties of hydrates A and B, the HSA hydrate and lime A (from which hydrate A and the HSA hydrate were made) are presented in table 2. In the FSI and boiler economizer systems, the HSA hydrated lime was tested against the hydrate A. However, in the Coolside tests, HSA hydrate was tested against hydrate B, since this material has been shown to be the best-performing commercial sorbent under Coolside conditions.

Chemical analyses of hydrated limes indicate that the sorbents contained over 96 wt% CaO after ashing. The mass mean diameters and surface areas of the HSA hydrated limes varied between 1.6 and 2.7 micrometers and 35 to 44 m<sup>2</sup>/g (except for one batch which was 31 m<sup>2</sup>/g), respectively, depending on the hydration batch. These samples, however, had surface areas well above the 20-23 m<sup>2</sup>/g surface areas typical for commercial hydrates. The pore volume of the HSA hydrate was 0.35 cm<sup>3</sup>/g compared to only 0.08 cm<sup>3</sup>/g for its commercial counterpart. The XRD results showed that the HSA hydrate had smaller Ca(OH)<sub>2</sub> grain size and lower crystallinities when compared to commercial material.

### Pilot-Scale SO<sub>2</sub> Removal Tests

FSI tests - The results for FSI tests are presented in table 3. The average baseline SO<sub>2</sub> concentrations under the test conditions were 3140 ppm for IBC-101, 2410 ppm for IBC-102, 2890 ppm for IBC-106 and 1000 ppm for IBC-109. The trend in the SO<sub>2</sub> concentration is consistent with the total sulfur content of the coals reported in table 1. Figure 1 shows the estimated SO<sub>2</sub> removal percentages at Ca/S ratio of 2. The values were calculated by extrapolating linearly from the mean removals at both Ca/S ratios run for each coal/sorbent combination. For each coal tested, HSA hydrate removed more SO<sub>2</sub> than its commercial counterpart. SO<sub>2</sub> removal observed with the HSA hydrate ranged from 72 to 77% for the coals tested (excluding IBC-102) compared to 55 to 66% for hydrate A.

The SO<sub>2</sub> capture levels for the IBC-102 coal were only 57 and 42% with the HSA and commercial hydrates, respectively. The substantial decrease in SO<sub>2</sub> capture by the sorbents for this coal could be related to its higher pyritic sulfur content than for the other coals tested. The pyritic/organic sulfur ratio for IBC-102 was 2.3:1 compared to values less than 1:1 for the other coals. One explanation that could be offered is that a major fraction of the organic sulfur in coals is released as H<sub>2</sub>S in the initial stages of the combustion and is rapidly captured by the fresh sorbent. The SO<sub>2</sub> released by the oxidation of the pyrite, which follows the pyrolysis stage, then reacts with the partially utilized sorbent at a much slower rate compared to the H<sub>2</sub>S reaction.<sup>16</sup> Therefore, sulfur capture by the sorbent is lowered when coal with a high concentration of pyritic sulfur is burned. This suggests that FSI is most beneficial for coals that are high in organic sulfur which cannot be removed by physical coal cleaning.

The enhanced performance of the HSA hydrate could be related to its smaller particle size and higher initial surface area. Laboratory tests conducted under FSI conditions at 2012°F with CaO derived from Ca(OH)<sub>2</sub> have revealed that the CaO conversion to CaSO<sub>4</sub> is inversely related to particle diameter to the 0.2 to 0.35 power<sup>7</sup>. In a recent study, however, the initial sulfation rate of CaO (7 to 100 micrometers) derived from several limestones and dolomites varied roughly inversely with the particle size, indicating pore diffusion was the rate controlling step under these test conditions (1650°F). Based on the data obtained in this work, SO<sub>2</sub> capture was inversely related to particle size to the 0.44 power (for capture values estimated at Ca/S ratios of 1 and 2).

The higher SO<sub>2</sub> capture of the HSA hydrate can also be attributed in part to its favorable pore structure. Pore volume analyses of raw sorbents, shown in figure 2, indicate the volume of pores between 0.01 and 0.1 micrometers (10 and 100 nm) is substantially higher for the HSA hydrate than for hydrate A. Pore volumes of hydrated limes are expected to correlate with pore volumes of the corresponding calcines. Due to the increase in molar volumes when converting from CaO to CaSO<sub>4</sub> (16.9 vs 46.0 cm<sup>3</sup>/mole), pore plugging is known to limit the sulfation reaction. Therefore, sorbents with a high volume of larger pores are expected to capture more SO<sub>2</sub>.

Boiler economizer tests - The results of these experiments are shown in figure 3. The HSA hydrate showed significantly greater SO<sub>2</sub> removals than hydrate A at all test conditions. The SO<sub>2</sub> reduction achieved with the HSA hydrate at 3000 ppm SO<sub>2</sub> and Ca/S of 2 was 58% at 900°F, 57% at 1000°F and 52% at 1100°F compared to only 32%, 30% and 28% for the commercial hydrate. At 500 ppm SO<sub>2</sub> and Ca/S ratio of 2, the average SO<sub>2</sub> removals for hydrate A and the HSA hydrate were 6.1 and 17%, respectively (an increase of 180%). The SO<sub>2</sub> removals observed for the HSA hydrate were also higher than for other commercial hydrates examined under similar test conditions.<sup>5</sup>

The superior performance of the HSA hydrate observed in this study is attributed, in part, to its high surface area and small particle size. The role of surface area and particle size can be explained in terms of two competing reactions under boiler economizer conditions,



The intrinsic rates (which are related to pore surface area of sorbent) of reactions (1) and (2) are very fast even at 900°F. However, because of the low concentration of SO<sub>2</sub> in the flue gas, reaction (1) is controlled by bulk diffusion of SO<sub>2</sub> for particles larger than 5 micrometers<sup>1,3</sup> (diffusion rate for spherical particles is inversely related to particle size to the second power), whereas reaction (2) is controlled by intrinsic rate. As a result, the relative rates for the reaction of CaSO<sub>3</sub> and CaCO<sub>3</sub> depend both on pore surface area and particle size of the sorbent. Increasing pore surface area would favor the carbonation reaction if particle diameter is held constant. Decreasing particle size and holding pore surface area constant would favor desulfurization reaction. Therefore, a sorbent with high pore surface area and small particle size would be expected to show high SO<sub>2</sub> removal efficiency under boiler economizer conditions. The average increase in sulfur capture observed for the two sorbents at 3000 ppm SO<sub>2</sub> and Ca/S ratio of 2 was 83%, which corresponds approximately to the difference in surface areas. However, at 500 ppm SO<sub>2</sub> and Ca/S ratio of 2, SO<sub>2</sub> captures were inversely related to particle diameter to the second power, indicating bulk diffusion limitation under these test conditions.

Coolside tests - Three different batches of HSA hydrate were examined in the Coolside pilot unit. The surface areas of the samples tested at Ca/S ratios of 0.54, 1.1 and

2.1 were 31, 34 and 39 m<sup>2</sup>/g, respectively. Figure 4 shows the effect of the Ca/S molar ratio on SO<sub>2</sub> removal at 25°F approach to saturation. The value shown for hydrate B at 2.1 Ca/S was obtained in this study. The removals shown for the same hydrate at 1.0 and 1.5 Ca/S are from Reference 2. The HSA hydrated lime showed higher SO<sub>2</sub> removals than the best-performing commercial hydrate. With the HSA hydrate at Ca/S ratios of 0.54, 1.1 and 2.1, the SO<sub>2</sub> removals were 15, 25 and 46% in the humidifier and 18, 33 and 56% across the entire system (humidifier + baghouse). Comparison of the data at Ca/S of 2.1 indicate that the HSA sorbent captured 35% more SO<sub>2</sub> than hydrate B in the humidifier and 15% more across the entire system. The maximum percent calcium utilizations for the HSA hydrate were 33.3, 31.7 and 26.3 as Ca/S ratio increased from 0.54 to 2.1. For hydrate B a 23.2% utilization was observed at Ca/S ratio of 2.1.

Figure 4 shows a linear SO<sub>2</sub> removal behavior at the Ca/S ratios tested. Normally, as is exhibited by hydrate B, a plot of SO<sub>2</sub> removal vs Ca/S ratio is curved because the effect diminishes as the Ca/S ratio increases. The straight-line behavior for the HSA hydrate may be due to the sample surface area variations mentioned above.

The Coolside data suggest that a major fraction of the SO<sub>2</sub> capture occurred during the two second residence time in the duct work. The higher SO<sub>2</sub> capture achieved by the HSA hydrate in the humidifier section and across the entire system suggests higher overall activity of the sorbent relative to hydrate B.

#### SUMMARY AND CONCLUSIONS

The HSA hydrated lime prepared by a proprietary process had considerably higher surface area and porosity, smaller particle size, and finer Ca(OH)<sub>2</sub> grain size than typical commercial hydrated lime. The results of the pilot-scale testing under FSI, boiler economizer, and Coolside conditions indicate that the HSA hydrated lime removed, depending on the test system, 15-180% more SO<sub>2</sub> than the commercial hydrated limes tested under similar conditions. The superior performance of the HSA hydrate was attributed to its favorable physical properties.

#### ACKNOWLEDGEMENTS

This work was funded in part by grants from the Illinois Coal Development Board through the Center for Research on Sulfur in Coal. Dr. Brian K. Gullett of the U. S. Environmental Protection Agency provided the FSI data.

#### REFERENCES

1. Bortz, S.J.; Roman, V.; Offen, G. R. First Combined FGD and Dry SO<sub>2</sub> Control Symposium. St. Louis, MO, Oct. 25-28, 1988, Paper no. 10-7.
2. Yoon, H.; Stouffer, M. R.; Rosenhoover, W.A.; Withum, J.A.; Burke, F.P. Eng. Prog. 1988, **7**(1), 82-89.
3. Beittel, R.J.; Gooch, J.; Dismukes E.; Muzio, L. Proc. Symp. on Dry SO<sub>2</sub> and Simul. SO<sub>2</sub>/NO<sub>x</sub> Control Technol. 1985, **1**, 16, EPA-600/0-85-020a (NTIS PB85-232353).
4. Snow, G.C.; Lorrain, J.M.; Rakes, S.L. Proc. Joint Symp. on Dry SO<sub>2</sub> and Simul. SO<sub>2</sub>/NO<sub>x</sub> Control Technol. 1986, **1**, 6-1, EPA-600/9-86-029a (NTIS PB87-120465).
5. Bortz, S.J.; Roman, V.P.; Yang, C.J.; Offen, G.R. Proc. Joint Symp. on Dry SO<sub>2</sub> and Simul. SO<sub>2</sub>/NO<sub>x</sub> Control Technol. 1986, **2**, 31.
6. Withum, J.A.; Lancet, M.S.; Yoon, H. Paper presented at the AIChE 1989 Spring Nat. Mtg, Houston, Texas. 1989

7. Gullett, B.K.; Bruce, K.R. First Combined FGD and Dry SO<sub>2</sub> Control Symposium, St. Louis, MO, Oct 25-28 1988, 6-7, EPA-600/9-89-0369(NTIS PB89-172159).
8. Newton, G.H.; Chen, S.L.; Kramlich, J.C. AIChE J. 1989, **35(6)**, 988-994.
9. Stouffer, M.R.; Yoon, H. AIChE J. 1989, **35(8)**, 1253-1262.
10. Bruce, K. R.; Gullett, B.K.; Beach, L.O. AIChE J. 1989, **35(1)**, 37-41.
11. Yoon, H.; Stouffer, M.R.; Rosenhoover, W.A.; Statnick, R.M. Proc. Second Pittsburgh Coal Conference, Pittsburgh, PA, Sept 16-18 1985, 223-242.
12. Klug, H.P.; Alexander, L.E. "X-ray Diffraction Procedures for Polycrystalline and Amorphous Materials," John Wiley and Sons, New York 1974, 657-659.
13. Gullett, B.K.; Briden, F.E. U. S. Environmental Protection Agency, AEERL, Research Triangle Park, NC, 1989, 62 pages, EPA-600/2-89-065.
14. Borgwardt, R.H.; Roache, N.F.; Bruce, K.R. Environ. Prog. 1984 **3**, 129.

Table 1. Average analyses of the coals (moisture free values).<sup>1,2</sup>

|                 | IBC-101 | IBC-102 | IBC-106 | IBC-109 |
|-----------------|---------|---------|---------|---------|
| Moisture        | 14.8    | 14.3    | 10.5    | 9.2     |
| Vol Matter      | 40.7    | 39.9    | 39.7    | 35.0    |
| Fixed Carbon    | 48.8    | 53.3    | 51.3    | 56.8    |
| H-T Ash         | 10.5    | 6.8     | 9.0     | 8.2     |
| Carbon          | 69.30   | 74.10   | 71.86   | 75.05   |
| Hydrogen        | 5.18    | 5.32    | 4.93    | 4.89    |
| Nitrogen        | 1.31    | 1.50    | 1.67    | 1.74    |
| Oxygen          | 9.31    | 8.92    | 8.76    | 8.53    |
| Sulfatic Sulfur | 0.05    | 0.06    | 0.01    | 0.00    |
| Pyritic Sulfur  | 1.22    | 2.26    | 1.86    | 0.50    |
| Organic Sulfur  | 3.08    | 0.98    | 1.90    | 0.63    |
| Py/Or Ratio     | 0.40    | 2.30    | 0.98    | 0.80    |
| Total Sulfur    | 4.36    | 3.30    | 3.77    | 1.13    |
| Total Chlorine  | 0.12    | 0.02    | 0.02    | 0.42    |
| Btu/lb          | 12659   | 13628   | 13226   | 13324   |

<sup>1</sup> All values in wt% except where noted

<sup>2</sup> Analyses were performed by LECO analyzers and are different than those obtained by the ASTM methods and reported in reference 13.

Table 2. Properties of test sorbents

| Sorbent     | Ash<br>Analyses. (wt%) |      | Mean<br>diameter<br>(micrometers) | BET surface<br>area<br>(m <sup>2</sup> /g) | Pore<br>volume <sup>1</sup><br>(cm <sup>3</sup> /g) | Crystallite<br>size<br>(angstroms) |
|-------------|------------------------|------|-----------------------------------|--|---|------------------------------------|
|             | CaO                    | MgO  |                                   |  |   |                                    |
| Lime A      | 96.1                   | 0.52 | ---                               | 1.6  | ---   | ---                                |
| Hydrate A   | 99.0                   | 0.57 | 3.5                               | 20.6                                       | 0.08  | 220                                |
| HSA hydrate | 96.5                   | 1.20 | 2.0 <sup>2</sup>                  | 38.0 <sup>3</sup>                          | 0.35  | 150                                |
| Hydrate B   | 97.7                   | 0.55 | 3.1                               | 23.2                                       | ---   | ---                                |

<sup>1</sup> Pores smaller than 0.25 micrometers.

<sup>2</sup> The value is an average. The range was 1.6 to 2.7 micrometers.

<sup>3</sup> The value is an average. The range was 35 to 44 m<sup>2</sup>/g.

Table 3. Furnace Sorbent Injection (FSI) data.<sup>1</sup>

| Coal<br>(%) | Sorbents<br>Ca/S | Baseline SO <sub>2</sub> | Removal<br>(ppm) | Ratio |
|-------------|------------------|--------------------------|------------------|-------|
| IBC-101     | Hydrate A        | 3161                     | 28.8             | 0.85  |
|             | Hydrate A        | 3161                     | 56.6             | 1.70  |
|             | HSA hydrate      | 3120                     | 36.6             | 0.79  |
|             | HSA hydrate      | 3120                     | 61.4             | 1.58  |
| IBC-102     | Hydrate A        | 2541                     | 25.6             | 0.88  |
|             | Hydrate A        | 2541                     | 42.1             | 1.75  |
|             | HSA hydrate      | 2288                     | 32.8             | 0.85  |
|             | HSA hydrate      | 2288                     | 50.3             | 1.70  |
| IBC-106     | Hydrate A        | 2918                     | 36.5             | 1.10  |
|             | Hydrate A        | 2918                     | 63.7             | 2.21  |
|             | HSA hydrate      | 2862                     | 59.8             | 1.07  |
|             | HSA hydrate      | 2862                     | 78.7             | 2.14  |
| IBC-109     | Hydrate A        | 1032                     | 40.8             | 0.92  |
|             | Hydrate A        | 1032                     | 52.7             | 1.84  |
|             | HSA hydrate      | 960                      | 47.1             | 1.16  |
|             | HSA hydrate      | 960                      | 80.6             | 2.32  |

<sup>1</sup> Data from reference 13.

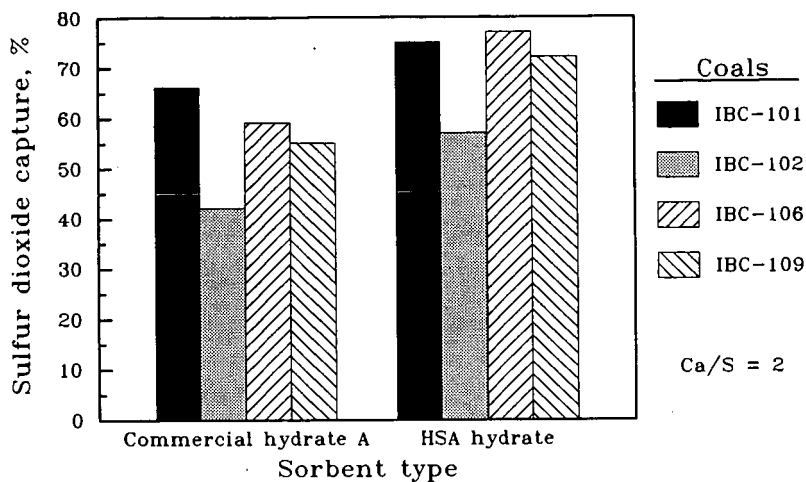


Figure 1. Furnace sorbent injection pilot-plant data

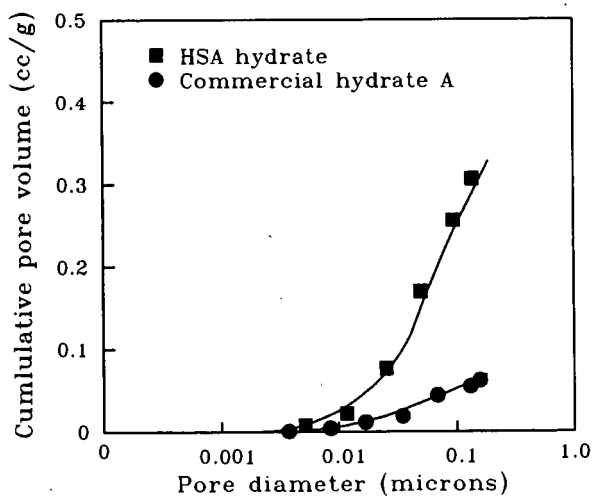


Figure 2. Pore size distribution data

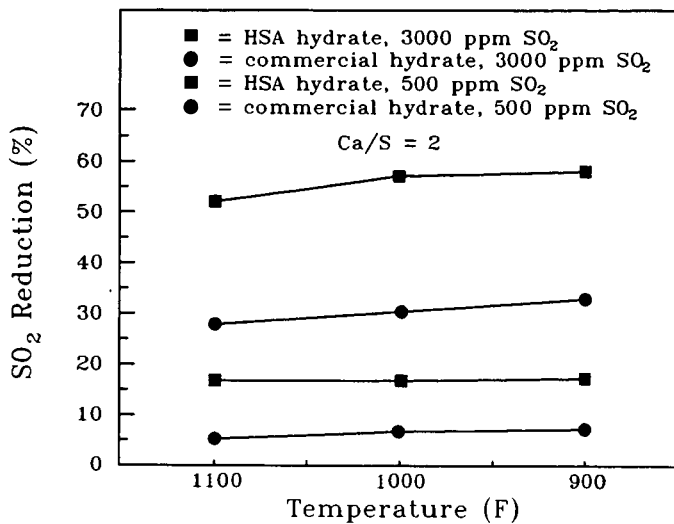


Figure 3. Boiler economizer pilot-plant data

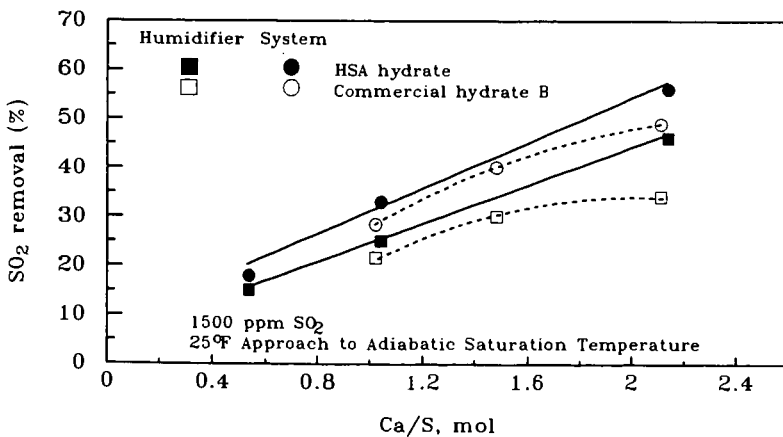


Figure 4. Coolside pilot-plant data

## CHEMICAL REGENERATION OF Fe(II)-EDTA IN WET SCRUBBERS

Y. Joseph Lee and Lewis B. Benson  
Dravo Lime Company, Pittsburgh, PA 15225

Key Words: Fe(II)-EDTA, chemical reduction, NO<sub>x</sub> removal

### INTRODUCTION:

Transition metal chelates have attracted the attention of researchers for the past two decades primarily because of the effectiveness of Fe(II)-EDTA in removing nitric oxide (NO) from the flue gas and its likely compatibility with wet scrubbers. However, Fe(II)-EDTA tends to get oxidized in the scrubbers and Fe(III)-EDTA is not reactive for NO removals. Several reducing agents have been proposed. The purpose of this paper is to evaluate these reducing agents including sulfite or bisulfite, the most logical ones in wet scrubbers.

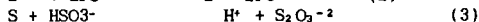
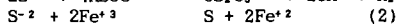
### EXPERIMENTS:

Jacketed reactors were used to conduct experiments at desired temperatures. 1, 10-phenanthroline method was used to determine ferrous ions (Walker and Perry, 1989). Total iron was measured by atomic absorption. Ethylene diamine tetraacetic acid (10% excess), ferrous ammonium sulfate, and ferric ammonium sulfate were used to prepare Fe-EDTA. Sodium carbonate powder and dilute sulfuric acid were used to adjust pH.

### RESULTS AND DISCUSSIONS:

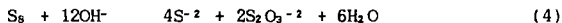
Several reducing agents were tested in batch reactors for Fe(II)-EDTA regeneration. Table 1 lists the related redox potentials. As indicated by the redox potentials, several common metals such as Fe, Zn and Al, are expected to be able to reduce Fe(III)-EDTA to Fe(II)-EDTA. Iron powder, aluminum powder and zinc dust were used to reduce 10 mM Fe(III)-EDTA. The results are summarized in Figure 1. Iron was capable of reducing Fe(III)-EDTA to Fe(II)-EDTA, which was tested and abandoned because of its poor utilization and ferric hydroxide precipitation problem (Staub, 1988). Compared to zinc or alumina, the reducing rate of Fe(III)-EDTA by iron powder was substantially lower probably due to the adverse effect of the magnetic stirring bar on iron powder distribution. Alumina was not reactive at pH 5.5. However, when the pH was raised to 9.0 its reactivity towards Fe(III)-EDTA reduction was substantially higher. Obviously, the higher pH helped dissolve the inert Al<sub>2</sub>O<sub>3</sub> film on the surface of alumina. Zinc is much more effective in reducing Fe(III)-EDTA primarily because of the unit surface area of the zinc we used was substantially higher than those of iron and alumina. Although zinc and alumina are effective and efficient in reducing Fe(III)-EDTA to Fe(II)-EDTA, they are probably not adequate for Fe(II)-EDTA regeneration because the stability constants of Zn-EDTA and Al-EDTA are larger than that of Fe(II)-EDTA. If Zn-EDTA and Al-EDTA are reactive towards NO removal, they should be used in the first place because Zn-EDTA and Al-EDTA cannot be oxidized.

Hydrogen sulfide has been proposed to reduce Fe(III)-EDTA to Fe(II)-EDTA. This approach was not generally accepted because of the toxicity and the odor problem of H<sub>2</sub>S. However, H<sub>2</sub>S can be converted to CaS or Na<sub>2</sub>S quite easily by reacting with Ca(OH)<sub>2</sub> and NaOH respectively. There are two possible reactions in scrubbing liquor when sulfide is added.



Sulfite/bisulfite competes with ferric for sulfide. The results indicated that 5 mM sulfide converted 6 mM Fe(III)-EDTA to Fe(II)-EDTA instantaneously with or without the presence of 0.1 M sulfite. In other words, the utilization of sulfide in reducing Fe(III)-EDTA was around 60%. There might be some unidentified reactions that reduce the utilization of sulfide as a reducing agent for Fe(II)-EDTA regeneration. As indicated by equations 1-3, thiosulfate will be accumulated when sulfide is used to reduce Fe(III)-EDTA. Thiosulfate was recognized as an effective free radical scavenger and was applied to wet FGD to inhibit sulfite oxidation successfully (Owens and Rochelle, 1985). Still, the effect of accumulated thiosulfate on the performance of wet scrubbers needs further study.

Theoretically, alkaline hydrolysis of sulfur (Lee et al., 1990)



can achieve a 50% conversion to sulfide as indicated by reaction 4. When the reaction is not complete, a polysulfide mixture instead of sulfide is the product. To investigate the possibility of using the sulfide/polysulfide product as the reducing agent for Fe(II)-EDTA regeneration, sodium tetrasulfide (Na<sub>2</sub>S<sub>4</sub>) was used to reduce Fe(III)-EDTA. The results indicated that the sulfide sulfur of the tetrasulfide was as good as sulfide in terms of reducing Fe(III)-EDTA to Fe(II)-EDTA. Unsurprisingly, the elemental sulfur of tetrasulfide did nothing except react with sulfite/bisulfite to form thiosulfate. Because alkaline hydrolysis of sulfur (reaction 4) is an inexpensive source of reducing agent, effects of accumulated thiosulfate on the performance of scrubbers deserve further investigation.

Obviously, the most ideal reducing agent for Fe(II)-EDTA regeneration in wet scrubbing system is sulfite/bisulfite. Unfortunately, the reaction rate at scrubber operating temperature (~50°C) is too slow to be practical. It is well known that the rate can be accelerated by raising the temperature, however, the effects of pH on the kinetics were reported inconsistently. Sada et al. (1984) judged that Fe(III)-EDTA reduction by sulfite/bisulfite should be enhanced by raising pH probably based on Le Chatelier principle and the following reaction.



Sada et al. (1988) reported later that reaction 5 was first order in both Fe(III)-EDTA and HSO<sub>3</sub><sup>-</sup>. In other words, Fe(III)-EDTA reduction by sulfite/bisulfite was supposed to be favored by lowering the pH of the

solution. It is contradictory to our result (Figure 2); and our result is consistent with data of Walker et al. (1988). Furthermore, Weisweiler et al. (1986) showed that NO removal was enhanced by raising pH in an ejector type 16-liter gas-liquid contactor. The mechanism is not clear yet, but our preliminary data (not shown) indicated that both Fe(II)-EDTA and dithionate suppressed the forward reaction of reaction 5. Furthermore the pH may significantly affect the activity of Fe(II)-EDTA and the stability of dithionate.

Since the regeneration of Fe(II)-EDTA by sulfite/bisulfite is not good enough to maintain high NO<sub>x</sub> removal, the search for efficient and affordable additives or other reducing agents has been in progress. Sodium thiosulfate was tested. It itself did not show any capability for Fe(II)-EDTA regeneration. However, in the presence of sulfite/bisulfite (0.05 M S(IV)), at pH 7, 10 mM thiosulfate tripled the initial rate of Fe(II)-EDTA (10 mM) reduction. However, a couple hours later, the cumulative conversion of ferric to ferrous EDTA was not affected by the addition of thiosulfate.

Several organic "reducing agents" were also tested for the reduction of Fe(III)-EDTA to Fe(II)-EDTA. Most of these organic compounds were not satisfactory. For example, methanol can be oxidized to formaldehyde, which can then be oxidized to formic acid, and then decomposed to carbon dioxide. Based on standard redox potentials, one would predict that Fe(III)-EDTA could be reduced to Fe(II)-EDTA by each oxidation reaction mentioned above. Unfortunately, neither methanol, formaldehyde or formic acid showed any reducing capability. Both tartaric acid and maleic acid are apt to be oxidized in the air. Oxalic acid, when decomposed to carbon dioxide, was predicted to be able to reduce Fe(III)-EDTA. Unfortunately, none of these three organic acids gave positive results. However, some of the aforementioned organic compounds may act as antioxidants which will prolong the lifetime of Fe(II)-EDTA by sacrificing themselves. Maleic acid is of particular interest because it is available as waste products and it was reported to be easily oxidized under FGD conditions (Lee, 1986).

One of the most interesting organic reducing agents we studied so far is ascorbic acid or vitamin C. It was reported to be a good reducing agent for Fe(II)-EDTA regeneration, in the presence of dithionite (Holter et al., 1987). We found that ascorbic acid was a very good reducing agent even in the absence of dithionite. Furthermore, 1 molecule of ascorbic acid can reduce 10 molecule of Fe(III)-EDTA in a couple hours (figure 3). Also tested was the D-form or the optical isomer of ascorbic acid. The D-isomer demonstrated similar effect on Fe(III)-EDTA reduction as one would expect. In other words, the racemic mixture, which should be substantially cheaper than vitamin C, would be as good as L-ascorbic acid in terms of Fe(II)-EDTA regeneration. The mechanism and the products of this reaction are not clear to the authors yet.

ACKNOWLEDGMENT

The Authors would like to thank Mr. Jeff Henk, Ms. Pat Kerr and Mr. Jerry Hoffman for their help in performing the experiments, typing the paper and preparing the figures, respectively.

REFERENCE

Holter, H. et al., "Process for Stripping Nitrogen Oxides and Sulfur Oxides as Well as Optionally Other Noxious Elements of Flue Gas from Combustion Plants," United States Patent 4,670,234 (1987).

Lee, Y., L. Benson, and R. O'Hara, "Production and Application of Thiosulfate in Lime-Based Wet FGD," ACS Annual Meeting, Washington, D.C. (1990).

Lee, Y. and G. Rochelle, "Oxidative Degradation of Organic Acids Conjugated with Sulfite Oxidation in Flue Gas Desulfurization: Products, Kinetics, and Mechanism," Environ. Technol. 21 (3) 266-272 (1987).

Walker, R. and H. Pennline, "Optimization of a Flue Gas SO<sub>2</sub>/NO<sub>x</sub> Cleanup Process Utilizing Electrodialysis," AIChE 1988 Summer Meeting, Denver, Colorado, (1988).

Weisweiler, W., B. Retzlaff, and L. Raible, "Simultaneous Absorption of Sulfur Dioxide and Nitrogen Monoxide in Aqueous Solutions of Iron-Chelate Complexes," Int. Chem. Eng. 26 (4), 574-581 (1986).

TABLE 1  
RELATED STANDARD REDUCTION POTENTIALS FOR Fe(II)-EDTA REGENERATION

| Reduction Reaction  | E <sub>o</sub> |
|---|----------------|
| Fe(III)-(Phenanthroline) <sub>3</sub> <sup>3+</sup> + e <sup>-</sup> → Fe(II)-(Ph) <sub>3</sub> <sup>2+</sup>                         | 1.14           |
| Fe <sup>3+</sup> + e <sup>-</sup> → Fe <sup>2+</sup>  | 0.77           |
| S <sub>2</sub> O <sub>6</sub> <sup>-2</sup> + 4H <sup>+</sup> + 2e <sup>-</sup> → 2H <sub>2</sub> SO <sub>3</sub>                     | 0.6            |
| S <sub>4</sub> O <sub>6</sub> <sup>-2</sup> + e <sup>-</sup> → 2S <sub>2</sub> O <sub>3</sub> <sup>-2</sup>                           | 0.09           |
| Fe(III)-EDTA <sup>-</sup> + e <sup>-</sup> → Fe(II)-EDTA <sup>-2</sup>  | -0.177*        |
| 2SO <sub>4</sub> <sup>-2</sup> + 4H <sup>+</sup> + 2e <sup>-</sup> → S <sub>2</sub> O <sub>6</sub> <sup>-2</sup> + 2H <sub>2</sub> O  | -0.2           |
| CO <sub>2</sub> + 2H <sup>+</sup> + 2e <sup>-</sup> → HCOOH   | -0.2           |
| Fe <sup>2+</sup> + 2e <sup>-</sup> → Fe   | -0.409         |
| S + H <sub>2</sub> O + 2e <sup>-</sup> → HS <sup>-</sup> + OH <sup>-</sup>  | -0.478         |
| 2CO <sub>2</sub> + 2H <sup>+</sup> + 2e <sup>-</sup> → H <sub>2</sub> C <sub>2</sub> O <sub>4</sub>                                   | -0.49          |
| S + 2e <sup>-</sup> → S <sup>2-</sup>   | -0.508         |
| 2SO <sub>3</sub> <sup>-2</sup> + 3H <sub>2</sub> O + 4e <sup>-</sup> → S <sub>2</sub> O <sub>3</sub> <sup>-2</sup> + 6OH <sup>-</sup> | -0.58          |
| Zn <sup>2+</sup> + 2e <sup>-</sup> → Zn   | -0.76          |
| SO <sub>4</sub> <sup>-2</sup> + H <sub>2</sub> O + 2e <sup>-</sup> → SO <sub>3</sub> <sup>-2</sup> + 2OH <sup>-</sup>                 | -0.92          |
| 2SO <sub>3</sub> <sup>-2</sup> + 2H <sub>2</sub> O + 2e <sup>-</sup> → S <sub>2</sub> O <sub>4</sub> <sup>-2</sup> + 4OH <sup>-</sup> | -1.12          |
| Al <sup>3+</sup> + 3e <sup>-</sup> → Al(0.1F NaOH)  | -1.706         |
| H <sub>2</sub> AlO <sub>3</sub> <sup>-</sup> + H <sub>2</sub> O + 3e <sup>-</sup> → Al + 4OH <sup>-</sup>                             | -2.35          |

Sources

CRC Handbook of Chemistry and Physics 53rd Ed. (1972-1973)

\*W. R. Grace Technical Information

**Figure 1 Fe(II)-EDTA Regeneration by Al, Zn, and Fe Powdered Metals**

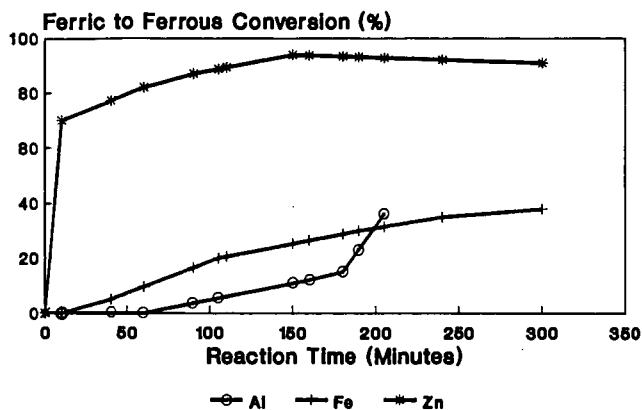


**Figure 2 pH and Temperature Effects on Fe(II)-EDTA Regeneration by Sulfite**

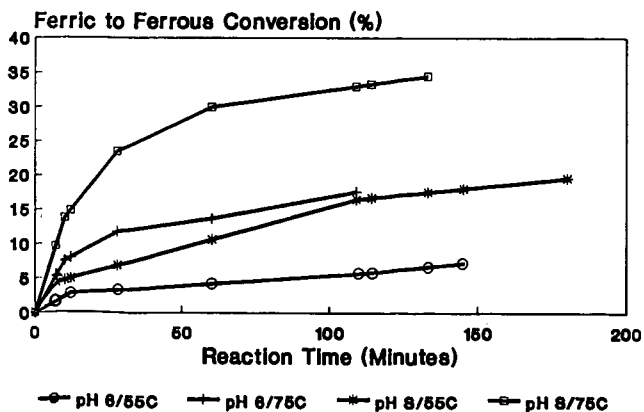
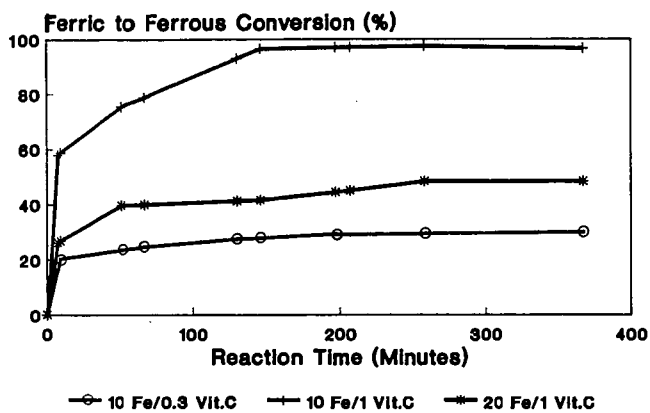


Figure 3 Fe(III)-EDTA Reduction  
by L-Ascorbic Acid (Vitamin C)



THERMOCHEMISTRY OF THE Fe-O-S SYSTEM AS A  
DESULFURIZER IN COAL COMBUSTION ATMOSPHERES:  
PART I - Fe-FeO-LIQUID EQUILIBRIUM

M. T. Hepworth, K. J. Reid, J. C. Wang and S. Zhong  
Mineral Resources Research Center  
University of Minnesota, 56 East River Road  
Minneapolis, Minnesota 55455

Key words: Iron oxysulfide, slagging burner, desulfurization

INTRODUCTION

Development in slagging combustors for utility coal combustion is being driven by several factors:

- \* Removal of coal combustion residues as dense constituents at the source of combustion to reduce ash transfer to heat exchangers and down-stream fly ash capture devices,
- \* Incorporation of staged-combustion to minimize NO<sub>x</sub> emissions,
- \* Utilization of added sorbents to reduce SO<sub>x</sub> emissions,
- \* Capability of operation at elevated pressures suitable for combined cycle operation.

A recent survey<sup>1</sup> indicated that lime or limestone was currently the only sorbent being injected in slagging utility burners for those systems close to, or currently undergoing commercial development. Some researchers, notably Avco<sup>2</sup> have experimented with added iron as a sorbent material with initial success. The results of some preliminary studies by AMAX on iron oxide additions to the reducing stage of a small coal burner was reported<sup>3</sup> to result in up to 90 percent sulfur removal into a compact residue. This residue appeared to be relatively inert with respect to sulfur re-emission when exposed to moisture. Avco confirm these preliminary findings in experiments conducted late in 1989.

This paper is written entirely from a thermodynamic point of view. It compares the degree of desulfurization which can be achieved using an iron system with a calcium-based system operating under both reducing conditions (to produce calcium sulfide) and oxidizing conditions (to produce calcium sulfate). For this study calculations were made on an Illinois #2 coal as the fuel. They are restricted to those sulfur potentials which occur for the four phase equilibrium: gas + iron + wustite (FeO) + liquid iron oxysulfide.

Iron may be considered a potential competitor to lime as a sorbent for several reasons:

- \* It forms a series of low-melting-point liquid solutions with iron and oxygen under reducing conditions. These liquids should be highly reactive with respect to absorption of sulfur in the gases which they contact. Because they are liquids rather than solids, good internal mixing under the high shear conditions of cyclonic burners should enhance the kinetics of absorption and also achieve sulfur absorption closer to the predicted stoichiometry than would occur with a solid sorbent.

- \* However, lime, being a solid, has been shown to require from two-to-five times the stoichiometric ratio of calcium-to-sulfur<sup>4</sup> in order to produce a high degree of desulfurization.
- \* Iron in the form of taconite concentrates (magnetite) is cost-competitive with lime at locations close to Great Lakes' ports (approximately \$30/short ton, FOB).

#### THERMODYNAMIC ANALYSIS

Calculations are based upon a Western Illinois Coal (Illinois No. 2), described as "Colchester, low ash, high pyritic sulfur" from sample IBC 102<sup>5</sup>. This coal, of the assay given below, was factored into the calculations as 100 grams of coal on dry basis plus 14.2 grams moisture:

| <u>Constituent</u> | <u>% by Wt.</u>            |
|--------------------|----------------------------|
| Carbon             | 73.92                      |
| Hydrogen           | 5.29                       |
| Nitrogen           | 1.52                       |
| Total sulfur       | 3.29                       |
| Oxygen             | 9.02 (not included in ash) |
| Ash                | <u>6.9</u>                 |
| Total              | 100.0 (dry basis)          |
| Moisture           | 14.2                       |
| BTU/lb             | 13,582                     |

An interactive computer program was developed which enables coal assays to be varied as well as combustion conditions including temperature, total pressure coal composition, moisture content, volume of air, etc. Data were taken from Kubaschewski and Alcock<sup>6</sup> for the thermodynamics of the gas phase interactions and for the stabilities of the calcium compounds. The iron oxygen-sulfur systems incorporates data from Darken and Gurry<sup>7</sup>, Bog and Rosenqvist<sup>8</sup>, Rosenqvist and Hartvig<sup>9</sup>, and Burgmann et al.<sup>10</sup> as reported by Turkdogan and Kor.<sup>11</sup>

The results of these calculations are shown in Figure 1 for the system Ca-S-O. This figure is a predominance diagram in which the equilibrium phase regions are designated on a logarithmic plot of partial pressures of sulfur (taking the dimer as the predominant elemental sulfur species) on the ordinate and log oxygen partial pressure as a measure of the chemical potential of oxygen on the abscissa. The solid lines represent conditions at 1000° C. and the dashed lines at 1300° C., respectively. As is expected, calcium sulfide is oxidized upon increasing the oxygen potential to the sulfate form and can only be maintained under the reducing conditions shown. As temperature is increased (dashed lines) the transition from sulfide to sulfate occurs under more oxidizing conditions. Also as temperature is increased the equilibrium between sulfide and oxide occurs at lower sulfur pressures in the equilibrium between CaS and CaO; however, the sulfur pressures for the equilibrium between CaO and CaSO<sub>4</sub> phases occur for higher sulfur pressures as temperature is raised.

Using the interactive program and the coal composition given above, the calculations in Figure 2 on the CaO/CaS/gas system show the anticipated equilibrium sulfur concentration reported as pounds of SO<sub>2</sub> per million BTU against temperature. For this plot the partial pressure of oxygen was arbitrarily taken at 10<sup>-12</sup> atmospheres with a total gas pressure of 1 atmosphere. The thermodynamic conditions are for the reducing stage of a two-stage combustor; however, the calculations for the sulfur dioxide emissions (ordinate) are based upon stoichiometric conditions existing in the second stage of the combustor. Figure 2 substantiates the conditions borne out in Figure 1; that is, high temperatures for the calcium sulfide system yield better desulfurization.

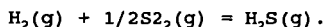
The converse is true for lime used as a sorbent under oxidizing conditions; i. e., with calcium sulfate as the product of reaction. Figure 3 shows that for temperatures much above 1150° C., the sulfur pressure rises rapidly. The conditions chosen were for an oxygen pressure of 0.05 atmospheres, or a slight excess of oxygen over stoichiometric requirements. In Figures 2 and 3 the theoretical dosage of lime is also plotted. As the lime reacts with sulfur, the dosage of lime required, of course, increases (Figure 1); whereas, the converse is true for Figure 3 where lime becomes less effective as a desulfurizer.

Figure 4 is a ternary projection of the liquidus surfaces in the Fe-O-S system showing the phase pyrrhotite (FeS) at the lower right hand corner. The liquid phase is seen to be in the thermal "trough" with a ternary eutectic of 920° C. From this ternary eutectic the labeled isotherms diverge outward to form the steep walls of this valley. The region in this paper for which calculations were made is the heavy diagonal line toward the left-hand wall of this trough which marks the boundary between the regions of iron/wustite/and liquid.

Data summarized by Turkdogan and Kor have been employed in our calculations. Figure 5 is a plot of the conditions of oxygen and sulfur potential as a function of temperature to maintain this four phase equilibrium (three condensed phases plus gas). This plot is not for a system of constant composition but for the composition along the solid line shown in the previous figure. As temperature rises, the oxygen partial pressure is shown to rise, but interestingly, the sulfur partial pressure shown on a log scale drops sharply. Part of this drop can be attributed toward the increasing solubility limit of the liquid phase (closer to lower sulfur concentrations); nevertheless, the rapid drop in sulfur partial pressure is steeper than would be predicted merely by a shift in composition to lower sulfur contents. Even at 1300°C the chemical potential of sulfur, as measured by the parameter,  $-RT \ln P_{S_2}$ , is about 45,000 calories per gram mole corresponding to a partial pressure of sulfur of  $5.58 \times 10^{-7}$  atm. This is a fortuitous aspect of the iron-oxygen-sulfur system; i. e., the thermodynamic calculations on desulfurization show improvement with higher temperatures. Figure 6 is a plot for the Fe-O-S system similar to those for the lime-based systems in which this improved degree of desulfurization with increasing temperature is shown. The increased dosage of iron is also shown. For example at 1300°C an iron dosage for the coal composition for these calculations would be 15 grams per 100 grams of coal.

One of the objectives of this study is to develop an interactive computer program such that an operator of a slagging combustor can enter coal compositions and combustion conditions and determine the optimum process conditions required. Figure 7 shows the air requirements for 100 grams of dry coal and the theoretical percent sulfur removal which can be achieved.

Figure 8 shows the calculated concentrations of the major gas species as a function of temperature for the equilibrium between Fe/FeO/liquid/gas. The predominant species for these reducing conditions (corresponding to a combustion stoichiometry of approximately 55% of the required air for complete combustion) are N<sub>2</sub> and CO followed by CO<sub>2</sub>, H<sub>2</sub>, and H<sub>2</sub>O in that order. The total sulfur pressure is the sum of all the sulfur-bearing species with H<sub>2</sub>S being the predominant sulfur carrier. Lower rank coals with higher hydrogen water vapor contents would be expected to carry more sulfur into the gas phase. Since the pressure of the sulfur species, S<sub>2</sub>, is fixed by the Fe-O-S equilibria, the actual amount of sulfur in the gas phase is determined principally by the equilibrium:



This equilibrium has an equilibrium constant somewhat greater than unity. Also the pressure of H<sub>2</sub>S is proportional only to the square root of the sulfur pressure but varies linearly with hydrogen pressure. It follows, then, that iron oxysulfide would perform best on dry, high-rank coals.

#### CONCLUSIONS

The following can be concluded from this analysis:

- \* In the Fe-O-S system for the four-phase contact, Fe/FeO/liquid/gas, higher temperatures result in greater degrees of desulfurization for the range of temperatures studied.
- \* Lime added under oxidizing conditions to form sulfate as a reaction product is not practical as a sulfur sorbent at temperatures above 1175°C.
- \* Inference is made that for iron oxysulfide as a sorbent, this liquid phase should exhibit a higher degree of utilization in liquid droplets than solid lime sorbents. Furthermore the kinetics of liquid/gas interactions should be more favorable than solid/gas interactions. This hypothesis will require further study in a dynamic burner system.
- \* Further calculations are required to determine the process conditions to achieve effective sulfur removal for the two phases, liquid/gas. These calculations should be made for a range of coals of varying hydrogen and water contents.

#### REFERENCES

1. Hepworth, M. T. and Reid, K. J.: Slagging Combustor Review, Final Report MRRC, University of Minnesota December, 1988.

2. Private Communication: R. Diehl Avco Research Laboratories, Everett, Mass.
3. Hepworth, M. T. and Wicker G. R., "Iron Oxide as a Desulfurizing Agent in a Slagging Coal Combustor", Pyrometallurgy '87, Institution of Mining and Metallurgy, London, 1987, and Hepworth, M. T., U. S. Patents 4,572,085 (2/25/86), 4,598,652 (7/8/86), and 4,599,955 (7/15/86).
4. Lachapelle, David G.: "EPA's LIMB Technology Development Program," Chemical Engineering Progress, May 1985 pps. 56-62.
5. Harvey, Richard D.: Illinois Geological Survey, Letter of 9/8/89 to M.T. Hepworth.
6. Kubaschewski, O. and Alcock, C. B.: Metallurgical Thermochemistry, Pergamon Press, 1979.
8. Bog, S. and Rosenqvist: The Physical Chemistry of Metallic Solutions and Intermetallic Compounds, Paper 6B, NPL Symposium No 9, Vol II, 1959.
7. Darken, L. S. and Gurry, R. W., J. Am. Chem. Soc., 1945, Vol 67. pps. 1398-1412; 1946, Vol 68, pps. 798-816.
9. Rosenqvist, T. and Hartvig, T.: Roy. Norweg. Concil Sci. and Ind. Res., Rep. No 12, Part II, 1958.
10. Burgmann, W., Urbain, G., and Froberg, M. G.: IRSID Saint Germain-en-Laye, France, January 1968.
11. Turkdogan, E. T. and Kor, G. J. W.: "Sulfides and Oxides in Fe-Mn Alloys: Part I, Phase Relations in the Fe-Mn-S-O System", Metallurgical Transactions, Vol 2, June 2971 pps 1561-1578.

#### ACKNOWLEDGEMENT

The authors wish to express their appreciation to the Department of Energy contract #DOE/DE-FG22-89PC89778 for funding this study.

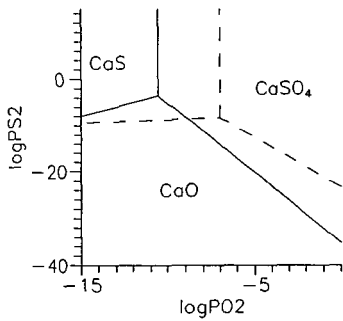


Figure 1. Predominance Diagram  
Ca-S-O System.  
Solid Lines - 1000° C.  
Dashes Lines - 1300° C.

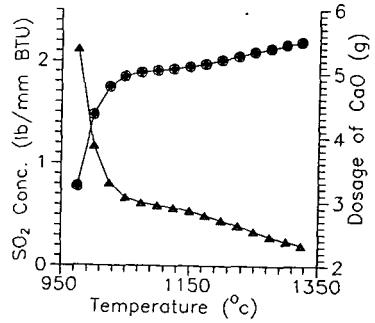


Figure 2. CaO/CaS/Gas  
Stoichiometric SO<sub>2</sub>  
Conc. vs. Temp  
at Oxygen Pressure: 10<sup>-12</sup>  
Atm.  
△ SO<sub>2</sub>  
○ Dosage of CaO

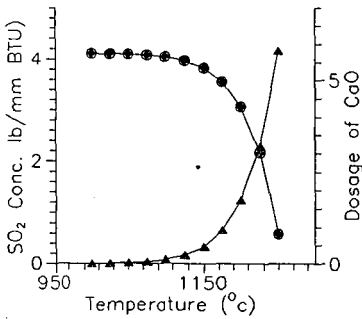


Figure 3. CaO/CaSO<sub>4</sub>/Gas  
Stoichiometric SO<sub>2</sub>  
at Oxygen Pressure: 0.05  
Atm.  
△ SO<sub>2</sub>  
○ Dosage of CaO

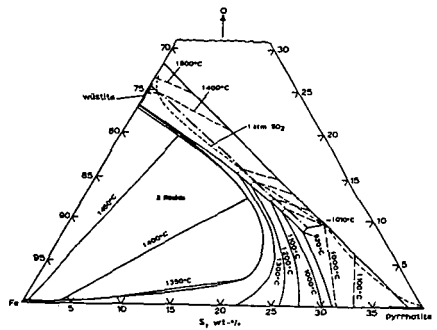


Figure 4. Ternary Section Fe/FeS/O System:  
Projection Liquidus Surface.  
After: Bog and Rosenqvist<sup>8</sup>  
Hilty and Crafts<sup>12</sup>

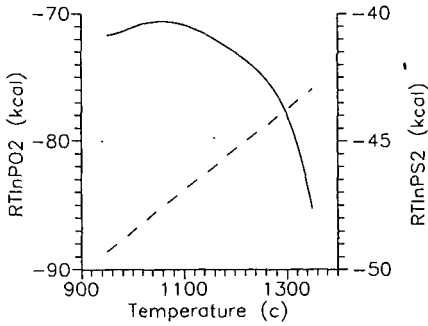


Figure 5. Fe/FeO/Liquid/Gas System  
Chemical Potentials S, O.  
— Sulfur  
--- Oxygen

After: Turkdogan et al.<sup>11</sup>

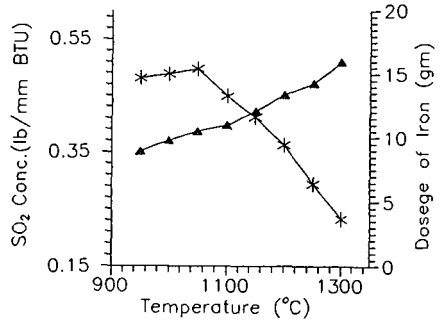


Figure 6. Fe/FeO/Liquid/Gas System  
Stoichiometric SO  
Conc. vs. Temp.  
\* SO<sub>2</sub> Concentration  
△ Dosege of Iron

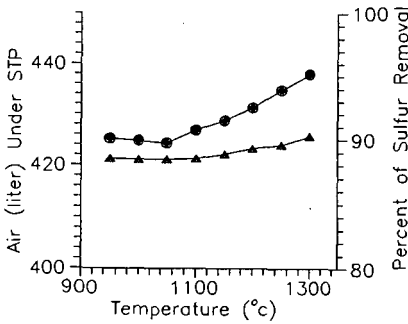


Figure 7. Fe/FeO/Liquid/Gas System  
△ Air Dosage/100g Dry Coal &  
○ % Sulfur Removal vs. Temp.

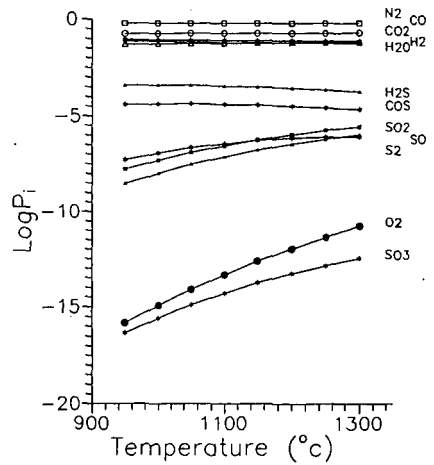


Figure 8. Calculated Partial Pressure (atm.)  
vs. Temperature for Coal Combustion  
Products in Equilibrium with  
Fe/FeO/Liquid

## COMPUTER MODELING OF THE CHEMISTRY OF AQUEOUS SCRUBBER SYSTEMS

David Littlejohn and Shih-Ger Chang  
Lawrence Berkeley Laboratory  
1 Cyclotron Road  
Berkeley, CA 94720

### Abstract

The chemistry occurring in aqueous flue gas scrubbing solutions can be quite complicated, due to the large number of chemical species present and the many physical processes involved. These include gas absorption into solution, gas and solution kinetics involving both nitrogen oxides and sulfur oxides, oxidation and hydrolysis reactions in solution, and liquid-solid interactions. Simple models that neglect the solution kinetics which can occur in scrubbers cannot be expected to accurately model aqueous-based scrubber chemistry. We have developed a computer model which incorporates the aqueous solution kinetics of nitrogen oxyanions, sulfur oxyanions, nitrogen-sulfur compounds, and other species. The model can be adapted to predict the chemistry in a wide range of aqueous-based scrubber systems. It can be used to study the effect of changes in the operating conditions of the scrubbers. The results of the model can be compared with experimental observations to determine how well the chemistry of the solutions is understood.

**Key Words:** Wet scrubber chemistry, nitrogen sulfur compounds, computer modeling

### Introduction

A good understanding of the chemistry occurring in wet flue gas scrubbing systems is important. The chemistry will influence the  $\text{NO}_x$  and  $\text{SO}_2$  removal and the product distribution, as well as factors such as scaling. A large number of compounds can be formed in scrubber solutions.<sup>1</sup> The compounds present depend, in part, on the type of scrubber chemistry utilized. Nitrogen-sulfur compounds will form under neutral to acidic conditions when both nitrite ion and bisulfite ion are present in significant quantities.<sup>1</sup> The term nitrogen-sulfur compound is used to collectively refer to hydroxyimidodisulfate (HADS), hydroxysulfamic acid (HAMS), nitridotrisulfate (ATS), imidodisulfate (ADS), sulfamate, and hydroxylamine. The compounds have been observed in a number of wet scrubber solutions.<sup>2,3</sup> These compounds can interfere with the recovery of desirable byproducts from scrubber solutions. They will also build up in scrubber solutions and must eventually be treated or removed.

To develop an understanding of the solution chemistry of wet scrubbers, a chemical kinetic computer modeling program has been developed. It allows simulation of the known reactions occurring in solution and calculation of reaction rates and concentration of aqueous species.

## The Model

Exact equations for calculating the concentrations of species involved in chemical reactions can only be established for the simplest reaction systems. Approximations, such as the steady-state approximation, permit estimation of concentrations and rates of reaction in more complicated chemical systems under suitable conditions, provided that the system is not too complicated. A different approach is required to accurately calculate concentrations and rates in complex reaction systems, particularly where conditions are rapidly changing.

In the 1970's, work by Whitten<sup>4</sup> and others led to the development of matrix-based computer calculations to simulate complicated chemical kinetic systems. The system of chemical reactions is converted into a series of ordinary differential equations. A method to integrate a system of ordinary differential equations was developed by Gear<sup>5</sup> and modified by Hindmarsh<sup>6</sup> at Lawrence Livermore National Laboratory. This routine is the basis for most chemical kinetic modeling schemes. The program performing the Gear routine has subsequently been modified to handle sparse matrices and improve its operating efficiency.<sup>7</sup> This version of the Gear routine is the basis of the chemical kinetic modeling program used in this work. It is similar to modeling routines that have been used to simulate air pollution chemistry for a number of years.<sup>8</sup>

## Results and Discussion

The chemistry of the nitrogen-sulfur compounds in solution has been studied extensively for many years, and is, for the most part, reasonably well understood. The rate constants for the reactions involving nitrogen-sulfur compounds, along with those for other important reactions, are incorporated into the computer model. The initial conditions for the calculation are also included as input. These include temperature or temperature vs time profile, initial concentration of species, pH and length of time of the calculation. The program generates a list of reaction rates vs time and concentration vs time for all species included in the calculation. In this way, we can explore the effect of variables such as temperature, pH, concentrations, and additives on the scrubber chemistry.

The chemical reaction database used as input into the model is listed in Table 1. Depending on conditions, some of the reactions are unimportant and are not included in the calculation to reduce the processing time. Tests are performed to ensure the absence of a reaction does not significantly alter the results of the calculation. Updated or additional reaction rate constants can be incorporated into the database as new measurements become available.

Examples of the calculations are shown in Figure 1 and Figure 2. Figure 1 illustrates the effect of pH on the generation and interconversion of nitrogen-sulfur compounds. Calculations were done at pHs of 3, 5 and 7 at a temperature of 40°C for a batch reactor exposed to concentrations of SO<sub>2</sub> = 2000 ppm, NO = 450 ppm and NO<sub>2</sub> = 50 ppm. Increasing the solution pH significantly increases the total concentration of nitrogen-sulfur compounds and favors ATS and ADS as products. Figure 2 illustrates the effect of temperature on the system of nitrogen-sulfur compounds. Calculations were done at temperatures of 20°C (68°F), 40°C (104°F), and 60°C (140°F) at a pH of 5 for a batch reactor exposed to concentrations of SO<sub>2</sub> = 2000 ppm, NO = 450 ppm, and NO<sub>2</sub> = 50 ppm. Increasing the solution temperature

also increases the total concentration of nitrogen-sulfur compounds. Higher temperatures increase the concentrations of ATS and ADS relative to HADS and HAMS.

These calculations illustrate what can be studied using the computer model. The influence of a number of scrubbing system parameters can be investigated relatively rapidly. The model does require accurate information on kinetics, gas concentrations, and solubilities for all compounds that have a significant influence on the chemistry to provide realistic results.

The chemical kinetics modeling program is still under development to increase its versatility. We are in the process of incorporating precipitation processes in the model to simulate the formation of solids. This will allow more accurate investigation of some scrubber chemistries, such as lime/limestone-based scrubbing systems. Measurement of the solubilities of the nitrogen-sulfur compounds is currently in progress,<sup>9</sup> and the results of this study will be incorporated into the model.

The model is also being developed to incorporate the effects of ionic strength and activities of the ions in solution on the reactions used. Scrubbing solutions are generally at conditions that are far from those of ideal solutions. By incorporating ionic strength and ionic interactions into the model, we should be able to obtain more accurate simulation of the chemistry of scrubbing solutions.

This work was supported by the Assistant Secretary for Fossil Energy, Office of Coal Utilization Systems, U.S. Department of Energy under Contract No. DE-AC03-76SF00098 through the Pittsburgh Energy Technology Center, Pittsburgh, PA.

## References

1. Chang, S.G.; Littlejohn, D.; Lin, N.H. Flue Gas Desulfurization; Hudson, J.L.; Rochelle, G.T., Eds.; ACS Symposium Series 188; American Chemical Society: Washington, DC, 1982; pp 127-152.
2. Littlejohn, D.; Chang, S.G. "Identification of Species in a Wet Flue Gas Desulfurization and Denitrication System by Laser Raman Spectroscopy". *Environ. Sci. Technol.* **1984**, *18*, 305-310.
3. Littlejohn, D.; Chang, S.G. "Determination of Nitrogen-Sulfur Compounds by Ion Chromatography". *Anal. Chem.* **1986**, *58*, 158-160.
4. Whitten, G.Z. "Rate Constant Evaluations Using a New Computer Modeling Scheme". Presented at the 167th National Meeting of the American Chemical Society, San Francisco, CA.
5. Gear, C.W. Numerical Initial Value Problems in Ordinary Differential Equations; Prentice Hall, Englewood Cliffs, NJ, 1971.

- 6 Hindmarsh, A.C. "GEAR: Ordinary Differential Equation System Solver" Report UCID-30001, rev.3; Lawrence Livermore National Laboratory, Livermore, CA, 1974.
- 7 Spellman, J.W.; Hindmarsh, A.C. "GEARS: Solution of Ordinary Differential Equations Having a Sparse Jacobian Matrix" Report UCID-30116; Lawrence Livermore National Laboratory, Livermore, CA, 1975.
- 8 Whitten, G.Z.; Hogo, H. "CHEMK; A Computer Modeling Scheme for Chemical Kinetics". Report No. EF78-107R, Systems Applications, Inc., San Rafael, CA, 1979.
- 9 Littlejohn, D.; Chang, S.G. to be published.

Table 1

Chemical Reactions Related to Aqueous Scrubber Chemistry

| Reaction |   | k, K or H <sup>a</sup>  | E <sub>act</sub> <sup>b</sup> |
|----------|---|-------------------------|-------------------------------|
| 1.       | SO <sub>2</sub> (gas) ⇌ SO <sub>2</sub> (aq)  | 1.24                    |                               |
| 2.       | NO(gas) ⇌ NO(aq)  | .0019                   |                               |
| 3.       | NO <sub>2</sub> (gas) ⇌ NO <sub>2</sub> (aq)  | .007                    |                               |
| 4.       | CO <sub>2</sub> (gas) ⇌ CO <sub>2</sub> (aq)  | .034                    |                               |
| 5.       | HNO <sub>2</sub> (gas) ⇌ HNO <sub>2</sub> (aq)  | 60                      |                               |
| 6.       | NO + NO <sub>2</sub> + H <sub>2</sub> O (gas) ⇌ HNO <sub>2</sub> + HNO <sub>2</sub>   | 5.3 × 10 <sup>-2</sup>  |                               |
| 7.       | SO <sub>2</sub> (aq) ⇌ HSO <sub>3</sub> <sup>-</sup> + H <sup>+</sup>   | 1.5 × 10 <sup>-2</sup>  |                               |
| 8.       | CO <sub>2</sub> (aq) ⇌ HCO <sub>3</sub> <sup>-</sup> + H <sup>+</sup>   | 4.3 × 10 <sup>-7</sup>  |                               |
| 9.       | HSO <sub>3</sub> <sup>-</sup> ⇌ SO <sub>3</sub> <sup>2-</sup> + H <sup>+</sup>  | 1.2 × 10 <sup>-7</sup>  |                               |
| 10.      | HNO <sub>2</sub> (aq) ⇌ NO <sub>2</sub> <sup>-</sup> + H <sup>+</sup>   | 5.8 × 10 <sup>-4</sup>  |                               |
| 11.      | HSO <sub>4</sub> <sup>-</sup> ⇌ SO <sub>4</sub> <sup>2-</sup> + H <sup>+</sup>  | 1.2 × 10 <sup>-2</sup>  |                               |
| 12.      | HSO <sub>3</sub> <sup>-</sup> + HSO <sub>3</sub> <sup>-</sup> ⇌ S <sub>2</sub> O <sub>5</sub> <sup>2-</sup> + H <sub>2</sub> O                        | 6.5 × 10 <sup>-2</sup>  |                               |
| 13.      | NO(aq) + NO <sub>2</sub> (aq) → HNO <sub>2</sub> (aq) + HNO <sub>2</sub> (aq)   | 1.6 × 10 <sup>8</sup>   |                               |
| 14.      | HNO <sub>2</sub> (aq) + HNO <sub>2</sub> (aq) → NO(aq) + NO <sub>2</sub> (aq)   | 14                      |                               |
| 15.      | H <sup>+</sup> + HNO <sub>2</sub> (aq) → NO <sup>+</sup> + H <sub>2</sub> O   | 4.08 × 10 <sup>2</sup>  | 11.5                          |
| 16.      | HNO <sub>2</sub> + HSO <sub>3</sub> <sup>-</sup> → ONSO <sub>3</sub> <sup>-</sup> + H <sub>2</sub> O  | 2.43                    | 12.1                          |
| 17.      | NO <sup>+</sup> + HSO <sub>3</sub> <sup>-</sup> → ONSO <sub>3</sub> <sup>-</sup> + H <sup>+</sup>   | c                       |                               |
| 18.      | ONSO <sub>3</sub> <sup>-</sup> + HSO <sub>3</sub> <sup>-</sup> → HON(SO <sub>3</sub> ) <sub>2</sub> <sup>2-</sup>                                     | c                       |                               |
| 19.      | HON(SO <sub>3</sub> ) <sub>2</sub> <sup>2-</sup> + H <sup>+</sup> → HONHSO <sub>3</sub> <sup>-</sup> + H <sup>+</sup> + HSO <sub>4</sub> <sup>-</sup> | 2.1 × 10 <sup>11</sup>  | 17.6                          |
| 20.      | HON(SO <sub>3</sub> ) <sub>2</sub> <sup>2-</sup> → HONHSO <sub>3</sub> <sup>-</sup> + HSO <sub>4</sub> <sup>-</sup>                                   | 1.67 × 10 <sup>11</sup> | 23.0                          |

Table 1  
(continued)

|  |   |  |                         |      |
|--|---|--|-------------------------|------|
| 21. HONHSO <sub>3</sub> <sup>-</sup> + H <sup>+</sup>                                | → | NH <sub>2</sub> OH + H <sup>+</sup> + HSO <sub>4</sub> <sup>-</sup>              | 6.2 × 10 <sup>12</sup>  | 26.3 |
| 22. HON(SO <sub>3</sub> ) <sub>2</sub> <sup>2-</sup> + HSO <sub>3</sub> <sup>-</sup> | → | N(SO <sub>3</sub> ) <sub>3</sub> <sup>3-</sup> + H <sub>2</sub> O                | 3.4 × 10 <sup>10</sup>  | 19.2 |
| 23. N(SO <sub>3</sub> ) <sub>3</sub> <sup>3-</sup> + H <sup>+</sup>                  | → | HN(SO <sub>3</sub> ) <sub>2</sub> <sup>2-</sup> + HSO <sub>4</sub> <sup>-</sup>  | 1.5 × 10 <sup>13</sup>  | 16.5 |
| 24. HN(SO <sub>3</sub> ) <sub>2</sub> <sup>2-</sup> + H <sup>+</sup>                 | → | H <sub>2</sub> NSO <sub>3</sub> <sup>-</sup> + HSO <sub>4</sub> <sup>-</sup>     | 2.54 × 10 <sup>14</sup> | 23.5 |
| 25. HON(SO <sub>3</sub> ) <sub>2</sub> <sup>2-</sup> + HSO <sub>3</sub> <sup>-</sup> | → | HN(SO <sub>3</sub> ) <sub>2</sub> <sup>2-</sup> + HSO <sub>4</sub> <sup>-</sup>  | 1.5 × 10 <sup>10</sup>  | 19.0 |
| 26. HONHSO <sub>3</sub> <sup>-</sup> + HSO <sub>3</sub> <sup>-</sup>                 | → | HN(SO <sub>3</sub> ) <sub>2</sub> <sup>2-</sup> + H <sub>2</sub> O               | 1.4 × 10 <sup>13</sup>  | 24.5 |
| 27. HONHSO <sub>3</sub> <sup>-</sup> + HSO <sub>3</sub> <sup>-</sup>                 | → | H <sub>2</sub> NSO <sub>3</sub> <sup>-</sup> + HSO <sub>4</sub> <sup>-</sup>     | 6.0 × 10 <sup>12</sup>  | 24.5 |
| 28. NH <sub>2</sub> OH + SO <sub>2</sub> (aq)  | → | H <sub>2</sub> NSO <sub>3</sub> <sup>-</sup> + H <sub>2</sub> O + H <sup>+</sup> | 1.74 × 10 <sup>11</sup> | 13.4 |
| 29. NH <sub>2</sub> OH + SO <sub>2</sub> (aq)  | → | NH <sub>4</sub> <sup>+</sup> + HSO <sub>4</sub> <sup>-</sup>                     | 1.06 × 10 <sup>2</sup>  | 3.0  |
| 30. H <sub>2</sub> NSO <sub>3</sub> + HNO <sub>2</sub>                               | → | HSO <sub>4</sub> <sup>-</sup> + H <sub>2</sub> O                                 | 1.13 × 10 <sup>2</sup>  | 11.3 |
| 31. NO(aq) + HSO <sub>3</sub> <sup>-</sup>   | → | <sup>-</sup> ONSO <sub>3</sub> <sup>-</sup> + H <sup>+</sup>                     | 2.6 × 10 <sup>14</sup>  | 17.6 |
| 32. NO(aq) + SO <sub>3</sub> <sup>2-</sup>   | → | <sup>-</sup> ONSO <sub>3</sub> <sup>-</sup>                                      | 3.2 × 10 <sup>10</sup>  | 10.6 |
| 33. NO(aq) + <sup>-</sup> ONSO <sub>3</sub> <sup>-</sup>                             | → | <sup>-</sup> ON(NO)SO <sub>3</sub> <sup>-</sup>                                  | c                       |      |
| 34. <sup>-</sup> ON(NO)SO <sub>3</sub> <sup>-</sup>                                  | → | N <sub>2</sub> O + SO <sub>4</sub> <sup>2-</sup>                                 | 1.55 × 10 <sup>-3</sup> |      |
| 35. NO <sub>2</sub> (aq) + NO <sub>2</sub> (aq)                                      | → | HNO <sub>2</sub> (aq) + NO <sub>3</sub> <sup>-</sup> + H <sup>+</sup>            | 8.4 × 10 <sup>7</sup>   |      |
| 36. HSO <sub>3</sub> <sup>-</sup> + 2NO <sub>2</sub> (aq)                            | → | 2NO <sub>2</sub> <sup>-</sup> + 3H <sup>+</sup> + SO <sub>4</sub> <sup>2-</sup>  | 1.2 × 10 <sup>7</sup>   |      |

a. k in units of M<sup>-1</sup> sec<sup>-1</sup> or sec<sup>-1</sup>; K in units of M; H in units of M atm<sup>-1</sup>

b. In units of kcal mol<sup>-1</sup>

c. reactions 17,18 and 33 are assumed to be fast.

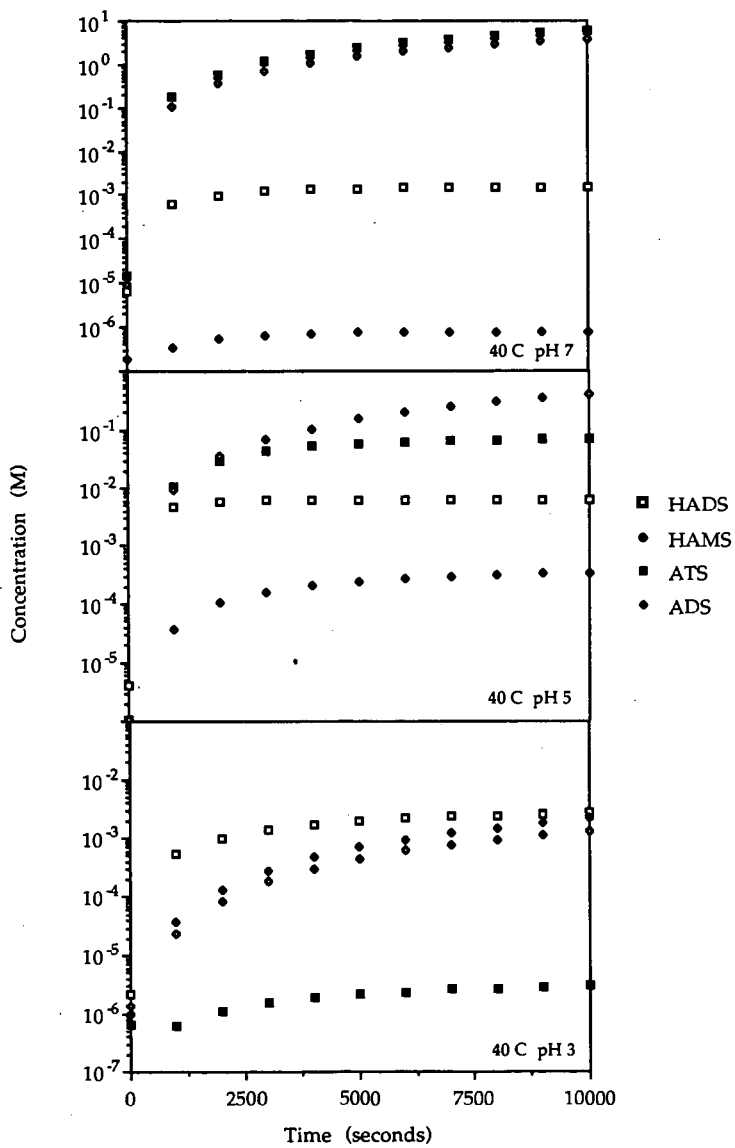


Figure 1

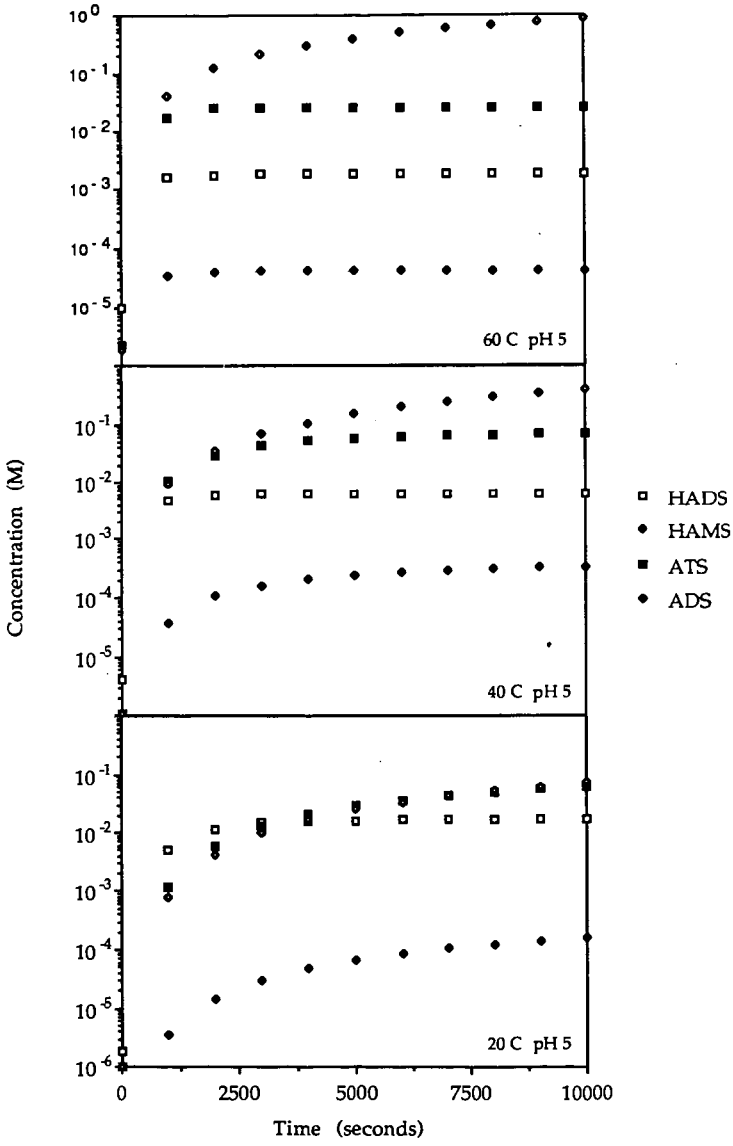


Figure 2

## NITROGEN OXIDE REBURNING WITH HYDROCARBON FUELS

Thomas E. Burch, Franz R. Tillman, Wei-Yin Chen\*, and Thomas W. Lester

*Department of Mechanical Engineering, Louisiana State University, Baton Rouge, LA 70803*

*\*Corresponding Author; Present Address: Department of Chemical Engineering, University of Mississippi, University, Mississippi 38677*

**Keywords:** Nitrogen Oxides, Reburning, Fuel Effects

### Introduction:

Reburning (or fuel staged combustion) is a furnace  $\text{NO}_x$  control process that utilizes the reduction powers of hydrocarbons. This concept and the term reburning were first proposed by Wendt, et al. (1973). However, reburning was not established as a practical  $\text{NO}_x$  reducing method until Takahashi, et al. (1983) reported greater than 50% reduction of NO in tests at Mitsubishi Heavy Industries. Reburning comprises three zones in the combustion process. The primary zone is the main heat release zone in which approximately 80% of the fuel is burned in a fuel lean (SR = 1.1) environment. This is followed by a reburning zone where additional fuel is added to give an overall fuel rich stoichiometry (ca. SR = 0.9). Finally additional air is provided in the burnout zone to complete the combustion process by burning off residual hydrocarbons in a fuel lean environment.

This study addresses the mechanisms of NO reduction in pulverized coal combustion using reburning. The interactions between NO and hydrocarbon constituents in the fuel, and the fate of fuel nitrogen are the focal points of this research. Nitrogen oxide reduction and formation mechanisms in reburning stage are investigated with a laboratory scale flow reactor. Feed to the reactor includes simulated flue gas and reburning fuels (methane, benzene, hexane, coal, and lignite). This paper discusses the implications of nitrogen product distribution as functions of second stage stoichiometry and reburning fuel type. In addition, a unique GC/MS technique established for the systematic analysis of flue gas will be presented.

### Experimental:

The experiments reported here were carried out in a ceramic flow reactor (Figure 1) with a simulated flue gas consisting of 16.8%  $\text{CO}_2$ , 1.95%  $\text{O}_2$ , and 0.1% NO in a helium base. These concentrations of  $\text{CO}_2$ ,  $\text{O}_2$ , and NO were chosen to be consistent with those of a coal primary flame operated at a stoichiometric ratio of 1.1. Helium, instead of nitrogen, was used as the base gas to minimize heating time due to its low heat capacity.

The flow reactor used for this research was an alumina tube (Coors Ceramics Co.) with an inside diameter of 0.75 in. and an overall length of 24 in. The central portion of the reactor tube was enclosed in a 12 in. long electrically heated furnace (Lindberg Model 55035) which provided tube temperatures up to 1150°C.

For experiments using coal as a reburning fuel, the delivery system was modified to incorporate a laboratory scale coal feeder shown schematically in Figure 2. Details of this device have been reported elsewhere (Burch, et al. 1990). The coal feeder required part of the gas flow (usually helium) to be diverted through the coal feeder for use as carrier gas.

The sampling train consisted of 0.25 in stainless steel transfer lines and switching manifold with stainless steel valves. Transfer lines from the reactor tube exit to the impinger were heat traced to prevent absorption of HCN and  $\text{NH}_3$ . The effluent was desiccated with anhydrous calcium sulfate before transfer to the instrument package through 0.25 in teflon tubing. For coal experiments, the sampling train was modified to allow the gaseous products (and particulate matter) to pass straight through the end of the reactor tube into a paper filter before entering the transfer lines. The filter was enclosed in a glass housing and heated to 100°C. Recovery tests showed no loss of HCN or  $\text{NH}_3$  in the filter. A 10  $\mu\text{m}$  filter was also added upstream of the desiccant dryer for coal experiments. The flow reactor was maintained near atmospheric pressure by providing an atmospheric vent downstream of the instrument package and monitoring the supply gas pressure in the mixing chamber.

HCN and  $\text{NH}_3$  were collected by diverting the reactor effluent through a straight tube impinger filled with 0.5 L of 0.1N  $\text{HNO}_3$  aqueous solution for a specified time interval. The captured solutions were pH adjusted using NaOH

and analyzed for CN- and dissolved ammonia with specific ion electrodes (Orion Research). Poisoning of the cyanide electrode by sulfur ions from coal combustion was prevented by adding an aqueous solution of  $PbNO_3$  prior to adding the NaOH. Sulfide ions were precipitated as  $PbS$ . Recovery of HCN and  $NH_3$  by this method was tested using known standards and found to be near quantitative for  $NH_3$  but only 70% for HCN. Thus  $NH_3$  values have been presented as measured while HCN values reported have been corrected for collection efficiency.

Qualitative analysis or separation of nitrogenous species were also performed by GC/MS. Samples of the reactive effluent were captured in 300  $cm^3$  stainless steel containers. To eliminate contamination from past runs the containers were heated under vacuum between runs to remove HCN and  $NH_3$  absorbed into the walls.

Two chromatographic columns were used for separation of the nitrogen compounds.  $N_2$  and NO were effectively separated from other fixed gases on a 20 ft x 1/8 in S.S. Hayesep D<sub>3</sub> column (Hayesep separations) at 25°C isothermal. Separation of  $NH_3$  and HCN was accomplished using an 8 ft x 1/8 in. S.S. Hayesep C column operated at 80°C for  $NH_3$  and 120°C for HCN. Due to active sites on the column, low concentrations of these specifics (less than 200 ppm) required several saturation injections and isothermal conditions to give quantifiable mass peaks. Lower concentrations of  $NH_3$  and HCN (less than 75 ppm) were analyzed by "loading" the column with repeated injection onto a cold column (25°C). The oven temperature was then rapidly raised to the desired operating temperature to facilitate elution. This procedure was repeated until the yields of the HCN and  $NH_3$  were stabilized, signifying that active sites were filled with species from the current sample.

GC/MS samples were injected via evaluated and heated static injection loops. For fixed gas analysis, a 10  $cm^3$  S.S. loop was used. For HCN and  $NH_3$  analysis a 40  $cm^3$  S.S. loop was used to help overcome low concentrations and active column sites.

## Results and Discussion:

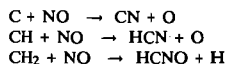
### - Gaseous Fuels Results

Reburning experiments were conducted for methane, hexane and benzene at a reburning temperature of 1100°C and an estimated reaction time of 0.2 seconds. The stoichiometry for these tests was varied from SR = 0.7 to 1.0. The resulting TFN (total fixed nitrogen; ie, all nitrogen species except  $N_2$ ) speciation profiles are illustrated in cumulative fashion by the curves in Figure 3 through 5.

The minimum TFN for each of these fuels occurred near SR = 0.95 under these conditions. However, the minimum value attained and the sensitivity to stoichiometry were found to be considerably different for the three fuels. Also, the TFN speciation in the neighborhood of the minimum TFN was radically different.

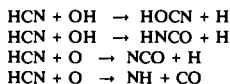
For methane the dominant fixed nitrogen species at the optimum stoichiometry was NO which accounted for more than 85% of the total. In benzene reburning, the contribution of NO at the optimum stoichiometry was only 2% of the total with HCN making up 75%. Hexane fell in between these two extremes with NO and HCN contributions of 33% and 60% respectively. It is interesting to note that hexane exhibited the lowest TFN.

Employing the mechanisms and sensitivity analysis of Miller and Bowman (1989) along with calculations conducted by Chen et al. (1989) it seems reasonable to view reburning as possessing two major kinetic barriers. The first barrier is the conversion of NO to HCN by combination with various hydrocarbon fragments such as



The accepted rate constants for these reactions are all within roughly one order of magnitude so the dominant mechanism in the conversion of NO to HCN is strongly dependent on the relative concentrations of the reducing species produced. Regardless of which mechanism dominates, there is general agreement that the end product is HCN, whether formed directly or by rapid conversion of intermediates such as CN.

The second major kinetic obstacle appears to be oxidation of HCN via one of the following reactions:



Having accomplished this step the subsequent conversion to N atoms is rapid. N atoms are then recycled to form NO or react with NO to form N<sub>2</sub>.

Using this two barrier concept many of the salient features of reburning can be interpreted. First the concentration and longevity of reducing species at near stoichiometric conditions is so low that substantial quantities of the initial NO remains unreacted. As the stoichiometry is shifted to more fuel rich conditions, competition from other oxidizing species decreases allowing concentrations of reducing species to build and react with NO. Thus at richer stoichiometries, most of the NO is converted to HCN. Actually the concentration of reducing species appears to peak somewhere around SR = 0.9, then slowly declines as the stoichiometry becomes more fuel rich. However, the general trend described above appears valid.

The concentration of oxidizing species needed to overcome the second barrier follows an opposite trend. At lean stoichiometries the populations of O and OH are high, effectively converting most form HCN to subsequent species. As the stoichiometry becomes richer the concentration of oxidizing species is depleted by reaction with abundant reducing species.

Thus, in leaner stoichiometries, the dominant kinetic barrier appears to be the initial reduction of NO whereas in rich stoichiometries the conversion of HCN to subsequent species is the major obstacle. The optimum stoichiometry is then defined by a compromise between these processes. Based on this admittedly simplistic argument the behaviour exhibited in Figures 3 through 5 can be interpreted.

For methane, the fact that the minimum TFN contains primarily NO indicates that reduction of NO to HCN is the limiting factor. The carbon to hydrogen ratio of methane (1 to 4) may not provide enough of the appropriate reducing species to effectively convert NO to HCN until the stoichiometry becomes too fuel rich to sustain good populations of O and OH.

Although any comments on the breakup of hexane and benzene is somewhat speculative, one might expect these fuels which are more carbon rich to produce CH<sub>i</sub> (i > 0, 1, 2) fragments in greater numbers at stoichiometries lean enough to still support substantial O and OH populations. The hexane curves (Figure 4) seem to follow this reasoning in that more of the NO has apparently been converted to HCN at SR = 0.95 where a substantial quantity of the HCN produced was converted to subsequent species leading to N<sub>2</sub>.

Benzene shown in Figure 5, continued the trend of increasing reduction of NO to HCN as the carbon content of the fuel increased. However, the expected attending conversion of HCN to N<sub>2</sub> at this relatively lean stoichiometry was not observed. Perhaps the benzene oxidation mechanism is such that O and OH species are consumed too rapidly (or not produced at all) to allow for the conversion of HCN.

The timing of peak concentrations of important species is also critical. Since the conversion of HCN to N<sub>2</sub> by necessity succeeds the reduction of NO to HCN, high populations of NO reducing species occurring after O and OH have been depleted serve to reduce NO but not TFN.

One final observation is that the true optimum stoichiometry for benzene (or methane) may not have been found. The high levels of HCN at SR = 0.95 would seem to suggest that a leaner stoichiometry might yield a better conversion of HCN to N<sub>2</sub> without seriously impairing the reduction of NO to HCN. Similarly, the high NO and low HCN exhibited by methane at SR = 0.95 would indicate a slightly richer stoichiometry might improve overall TFN levels.

#### *Coal Results*

Reburning experiments were conducted for a Pittsburgh #8 bituminous coal and a North Dakota lignite with reburning conditions identical to those used for gaseous fuels. The analyses of the two coals used are given in Table 1.

Each of the coals were sieved between 200 and 270 mesh to provide a uniform particle size for feeding and to eliminate particle size considerations in comparison of results.

Char samples were collected from reburning experiments ranging from  $SR = 0.7$  to  $SR = 1.0$ . Analysis of these samples for each coal showed no more than a statistical variation in nitrogen retained in the char. On average, lignite char retained 50% of the nitrogen contained in the coal whereas bituminous char contained 58% of the original nitrogen. Apparently, reburning with these conditions involves primary devolatilization with little or no char oxidation taking place. Average data were used to determine char nitrogen with ash as a tracer.

The cumulative TFN speciation for the Pittsburgh #8 coal is shown in Figure 6. The most notable feature of this graph is that the minimum gas phase TFN occurs at  $SR2 = 0.85$  whereas for gaseous fuels  $SR = 0.95$  produced minimum TFN. This is reasonable if reburning is considered to be controlled primarily by homogeneous gas phase reactions. Since part of the hydrogen were retained in the solid phase as char, the gas phase stoichiometry was somewhat leaner than the overall stoichiometry.

The gas phase TFN exhibited by the Pittsburgh #8 coal appears very similar to a stretched version of the hexane distribution both in minimum TFN value and speculation. However, the retained char nitrogen added considerably to the fixed nitrogen pool and accounted for more than 65% of the total at  $SR = 0.85$ .

Lignite reburning produced more novel results as shown in Figure 7. The minimum TFN for lignite occurred at  $SR = 0.9$  owing partially to higher volatility of combustible species. Surprisingly, reduction of NO was nearly complete for stoichiometries below  $SR = 0.85$  achieving levels below 1 ppm. Another unusual feature is that for all stoichiometries below  $SR = 0.90$  the gas phase TFN is totally dominated by  $NH_3$ . HCN levels never exceeded 17 ppm at any stoichiometry.

Although fuel rich combustion and pyrolysis experiments reported in the literature (eg. Chen, et al., 1982) have shown high levels of  $NH_3$  from lignites the results presented here differ in that much of the gas phase nitrogen in these experiments did not originate in the coal. The extremely low NO and HCN levels (normally the dominant species in reburning) suggest that most of the original NO has been converted to either  $NH_3$  or  $N_2$ . These peculiar results spanned an effort to isolate the reason for this behavior and to see if the low NO, low HCN, and high  $NH_3$  levels were related.

Heterogeneous reactions of NO are usually discounted in reburning as too slow to be of any consequence. However, a suitable gas phase mechanism could not be found so the search was directed toward heterogeneous mechanisms. The following sequence of tests was conducted and the corresponding results given.

The effect of char addition rate on surviving NO levels with varying gas composition was studied. The char was collected from lignite reburning at  $SR = 0.85$ . First, the standard gas composition used for other reburning experiments (i.e. 16.8%  $CO_2$ , 1.95%  $O_2$ , 1000 ppm NO, balance He) was used. For reference a char feed rate of 0.029 gm/min corresponds to the char loading found in lignite reburning at  $SR = 0.9$ . The results are shown in Curve 1 of Figure 8. As the char feed rate was increased, the surviving NO levels gradually decreased and then abruptly fell to less than 10 ppm. This precipitation decline was accompanied by the disappearance of measurable  $O_2$  in the reactor effluent. This suggested competition for active sites on the char surface.

The results shown in Curve 2 of Figure 8 were obtained by replacing the  $O_2$  in the feed gas with helium so that  $CO_2$  remained the only oxidizer competing with NO for active sites. The elimination of  $O_2$  had a profound effect in that very low surviving NO levels were measured with significantly reduced char feed rates. However, some competition for active sites persisted as evidenced by the reduction of  $CO_2$  to CO when char was fed.

Finally, the effect of char on surviving NO with only NO and He in the feed gas is shown in Curve 3 of Figure 8. Eliminating the  $CO_2$  from the feed gas further reduced the required char feed rate to the point that any char feed resulted in almost total elimination of NO from the reactor effluent.

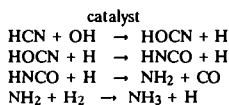
In all of the above tests only low levels of HCN and  $NH_3$  were formed because of the absence of available hydrogen. Also, the reaction was almost certainly heterogeneous instead of surface catalyzed gas phase since gas phase reactants were almost non-existent. DeSoete (1980) gives an excellent review of possible mechanisms.

Next attention was turned to the unusually high production of  $\text{NH}_3$  in lignite reburning. Again heterogeneous effects were suspected. To confirm this, a methane reburning experiment was conducted at  $\text{SR} = 0.9$  with char addition at a rate of approximately 0.0194 gm/min. The results of this experiment (shown in Table 2) were very similar to those from lignite reburning. The only difference of note was the lower NO level produced by methane/char reburning because of the richer gas phase stoichiometry.

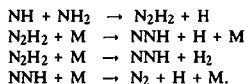
Next, lignite ash was produced by burning char in excess  $\text{O}_2$  at  $1100^\circ\text{C}$  and fed with methane at  $\text{SR} = 0.9$ . Again, high levels of  $\text{NH}_3$  were produced as shown in Table 2. However, in this experiment the surviving NO level was similar to that when reburning with methane alone. Also, the  $\text{NH}_3$  level was almost twice that of methane/char reburning.

Since the ash contained very little carbon, the direct heterogeneous reduction of NO on carbon was eliminated. This caused more of the nitrogen to be converted to HCN as in reburning with methane alone.

In the final experiments, (shown in Table 2) NO was replaced with approximately 500 ppm of HCN in methane/char reburning. Again the final TFN distribution was weighted heavily in favor of  $\text{NH}_3$ . Although not conclusive, these tests strongly indicate that increased  $\text{NH}_3$  production with lignite reburning was the result of HCN conversion in an ash catalyzed reaction. However, direct conversion by addition of  $\text{H}_2$  would seem unlikely. A mechanism such as the sequence



would be more plausible. In the mechanism, some of the HCN converted to  $\text{NH}_2$  would be subsequently converted to  $\text{N}_2$  via



Thus the lower total fixed nitrogen found in methane/ash versus methane alone would be accounted for.

The usually strong heterogeneous and/or catalytic effects observed with lignite char are particularly interesting in light of the apparent absence of such effects with bituminous char. The reason for this disparity is not known and may be due to differences in the nature of the chars.

The lignite ash (PSOC 1507) composition as reported by the Pennsylvania State University Coal Research Section was unusually rich in calcium oxide (23.2%), barium (6570 ppm), and strontium (4900 ppm). On the basis of concentrations alone, these seem to be the most likely candidates for catalysts.

The heterogeneous reduction of NO is most likely due to the large surface area of the very porous and friable lignite char. However, this may also be a catalytic effect. Several authors including Walker et al. (1968) have observed enhancement of char oxidation rates when the chars were impregnated with various transition metal compounds.

## Conclusions

The choice of fuels has a very definite impact on the TFN speciation and minimum TFN achievable in reburning. The estimated NO concentrations after burnout for the fuels tested in this work can be calculated based on 80% conversion of gas phase fixed nitrogen and 20% conversion of char nitrogen to NO. From these calculations, it would appear that the lignite has the greatest potential in spite of its fuel bound nitrogen.

The strong heterogeneous/catalytic activity of the lignite char could have important consequences for practical reburning enhancement. It appears that lignite char at least partially removes the current kinetic barriers in reburning

by directly converting NO to N<sub>2</sub> and by converting HCN to other nitrogenous species that are more readily converted to N<sub>2</sub>.

Addition of lignite char in methane, reburning reduced gas phase TFN by 71%. If the char could be produced with low nitrogen constant or used in smaller quantities without adversely affecting the desirable characteristics, overall TFN could be reduced to extremely low levels. Even the simple addition of lignite ash in methane reburning reduced TFN levels by 39% over methane alone. Although temperature, scale up, and mixing effects need to be studied and may impact the utility of this scheme, enhanced reburning by injection of suitable char/ash may show some promise.

### Acknowledgements

The work reported in this paper was funded by the U.S. Department of Energy, Pittsburgh Energy Technology Center under contract No. DE-AC22-88PC88859.

### References

- Burch, T.E., R.B. Conway, and W.Y. Chen, "A Practical Coal Feeder for Bench-Scale Combustion Requiring Low Feed Rates", submitted to Review of Scientific Instruments, Feb., 1990.
- Chen, S.L., M.P. Heap, D.W. Pershing, and G.B. Martin, "Fate of Coal Nitrogen during Combustion," Fuel, **61**(12), 1218 (1982)
- Chen, W.Y., T.W. Lester, L.M. Babcock, T.E. Burch, and F.R. Tillman, "Formation and Destruction of Nitrogen Oxides in Coal Combustion", Sixth Quarterly Report, DOE Contract No. DE-AC22-88PC88859, July 1989.
- DeSoete, G.G., "Mechanisms of Nitric Oxide Reduction on Solid Particles", Fifth EPA Fundamental Combustion Research Workshop, Newport Beach, January, 1980.
- Miller, J.A. and C.T. Bowman, "Mechanism and Modelling of Nitrogen Chemistry in Combustion", Prog. Energy Combustion Science, Vol. 15, p. 287, 1989.
- Takahashi, Y., T. Sengoku, F. Nakashima, S. Kaneko, and K. Tokuda, "Evaluation of Tangential Fired Low NO<sub>x</sub> Burner", Proc. 1982 Joint Symposium Stationary NO<sub>x</sub> Control, Vol. 1, "EPRI Report No. CS-3182, July, 1983.
- Walker, P.L., M. Shelef, and R.T. Anderson, "Catalysis of Carbon Gasification", Chemistry and Physics of Carbon, Vol. 4 (Walker, P.L., Ed.), Marcel Dekker, New York, NY, 287, 1968.
- Wendt, J.O.L., C.V. Sternling, and M.A. Matovich, "Reduction of Sulfur Trioxides and Nitrogen Oxides by Secondary Fuel Injection", Fourteenth Symposium (International) on Combustion, p. 897, The Combustion Institute, 1973.

Table 1. Analysis of Coals

|               | Pittsburgh #8,<br>Bituminous | North Dakota Lignite<br>(PSOC 1507) |
|---------------|------------------------------|-------------------------------------|
| Moisture*     | 2.02                         | 33.57                               |
| Carbon        | 70.48                        | 62.61                               |
| Hydrogen      | 4.66                         | 4.41                                |
| Oxygen (Diff) | 8.53                         | 18.23                               |
| Nitrogen      | 1.44                         | 0.83                                |
| Sulfur        | 3.35                         | 1.43                                |
| Ash           | 11.54                        | 12.49                               |
| Vol. Matter   | 33.25                        | 40.77                               |
| Fixed Carbon  | 55.21                        | 46.75                               |

\*Moisture is reported on an as received basis all other results are on a dry basis.

Table 2. Total Fixed Nitrogen Speciation with Addition of Lignite Char/Ash.

| Reburning Fuel        | CH <sub>4</sub> | Lignite | CH <sub>4</sub> /char | CH <sub>4</sub> /ash | CH <sub>4</sub> /char |
|-----------------------|-----------------|---------|-----------------------|----------------------|-----------------------|
| N in Feed             | NO              | NO      | NO                    | NO                   | HCN                   |
| Concentration, ppm    | 1000            | 1000    | 1000                  | 1000                 | 500                   |
| Effluent Species      |                 |         |                       |                      |                       |
| NO, ppm               | 90              | 32      | 5                     | 70                   | 1                     |
| HCN, ppm              | 308             | 12      | 9                     | 10                   | 12                    |
| NH <sub>3</sub> , ppm | 105             | 135     | 130                   | 227                  | 51                    |

Gas phase SR = 0.9 for all tests.

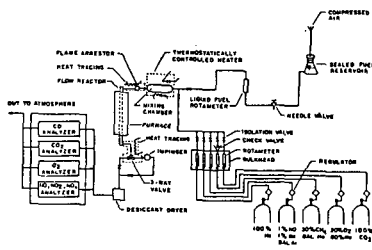


Figure 1. Schematic of experimental facility.

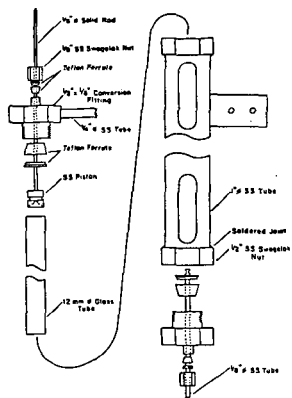


Figure 2. Exploded view of coal feeder assembly.

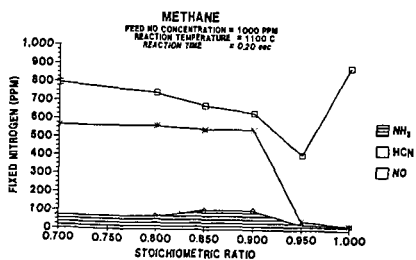


Figure 3. Cumulative total fixed nitrogen for methane reburning.

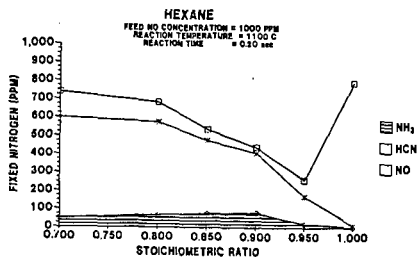


Figure 4. Cumulative total fixed nitrogen for hexane reburning.

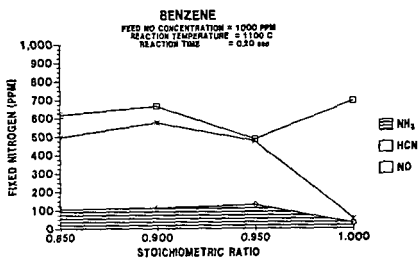


Figure 5. Cumulative total fixed nitrogen for benzene reburning.

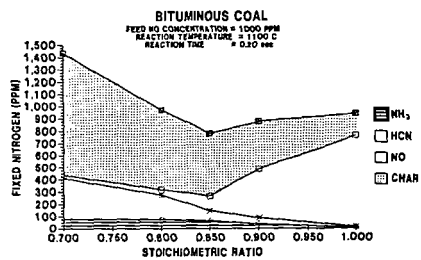


Figure 6. Cumulative total fixed nitrogen for reburning with Pittsburgh #8 bituminous coal.

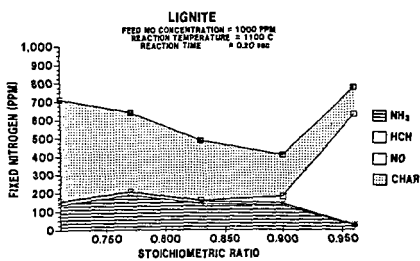


Figure 7. Cumulative total fixed nitrogen for reburning with Zap, North Dakota lignite.

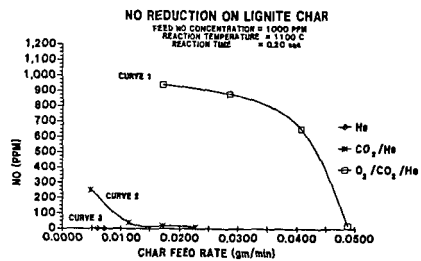


Figure 8. Influence of gas composition on heterogeneous reduction of NO with lignite char.

PROCESS DESIGN AND CHEMISTRY  
OF THE  
NOXSO PILOT PLANT DEMONSTRATION

Rita E. Bolli, John L. Haslbeck<sup>1</sup>, B. Dwight Coffin<sup>2</sup>, and L. G. Neill<sup>1</sup>

Ohio Edison Company  
Environmental and Special Projects Dept.  
76 South Main Street  
Akron, OH 44308

<sup>1</sup>NOXSO Corporation, Library, PA  
<sup>2</sup>MK-Ferguson Company, Cleveland, OH

Key Words: NOXSO, FGT (flue gas treatment), pollution (control technology).

ABSTRACT

Ohio Edison Company, NOXSO Corporation, MK-Ferguson, and W. R. Grace Co. are conducting a Proof-of-Concept (POC) test of the NOXSO flue gas treatment system at Ohio Edison's Toronto Plant in Toronto, Ohio. The project is co-funded by the U.S. Department of Energy's (DOE) Pittsburgh Energy Technology Center (PETC), the Ohio Coal Development Office and the project team. The pilot plant treats flue gas from either Boiler No. 10 or No. 11 at Toronto containing approximately 2300 ppm SO<sub>2</sub> and 350 ppm NO<sub>x</sub>. The pilot plant treats a volume of flue gas equivalent to 5 MW of power production, which makes the pilot plant roughly 1/20 the size of a commercial process module. This paper presents the design and process chemistry of the pilot test facility.

Background

On May 10, 1989, a consortium consisting of Ohio Edison, NOXSO Corporation, MK-Ferguson, and W. R. Grace Co. signed a cost-shared contract with the DOE/PETC to conduct a Proof-of-Concept (POC) test of the NOXSO process. The POC project will take approximately three years to complete, and the test will be conducted at Ohio Edison's Toronto Plant at Toronto, Ohio.

POC Test Site

The POC unit will treat flue gas from either Boiler No. 10 or No. 11 at Ohio Edison's Toronto Plant. Two sources of flue gas will be tapped so that the POC test can continue as long as one of the boilers is operating. A slipstream of flue gas will be taken from either boiler in the amount of 12,000 SCFM. The slipstream will be taken downstream of the Toronto Plant's electrostatic precipitators (ESPs) which remove 99 percent of the particulate matter from the flue gas. The Toronto boilers are pc-fired and burn Ohio coal containing 3.7 percent sulfur. The flue gas typically contains 2300 ppm SO<sub>2</sub> and 350 ppm NO<sub>x</sub>.

POC Test Schedule

Detailed design engineering has been completed and the major pieces of equipment have been ordered. Construction began in March 1990 and will be completed in November 1990. The test is scheduled to begin in January 1991 and will run through August 1991.

### POC Process Flow Diagram

The process flow diagram for the POC is shown in Figure 1. The system is best described by following the flow of flue gas, sorbent, and regeneration gas through the process.

Flue gas will be available from either Boiler No. 10 or No. 11 at the Toronto facility and will be taken downstream of the respective ESP. The base case condition will treat 12,000 SCFM of flue gas, equivalent to approximately 5 MWe. The flue gas, once past the ESP, will enter the NOXSO flue gas treatment system. The flue gas first passes through the adsorber feed blower and then is cooled by vaporizing a water stream sprayed directly into the duct work. The cooled flue gas then passes through the fluidized bed adsorber where  $\text{SO}_2$  and  $\text{NO}_x$  are simultaneously removed. The clean flue gas then enters a cyclone that returns entrained sorbent larger than 20 microns back to the adsorber fluid bed. Attrited sorbent smaller than 20 microns diameter will pass through the cyclone along with any flyash remaining in the flue gas, and the entire stream will pass through a baghouse for final particulate removal.

After the sorbent is loaded with  $\text{SO}_2$  and  $\text{NO}_x$ , it is removed from the adsorber and feeds the dense phase pneumatic conveying system. Fresh make-up sorbent is also added to the dense phase conveying system from the make-up sorbent bin. Compressed air is then used to lift the sorbent to the sorbent heater. The sorbent passes through a disengaging chamber where the lift air is separated from the sorbent. The sorbent heater is a three-stage fluidized bed where a hot air stream is passed countercurrent through the reactor raising the sorbent temperature from the adsorber temperature of  $250^\circ\text{F}$  to the regeneration temperature of  $1220^\circ\text{F}$ . During the heating process, loosely bound  $\text{SO}_2$  and  $\text{NO}_x$  are desorbed and transported away in the heating gas stream. The hot gas stream exiting the sorbent heater passes through a cyclone which returns entrained sorbent larger than 20 microns to the top bed. Finally, the hot air is combined with the clean flue gas from the adsorber and the combined streams pass through the baghouse for final particulate removal. Alternatively, the hot air from the sorbent heater may bypass the baghouse and combine with the clean flue gas downstream of the baghouse. The combined streams are then returned to the downstream side of the plant ESP from where the gas will exit the plant stack.

Once the sorbent reaches the regeneration temperature of  $1220^\circ\text{F}$ , it is fed by means of a J-valve to the moving bed regenerator. The J-valve is used to both control the solid feed rate to the regenerator and to isolate the sorbent heater from the regenerator. In the regenerator, sorbent is contacted with natural gas in a countercurrent fashion. The off-gases from both sections of the regenerator are then sent to an incinerator where all the sulfur species are oxidized to  $\text{SO}_2$ . Any excess  $\text{CH}_4$  that passes through the regenerator will also be oxidized to  $\text{CO}_2$  and  $\text{H}_2\text{O}$ . Both combustion air and natural gas are provided to maintain the incinerator flame. The incinerator exhaust is cooled with air to  $1200^\circ\text{F}$  and returned to the power plant duct.

From the steam treatment vessel, the sorbent is again transferred by means of a J-valve to the sorbent cooler. The sorbent cooler is also a three-stage fluidized bed and is also operated in a countercurrent manner. Ambient air passes first through the cooling air blower and then through the three fluid beds. The warm air exiting the cooler is further heated in a natural gas-fired

air heater before being used to heat the sorbent in the sorbent heater. The sorbent temperature is reduced in the cooler to the adsorber bed temperature (248°F) and is then gravity fed to the sorbent surge bin. Finally, by means of another J-valve, the sorbent is fed from the surge bin to the adsorber completing one full cycle.

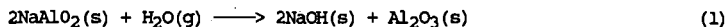
The POC facility differs from a commercial application of the NOXSO technology in two important areas. First, the POC facility does not include a Claus plant, which in the commercial design would be used to produce a sulfur by-product from the concentrated stream of SO<sub>2</sub> and H<sub>2</sub>S produced in the regenerator. This is because Claus technology is commercially available and, therefore, does not require testing at pilot scale. Second, the POC does not include NO<sub>x</sub> recycle to the coal combustor. In the commercial design, NO<sub>x</sub> in the air leaving the sorbent heater is recycled to the combustor as part of the combustion air. Since NO<sub>x</sub> formation in the coal combustor is a reversible reaction, addition of NO<sub>x</sub> to the combustion air suppresses the formation of NO<sub>x</sub> in the combustor. Since this is an important feature of the NOXSO process, the results of tests on NO<sub>x</sub> recycle are presented in this paper. However, NO<sub>x</sub> recycle is impractical in the POC test, since the POC treats less than 10 percent of the flue gas produced by Toronto Boiler 10 or 11.

#### NOXSO PROCESS CHEMISTRY

The NOXSO process chemistry is relatively simple. It involves the chemistry of adsorbing the SO<sub>2</sub> and NO<sub>x</sub> pollutants and the chemistry of regenerating the sorbent for reuse using natural gas as shown below.

##### Adsorption

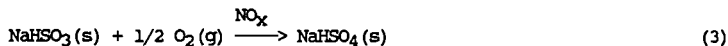
The NOXSO sorbent consists of NaAlO<sub>2</sub> on the surface of a gamma alumina substrate. Sodium aluminate adsorbs SO<sub>2</sub> according to the following reaction mechanism:



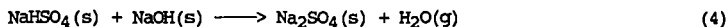
Sodium hydroxide reacts with SO<sub>2</sub> in the flue gas as follows:



The sodium bisulfite is subsequently converted to bisulfate in a reaction with O<sub>2</sub> in the flue gas with NO<sub>x</sub> acting as a catalyst.



The bisulfate combines with a neighboring active site to form sodium sulfate.

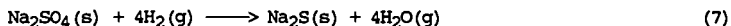
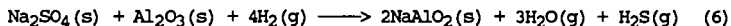


By a similar mechanism, sodium hydroxide adsorbs NO<sub>x</sub> from the flue gas to form NaNO<sub>2</sub> and NaNO<sub>3</sub>.

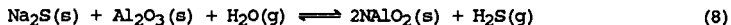
### Regeneration

Regeneration is accomplished by heating the spent sorbent in air followed by treatment with a reducing gas. The reducing gas is used solely to reduce sorbed sulfur compounds. Treatment with the reducing gas produces a mixture of sulfur compounds:  $\text{SO}_2$ ,  $\text{H}_2\text{S}$ , and elemental sulfur.

The chemistry of the regeneration step is complex, involving the reduction of sodium-sulfur and alumina-sulfur compounds. Reactions involving the reduction of sodium-sulfur compounds with hydrogen are as follows:



Reaction (7) above produces a sulfide which remains on the sorbent after it has been treated with the reducing gas. In tests to date, the sorbent has been treated with steam, following treatment with the reducing gas, to hydrolyze the sulfide to form  $\text{H}_2\text{S}$  according to reaction (8):



The product of  $\text{NO}_x$  chemisorption, in the case of both the sorbent and the alumina, is unstable at temperatures in the range 350–400°F. Therefore, the sorbent's activity toward  $\text{NO}_x$  is completely restored as the sorbent is heated to the sulfur regeneration temperature of 1220°F. The sorbent is heated with air in a fluidized bed. The concentrated stream of  $\text{NO}_x$  in air produced on heating the spent sorbent is recycled to the boiler with the combustion air.

The technical feasibility of returning the  $\text{NO}_x$  to the combustor was evaluated in two previous pilot tests. The data show that 65 percent and 75 percent of the  $\text{NO}_x$  returned to the combustor, depending upon the combustor configuration is reduced in the combustor. These tests proved that the technique is feasible although its use will result in a slightly higher equilibrium concentration of  $\text{NO}_x$  in the flue gas relative to the concentration prior to  $\text{NO}_x$  recycle.

### POC TEST UNIT DESIGN

#### Adsorber

Internals for the POC adsorber were designed by Dr. Frederick Zenz, a noted expert in the field of fluid bed engineering. The adsorber grid (gas distributor) is a flat perforated plate containing 72,700, 1/16" diameter holes spaced 0.45" center to center on a square pitch. To ensure smooth fluidization, the grid pressure drop was set at 30 percent of the pressure drop across the sorbent bed. The grid pressure drop sets the gas velocity through the grid plate and the grid hole area (given flue gas flow rate). The size of the grid holes is predicated on the observation that holes no larger than four times the particle diameter ( $d_p = 1409$  microns) will not weep on complete shutdown but will inevitably seal off by particle interference or blockage at the lip of the grid hole. A similar approach was used to design the grid plates in the three-staged fluid bed sorbent heater and cooler.

Sorbent is fed to the adsorber through a 6" line entering below bed level and sloped 60° for the horizontal to minimize attrition by minimizing the force of impact as sorbent particles "fall" into the bed. Sorbent leaves the bed by overflow into a 6" downcomer with a detachable section that may be changed to test different bed heights in the adsorber.

Flue gas enters the adsorber at a flow rate of 14,780 ACFM at 233°F. The chemical reactions in the adsorber are exothermic so that the adsorber bed temperature is 250°F. The superficial gas velocity in the adsorber is 2.8 ft/sec, approximately 2.4 times greater than the minimum fluidization velocity and a factor of three less than the terminal velocity of the smallest particle in the bed. At baseline conditions, the sorbent circulation rate is 9,673 pounds per hour into the adsorber. The adsorber settled bed height is two feet, and the sorbent residence time is 45 minutes.

#### Fluidized Bed Sorbent Heater/Cooler

A fluidized bed is used heat and cool the sorbent because of its extraordinarily effective thermal conductivity. In previous tests, a single stage fluidized bed was used. However, multistaged fluidized beds are preferred since adding more beds increases the efficiency at which the heat in gas and solids is utilized. Energy efficiency was not a primary concern in previous tests. Energy efficiency is a major concern in the POC test, since the POC unit is intended to duplicate the design of the commercial unit.

The fluidized bed internals (i.e., pipes to transport sorbent in and out, standpipes, gas distributor plates, etc.) were designed by Dr. Frederick Zenz in a manner similar to that discussed previously in connection with the fluidized bed adsorber.

#### Regenerator

Regeneration of the NOXSO sorbent consists of three steps: Heating to 1220°F, contacting with a reducing gas, and contacting with steam. In the first step, heating the sorbent, adsorbed NO<sub>x</sub> is desorbed from the sorbent surface. Measurements made during the LCTU tests show that from 76 percent to 99 percent of the adsorbed NO<sub>x</sub> was detected in the sorbent heater offgas. Within limits of measurement error, this represents complete regeneration of the sorbent with respect to NO<sub>x</sub>.

Besides NO<sub>x</sub>, some adsorbed SO<sub>2</sub> is released in the sorbent heater. Based on LCTU results, from 2.2 percent to 8.6 percent of the adsorbed SO<sub>2</sub> was detected in the sorbent heater offgas stream with an average of 6 percent.

After reaching the regeneration temperature of 1220°F, the sorbent is transferred from the sorbent heater to the moving bed regenerator. The adsorbed sulfur compounds are regenerated by contacting the sorbent with a reducing gas followed by steam. During the three completed test programs, H<sub>2</sub>, CO, H<sub>2</sub> + CO, H<sub>2</sub>S, and natural gas were used as the reducing gas. The offgas from the regenerator contains SO<sub>2</sub>, H<sub>2</sub>S, and elemental sulfur with the relative proportions dependent on the reducing gas used.

Each of the reducing gases, when coupled with steam treatment, successfully regenerated the sorbent. Natural gas required a higher temperature for regeneration (1130°F) compared to H<sub>2</sub> (1050°F) or H<sub>2</sub>S (950°F). Nonetheless, natural gas was chosen as the regenerant for the POC based on economic considerations, availability, and the fact that natural gas generates the most favorable product mix for a Claus plant feed.

Sorbent residence times were determined from laboratory experiments performed at W. R. Grace and NOXSO using methane followed by steam to regenerate the sorbent in a fixed-bed reactor. The required sorbent contacting time with reducing gas was found to be 30 minutes and with steam 20 minutes. With residence time and sorbent circulation rate fixed, the regenerator inventory and hence volume can be calculated according to:

$$V = I / \rho = W(RT_s) / \rho$$

where V = sorbent volume, ft<sup>3</sup>  
 I = sorbent inventory, lbs  
 $\rho$  = sorbent bulk density, lb/ft<sup>3</sup>  
 W = sorbent circulation rate, lb/hr  
 RT<sub>s</sub> = sorbent residence time in regenerator, hr

THE POC regenerator consists of two distinct moving bed reactors encased in a single, cylindrical shell, four feet in diameter and approximately 40 feet high. (Note: The POC regenerator is intentionally sized larger than required to allow testing of sorbent circulation rates and residence times beyond the range of baseline conditions.) Sorbent moves through the upper section of the regenerator and into a conical section which separates the natural gas and steam treatment sections of the reactor. To guard against "rat-holing," i.e., sorbent moving through the center of the reactor faster than along the walls, the angle of the cone is 70° which is greater than the sorbent's angle of internal friction. Natural gas is fed into the conical section through a series of concentric rings hung inside the cone. The rings provide a gas space between the moving bed of sorbent and the reactor wall and serve to distribute the gas within the bed.

The rings are placed at an angle of 45° to the horizontal. The sorbent's angle of repose is 23°. Sorbent leaving the upper section of the regenerator passes through a six-inch pipe into the steam treatment section. The steam treatment section is also a cylindrical vessel with a 70° cone at the bottom. Steam is fed into the cone through a series of rings identical to those in the upper section of the regenerator.

The POC will use a dense phase lift to convey the sorbent and no valves will open or close on the sorbent.

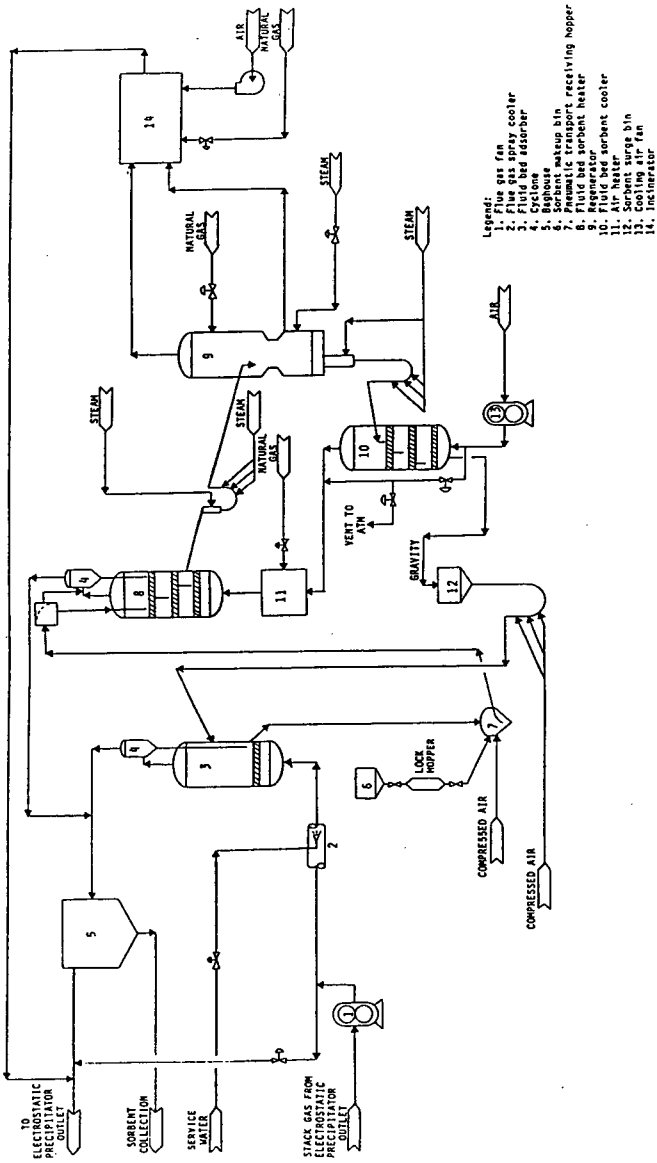
The transport system will be a dense phase pneumatic lift that should be much less attriting than the conveying system used in previous tests. The attrition rate of 0.03 percent/hr of the fluid bed inventory gives an attrition rate at the POC of about 6 lbs/hr at base case conditions.

#### PROCESS SUMMARY

The NOXSO process has the following operating advantages over both existing and developing sulfur removal processes:

- \* Simultaneous removal of SO<sub>2</sub> and NO<sub>x</sub> in a single reaction vessel.
- \* Produces no secondary pollution in the form of solid or liquid waste.
- \* Applicable to all coal types and sulfur contents.
- \* Completely dry process with no need for stack gas reheat.
- \* Cost effective when compared to conventional technology, i.e., flue gas desulfurization plus selective catalytic reduction.
- \* Applicable to new and retrofit installations

Figure 1  
 Proof-of-Concept Process Flow Diagram



COOLSIDE DESULFURIZATION DEMONSTRATION AT  
OHIO EDISON EDGEWATER POWER STATION

J. A. Withum, R. M. Statnick, H. Yoon, and F. P. Burke  
CONSOLIDATION COAL COMPANY  
Research & Development  
4000 Brownsville Road  
Library, PA 15120

**KEYWORDS:** FGD, Retrofit SO<sub>2</sub> Control, Duct Sorbent Injection

**ABSTRACT**

The Coolside Process is a duct sorbent injection process developed for retrofit SO<sub>2</sub> control in a coal-fired boiler. The attractive features of the process for retrofit use include low capital cost, low space requirements, and short construction time. The demonstration project was conducted on the 104 MWe Unit 4-Boiler 13 at the Ohio Edison Edgewater Power Plant, Lorain, Ohio, under a partial sponsorship of the U.S. Department of Energy (DOE) Clean Coal Technology Program. The full-scale test results confirmed the SO<sub>2</sub> removal capability of the process, as previously observed in pilot plant tests, and the soundness of the basic process design concept for operation in a utility environment. Additionally, the demonstration provided information on process equipment design improvements required for commercial operation.

This paper focuses on the process SO<sub>2</sub> removal performance observed in the demonstration. Potential research areas for improving the process performance based on the full-scale results are discussed.

**INTRODUCTION**

In 1986, Babcock & Wilcox, Consolidation Coal Company (Consol), the State of Ohio Coal Development Office, and Ohio Edison Company, under the sponsorship of the DOE Clean Coal Technology Program, agreed to demonstrate the Coolside and LIMB processes at the Ohio Edison Edgewater Station. The demonstration of the Coolside process was conducted from late July 1989 to mid-February 1990, using compliance (1.4 wt % S) and non-compliance (3 wt % S) bituminous coals from Ohio (Table 1). The objectives of the full-scale program were to verify the process performance in regard to short-term operability and SO<sub>2</sub> removal, to determine factors which could affect long-term operations, and to develop a data base to establish process economics and design parameters. The demonstration program included sorbent once-through and sorbent recycle operations. Key process variable effects were evaluated in short-term (6-8 hr) parametric tests and longer-term (1-14 day) process operability tests. Two different hydrated limes (Table 2) were tested. Prior to the demonstration, pilot-scale tests were conducted to select the hydrated limes to be tested and to develop process performance data applicable to the Edgewater site-specific conditions. The pilot data were used for demonstration program planning and data interpretation. This paper discusses full-scale Coolside desulfurization results at the Edgewater Station Unit 4-Boiler 13 in Lorain, Ohio. The discussion of the results is limited to the observations from once-through process tests. Recycle process tests (in which a portion of the collected ash is reinjected into the flue gas to increase overall sorbent utilization) were performed but the data are not included here because data analysis was not completed at the time this paper was written. Coolside pilot-scale process performance (1-5) and full-scale design and operation (6) were described elsewhere.

## PROCESS DESCRIPTION

Coolside desulfurization technology involves dry injection of hydrated lime into the flue gas downstream of the air preheater and flue gas humidification by water sprays (Figure 1).  $\text{SO}_2$  is captured by reaction with the entrained sorbent particles in the humidifier and by the dense sorbent bed collected in the particulate removal system. The humidification water serves a dual purpose. First, it activates the sorbent to enhance  $\text{SO}_2$  removal and, second, it conditions the flue gas and particulate matter to maintain efficient electrostatic precipitator (ESP) performance. Spent sorbent is removed from the gas along with fly ash in the existing particulate collector (ESP or baghouse). The sorbent activity can be significantly enhanced by dissolving sodium hydroxide (NaOH) or sodium carbonate ( $\text{Na}_2\text{CO}_3$ ) in the humidification water (3-5). Sorbent recycling can be used to improve the sorbent utilization if the particulate collector can handle the resulting increased solids loading. For reasons of convenience and cost, NaOH was used as the additive in the Edgewater demonstration.

## EDGEWATER HUMIDIFIER DESCRIPTION

The Edgewater equipment and process operations were described in detail elsewhere (6). Because humidification is crucial to the Coolside process, a short description of the Edgewater humidifier follows. The Edgewater humidifier was designed to avoid forming wet deposits on the walls. Figure 2 shows a drawing of the humidifier and the ductwork connecting it to the existing plant equipment. The humidification chamber was erected on the roof of the boiler house. Its dimensions were 14-feet 7-inches x 14-feet 7-inches, and 56-feet long. A 10 x 10 array of Babcock & Wilcox Company Mark 12 atomization nozzles at the humidifier entrance provided the fine water sprays for the flue gas humidification. The hydrated lime injector ports were located at the same vertical plane as the atomizer array. The humidifier was designed for a flue gas flow rate of one million pounds per hour, which gives about a 2.5 second humidifier residence time. However, air in-leakage through the air preheater resulted in a higher-than-design flue gas rate (1.3 million pounds per hour at full boiler load of 104 MWe). This increased flow necessitated that, at full load, a portion of the flue gas by-pass the humidification chamber. The original plant ductwork between the air preheater and the ESP was used for the flue gas by-pass. The data reported here, however, are only from tests at lower load in which all of the flue gas passed through the humidification chamber.

Thermocouples to measure flue gas temperature were located at the humidifier inlet and exit and at the ESP inlet. Humidification was controlled by varying the water flow rate to maintain a preset humidifier outlet temperature based on the thermocouples located at the humidifier exit. The flue gas was continuously monitored at the humidifier inlet and the ESP exit (stack) for  $\text{SO}_2$  and  $\text{O}_2$ .

## PROCESS DESULFURIZATION PERFORMANCE

### Desulfurization Performance Overview

The Edgewater program demonstrated that the Coolside process can routinely achieve up to 70%  $\text{SO}_2$  removal at the design conditions of 2.0 Ca/S and 0.19 Na/Ca molar ratios and 20°F approach to adiabatic saturation temperature using a commercial hydrated lime (Lime A). Use of an alternate hydrated lime (Lime B) gave somewhat lower  $\text{SO}_2$  removals, as did a 25°F approach; these effects will be discussed in detail later in this paper. A range of  $\text{SO}_2$  removals between 30 and 70% was achieved by controlling the Ca/S and Na/Ca molar ratios and the approach to adiabatic saturation temperature. The  $\text{SO}_2$  removals measured in these tests were confirmed by ash analysis results, as discussed in a later section. The  $\text{SO}_2$

removal results were consistent with projections based on Consol 0.1 MWe pilot plant and 1 MWe field test data.

Sorbent once-through utilizations of up to 35% were observed. This indicates that there is room for significant process improvement if the sorbent utilization can be increased through process optimization, including sorbent recycle. When calculating sorbent utilization, NaOH is included as a co-sorbent since it also captures  $\text{SO}_2$  as  $\text{Na}_2\text{SO}_3$  or  $\text{Na}_2\text{SO}_4$ .

The process was operated round-the-clock. During most operations, the ESP was able to handle the increased solids loading resulting from the sorbent injection and kept the flue gas opacity level below 5%. The acceptable performance of the ESP was largely the result of flue gas humidification. Without humidification, the ESP would not have been able to handle the increased solids loading and particle resistivity caused by sorbent injection (Z).

#### Variable Effects

Ca/S Ratio. The data obtained at Edgewater show an increase in  $\text{SO}_2$  removal with Ca/S ratio for the two hydrated limes tested (Figure 3). The  $\text{SO}_2$  removal using hydrated lime B at 23 to 26°F approach to adiabatic saturation are shown as squares, while the removals using hydrated lime A are shown as crosses for tests at 23 to 26°F approach, and as circles for 19 to 22°F approach to adiabatic saturation. No tests were performed using hydrated lime B at 19 to 22°F approach because, by this point in the test program, the humidification performance had deteriorated to the point where operation at 20°F set point caused the formation of large droplets, leading to wet deposits formation at the humidifier outlet. Using hydrated lime A,  $\text{SO}_2$  removals were 40, 50 and 70% at average Ca/S molar ratios of 1.1, 1.4 and 2.0, respectively. The process conditions were 19 to 22°F approach to adiabatic saturation; 0.17 to 0.24 Na/Ca molar ratio; and coal sulfur content between 2.0 to 2.8 wt %. The  $\text{SO}_2$  removals with hydrated lime B showed a similar trend, although they were lower than those with hydrated lime A. Although the observed  $\text{SO}_2$  removals at similar Ca/S ratios had some variation, Figure 3 clearly shows the trend of higher  $\text{SO}_2$  removals at higher Ca/S ratios. The Ca/S ratio is an important process variable to maintain  $\text{SO}_2$  removal at a desired level. As was shown in pilot plant (4,5) and other field tests (1),  $\text{SO}_2$  removal increases in a predictable manner with increasing Ca/S ratio.

The  $\text{SO}_2$  removals were calculated from the  $\text{SO}_2$  concentrations measured at the humidifier inlet and ESP outlet using continuous gas analyzers which were corrected to dry, excess-air-free conditions. Corrections for air in-leakage were made using continuous oxygen analyzer data collected at both locations. The moisture content was calculated based on measured wet bulb and dry bulb temperatures. The Ca/S ratio was calculated based on the measured  $\text{SO}_2$  concentration in the flue gas entering the humidifier, the measured flue gas flow rate into the humidifier, and the measured hydrated lime feed rate to the humidifier.

Approach to Adiabatic Saturation Temperature. At a constant Ca/S and Na/Ca molar ratio,  $\text{SO}_2$  removal was higher when the process was operated at closer approach to adiabatic saturation (or wet bulb) temperature. The effect of only a few degrees variation in the approach to adiabatic saturation can be observed by comparing the circles (19 to 22°F approach) with the crosses (23 to 26°F approach) in Figure 3. This comparison shows that, at equivalent Ca/S ratios, the observed  $\text{SO}_2$  removals were 6 to 10 percentage points (absolute) higher in the tests at 19 to 22°F approach than in tests at 23 to 26°F approach over the range of Ca/S ratios in the figure. The effect of larger variation in the approach to adiabatic saturation is given by Figure 4, which shows  $\text{SO}_2$  removal as a function of the approach to the

adiabatic saturation temperature using hydrated lime A at Ca/S molar ratios of 1.4 and 2.0; the Na/Ca molar ratio was 0.17 to 0.24. Although some variation occurred in the observed SO<sub>2</sub> removals at similar approach temperatures, the data demonstrate that the SO<sub>2</sub> removal is higher at closer approaches to adiabatic saturation temperature.

Variations in the approach to adiabatic saturation were not intended as part of the demonstration test program. The variations shown in Figure 4 occurred for two reasons. First, the approach varied because of variations in the humidifier exit temperature from the control point and some fluctuations in the flue gas wet bulb temperature. Second, the set point for the approach was increased from 20 to 25°F during the tests with lime A. This change was necessary because of the change in the humidifier performance.

Na/Ca Ratio. At constant Ca/S and approach to adiabatic saturation, the SO<sub>2</sub> removal was higher when NaOH was added to the humidification water. Using hydrated lime A at a 2.0 Ca/S molar ratio and 23 to 26°F approach to adiabatic saturation temperature, SO<sub>2</sub> removals were 60 to 65% in tests with additive (0.19 Na/Ca molar ratio) but only 35 to 45% in tests without additive. Since NaOH additive significantly enhances SO<sub>2</sub> removal, and demonstration of maximum SO<sub>2</sub> removal was the project goal, tests without NaOH were limited. Thus, no data were obtained at 1.0 Ca/S without additive, nor were data obtained at higher approaches without additive. The effect of sodium additive on SO<sub>2</sub> removal performance was established in previous pilot plant studies (3-5). The full-scale results were in good agreement with pilot data on the additive effect.

Effect of Different Hydrated Limes. Hydrated lime A gave higher SO<sub>2</sub> removals than hydrated lime B at similar process conditions. This is shown for the conditions 0.17 to 0.24 Na/Ca molar ratio and 23 to 26°F approach to adiabatic saturation temperature by comparing the crosses (Lime A) with the squares (Lime B) in Figure 3. This comparison shows that, at equivalent Ca/S ratios, the observed SO<sub>2</sub> removals were 5 to 10 percentage points (absolute) higher when using hydrated lime A than when using hydrated lime B over the range of Ca/S ratios in the figure. These results are consistent with pilot plant results that showed higher SO<sub>2</sub> removals when using hydrated lime A than when using hydrated lime B (5). Both are high calcium (>88% Ca(OH)<sub>2</sub> by wt) hydrated limes. Differences in physical properties, such as surface area, may have contributed to the performance differences. The BET surface areas were 22 to 24 m<sup>2</sup>/g for hydrated lime A and 15 to 18 m<sup>2</sup>/g for hydrated lime B. Previously reported work showed a correlation between sorbent surface area and SO<sub>2</sub> removal performance (5).

#### Comparison with Pilot Plant and Field Tests

In preparation for the demonstration tests at Edgewater, Consol conducted pilot plant tests on a 0.1 MWe scale and a 1 MWe scale. Figure 5 compares the SO<sub>2</sub> removals at Edgewater with those observed in the 0.1 MWe pilot plant (4,5) and 1 MWe field tests (1) for the conditions of 2.0 Ca/S and 0.19 Na/Ca molar ratios. The data shown from the Edgewater and the 1 MWe field tests were from tests at 20°F approach; the data from the pilot plant were from tests at 25°F approach to adiabatic saturation. The sorbent was hydrated lime A for the Edgewater and pilot plant data and a third lime, hydrated lime C for the field test data. In pilot plant tests, the SO<sub>2</sub> removals using hydrated lime C were about 5 to 10% (relative) lower than those using hydrated lime A (5). The 70% SO<sub>2</sub> removal achieved at Edgewater compares well with the 75% SO<sub>2</sub> removal observed in the 1 MWe field tests. In both of these tests, an ESP was used for particulate control. These removals were lower than the 85% SO<sub>2</sub> removal observed in pilot plant tests. However, a baghouse was used for particulate collection in the pilot plant. Because a

baghouse provides more effective gas-sorbent contact than an ESP, the SO<sub>2</sub> removals were expected to be somewhat lower at Edgewater than in the pilot plant tests. These results, along with the consistency in the variable effects of the pilot and Edgewater tests, as discussed above, indicate that the 0.1 MWe pilot plant unit is a reliable device for simulating process performance, for evaluating improved sorbents, or for conducting site-specific simulations.

In addition to the difference in the particulate removal device, differences in other design/operating factors of the Edgewater Coalside system from the pilot plant may have affected the comparison of SO<sub>2</sub> removal performances at Edgewater and at the pilot plant. These factors include water droplet size distribution, water droplet and hydrated lime distributions in the gas, and flue gas velocity and flow distribution. However, the effects of these differences on SO<sub>2</sub> removal were not quantifiable from the current Edgewater data.

#### Edgewater Data Reliability

Table 3 compares the sorbent utilizations based on the sulfur, Ca, and Na contents of the ESP hopper samples with the sorbent utilizations calculated from the process run data for tests using hydrated lime A. Samples also were taken during tests using hydrated lime B, but the analyses were not completed when this paper was written. The average difference between the two methods was 0.87% (absolute). This agreement is good, considering the relatively small size of the ESP samples (50-100 lbs) taken from a single ESP hopper, of which 100 grams was submitted for analysis, compared with the large amount of solids (2 to 10 tons/hr) collected by the ESP which had a total of twelve hoppers. A standard statistical F Test (8) on the data in Table 3 shows that the differences between the results of the two methods of determining sorbent utilization were not significant. Using the twelve process runs and the two methods of determining utilization in Table 3 as the sources of variance, the F-number for the method variance/residual variance was 0.87 for 1/11 degrees of freedom. This indicates that the probability that the two methods gave truly different results was not significant.

#### Directions for Desulfurization Performance Improvement

Since the observed sorbent utilization is low (25-35%), there is a significant potential for improving process economics by optimizing the process design for maximum SO<sub>2</sub> removal efficiency. Process optimization is possible in several areas. Improved dispersion of the sorbent in the flue gas may improve the SO<sub>2</sub> removal. Sorbent recycle, involving reinjection of spent sorbent recovered from the ESP, offers a straightforward means of enhancing the sorbent utilization as long as the ESP and the waste handling system installed in the plant can handle the increased solids loading. Sorbent recycle tests were performed during the Edgewater demonstration, but the data analysis was not completed at the time this paper was written.

In the longer term, optimization of the sorbent (hydrated lime) properties for SO<sub>2</sub> capture is expected to lead to an improved sorbent. Pilot plant tests have shown a positive correlation of hydrated lime surface area with sorbent utilization. Lime hydration methods that produce high surface area hydrates are being studied at Consoil R&D (9) and elsewhere (10). Additive incorporation during lime hydration also may provide more reactive sorbents (2,11).

#### CONCLUSIONS

The Edgewater Coalside testing demonstrated SO<sub>2</sub> removals up to 70% in an electric utility boiler burning an eastern United States high-sulfur coal.

- Sorbent utilizations at these SO<sub>2</sub> removals were typically 30 to 35%. The spent sorbent analyses confirmed the sorbent utilizations based on the continuous flue gas analyzers.
- The full-scale SO<sub>2</sub> removals were similar to pilot-scale SO<sub>2</sub> removals. This indicates that appropriate pilot-scale tests are a good predictor of full-scale performance for this technology.
- As observed in the pilot-scale tests, the process SO<sub>2</sub> removal depends on the primary process variables: Ca/S and Na/Ca molar ratios and the approach to adiabatic saturation.
- Differences in the hydrated lime affect the SO<sub>2</sub> removal level.

#### LEGAL NOTICE/DISCLAIMER

This report was prepared by Consolidation Coal Company, pursuant to a contract with Babcock & Wilcox Company. This report was prepared in accordance with a cooperative agreement partially funded by the U.S. Department of Energy, and neither Babcock & Wilcox Company, nor any of its subcontractors nor the U.S. Department of Energy, nor any person acting on behalf of either: a) makes any warranty or representation, express or implied, with respect to the accuracy, completeness, or usefulness of the information contained in this report, or that the use of any information, apparatus, method, or process disclosed in this report may not infringe privately-owned rights; or b) assumes any liabilities with respect to the use of, or for damages resulting from the use of, any information, apparatus, method or process disclosed in this report.

Reference herein to any specific commercial product, process, or service by trade name, trademark, manufacturer, or otherwise, does not necessarily constitute or imply its endorsement, recommendation, or favoring by the U.S. Department of Energy. The views and opinions of authors expressed herein do not necessarily state or reflect those of the U.S. Department of Energy.

#### REFERENCES

1. Yoon, H.; Ring, P.A.; Burke, F. P. "Coolside SO<sub>2</sub> Abatement Technology: 1 MW Field Tests". Proceedings, Coal Technology '85 Conference, Pittsburgh, PA, November 1985; Vol. V, pp 129-151.
2. Yoon, H; Stouffer, M. R.; Rosenhoover, W. A.; Statnick, R. M. "Laboratory and Field Development of Coolside SO<sub>2</sub> Abatement Technology". Proceedings, Second Annual Pittsburgh Coal Conference, Pittsburgh, PA, September 1985; pp 235-236.
3. Withum, J. A.; Rosenhoover, W. A; Yoon, H. "A Pilot Plant Study of the Coolside Desulfurization Process with Sorbent Recycle". Proceedings, Fifth Annual Pittsburgh Coal Conference, Pittsburgh, Pa, September 1988; pp 84-96.
4. Yoon, H; Stouffer, M. R.; Rosenhoover, W. A.; Withum, J. A.; Burke, F. P. "Pilot Process Variable Study of Coolside Desulfurization". *Environmental Progress* 1988, 7(2), 104-111.
5. Stouffer, M. R.; Rosenhoover, W. A; Yoon, H. "Pilot Plant Process and Sorbent Evaluation Studies for 105 MWe Coolside Desulfurization Process Demonstration". Third International Conference on Processing and Utilization of High Sulfur Coals, Ames, IA, November 1989; paper A-52.
6. Kanary, D. A.; Statnick, R. M.; Yoon, H.; McCoy, D. C.; Withum, J. A.; Kudlac, G. A. "Coolside Process Demonstration at the Ohio Edison Company Edgewater Unit 4-Boiler 13". Proceedings, 1990 EPA/EPRI SO<sub>2</sub> Control Symposium, New Orleans, LA, May 1990.
7. Fink, C. E.; McCoy, D. C.; Statnick, R. M. "Flue Gas Humidification With Boiler Limestone Injection for Improved ESP Performance and Increased SO<sub>2</sub> Removal". Proceedings, Coal Technology '85 Conference, Pittsburgh, PA, November 1985.

8. Miller, R. E. "CE Tutorial: Statistics. 4. Means and Variances". *Chemical Engineering* 1985, 107-110.
9. Withum, J. A.; Yoon, H. "Treatment of Hydrated Lime with Methanol for In-Duct Desulfurization Sorbent Improvement". *Environmental Science and Technology* 1989, 23(7), 821-827.
10. Moran, D. L.; Rostam-Abadi, M; Harvey, R. D.; Frost, R. R.; Sresty, G. C. "Sulfur Dioxide Sorption Reactivity of Hydrated Lime: Effect of Hydration Method". *Prepr., Div. Fuel Chem., Am. Chem. Soc.* 1987, 32(4), 508-516.
11. Yoon, H.; Withum, J.A.; Rosenhoover, W. A.; Burke, F. P. "Sorbent Improvement and Computer Modeling Studies for Coolside Desulfurization". Proceedings, Joint Symposium on Dry SO<sub>2</sub> and Simultaneous SO<sub>2</sub>/NO<sub>x</sub> Control Technology, Raleigh, NC; U.S. Environmental Protection Agency. U.S. Government Printing Office: Washington, DC, 1986; EPA-600/9-86-029b.

TABLE 1  
TYPICAL COAL ANALYSES\*

| Coal           | Proximate Analysis |          |                 |              | Ultimate Analysis |       |      |      |      |              |
|----------------|--------------------|----------|-----------------|--------------|-------------------|-------|------|------|------|--------------|
|                | Btu/lb             | Moisture | Volatile Matter | Fixed Carbon | Ash               | C     | H    | N    | S    | O (by diff.) |
| Compliance     | 13204              | 4.18     | 34.75           | 54.74        | 10.51             | 74.48 | 4.92 | 1.39 | 1.42 | 7.29         |
| Non-Compliance | 12695              | 4.12     | 37.98           | 48.91        | 13.11             | 70.72 | 4.88 | 1.25 | 3.02 | 7.02         |

\*All analyses except moisture are wt % dry basis.

TABLE 2  
TYPICAL HYDRATED LIME ANALYSES

| Hydrated Lime | BET Surface Area, m <sup>2</sup> /g | TGA Data, dry wt %  |                   |
|---------------|-------------------------------------|---------------------|-------------------|
|               |                                     | Ca(OH) <sub>2</sub> | CaCO <sub>3</sub> |
| A             | 23.2                                | 93.0                | 2.5               |
| B             | 16.7                                | 88.0                | 2.5               |

TABLE 3  
COMPARISON OF ESP ASH ANALYSES AND PROCESS RUN DATA

| Ca/S (mol) | Na/Ca (mol) | % SO <sub>2</sub> Removal | % Sorbent Utilization Based on           |                | Difference |
|------------|-------------|---------------------------|--|----------------|------------|
|            |             |                           | SO <sub>2</sub> Removal, Ca/S and Na/Ca* | Ash Analysis** |            |
| 1.56       | 0.00        | 41.1                      | 26.3                                     | 30.0           | -3.7       |
| 1.89       | 0.19        | 58.6                      | 28.3                                     | 22.9           | 5.4        |
| 1.21       | 0.28        | 46.9                      | 33.9                                     | 34.6           | -0.7       |
| 1.29       | 0.17        | 44.7                      | 32.5                                     | 31.8           | 0.7        |
| 1.45       | 0.18        | 52.7                      | 34.2                                     | 32.3           | 1.9        |
| 1.45       | 0.18        | 53.7                      | 34.9                                     | 33.8           | 1.1        |
| 1.40       | 0.21        | 48.2                      | 32.0                                     | 33.0           | -1.0       |
| 2.05       | 0.23        | 57.8                      | 26.7                                     | 29.2           | -2.5       |
| 1.49       | 0.11        | 45.7                      | 29.6                                     | 24.7           | 4.9        |
| 1.96       | 0.23        | 60.8                      | 29.2                                     | 32.9           | -3.7       |
| 1.03       | 0.00        | 29.1                      | 28.3                                     | 21.4           | 6.9        |
| 2.17       | 0.00        | 27.1                      | 12.5                                     | 11.4           | 1.1        |
| Average    |             |                           |  |                | 0.87       |

\*  $\frac{\% \text{ SO}_2 \text{ Removal}}{\text{Ca/S} + 0.5 (\text{Na/S})}$

\*\*  $\frac{\text{Total Sulfur}/32}{\text{CaO}/56 + \text{Na}_2\text{O}/62}$ , CaO and Na<sub>2</sub>O corrected for calcium and sodium in coal ash

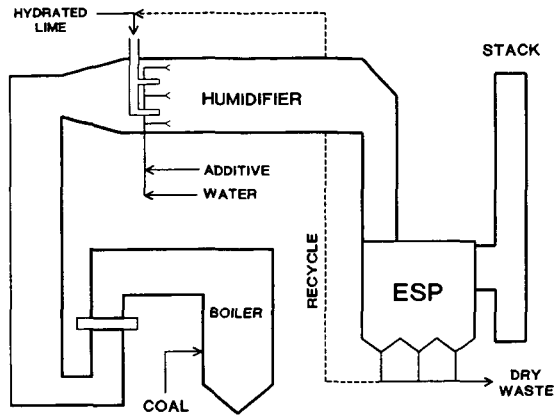


Figure 1. Coolside Process Schematic..

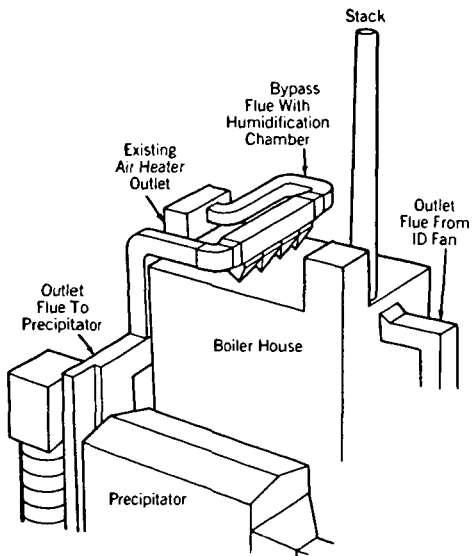


Figure 2. Edgewater Coolside Demonstration Process Equipment Layout.

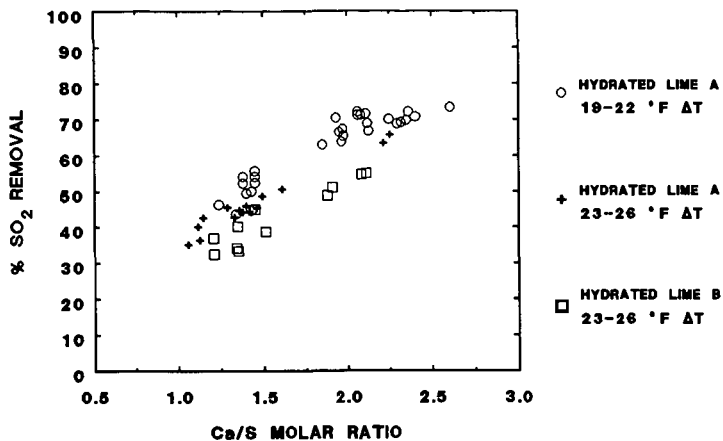


Figure 3. SO<sub>2</sub> Removal vs Ca/S Ratio. These data were obtained at a nominal Na/Ca mol ratio of 0.19. ΔT is the approach to adiabatic saturation at the humidifier outlet.

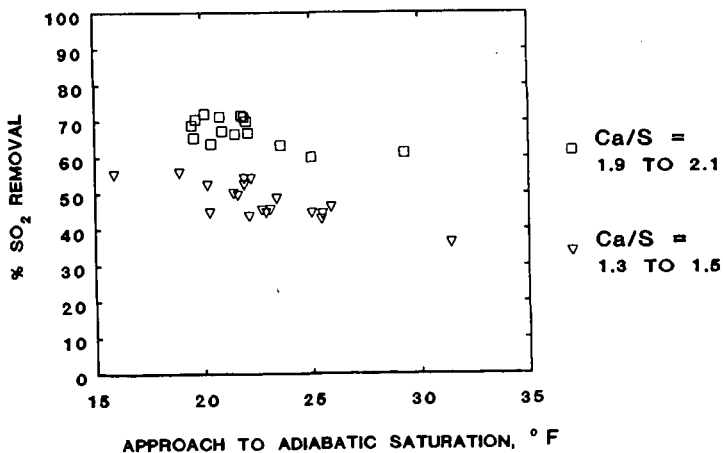


Figure 4. SO<sub>2</sub> Removal vs Approach to Adiabatic Saturation for Operation With Hydrated Lime A. The Na/Ca molar ratio was 0.17-0.24 in these tests.

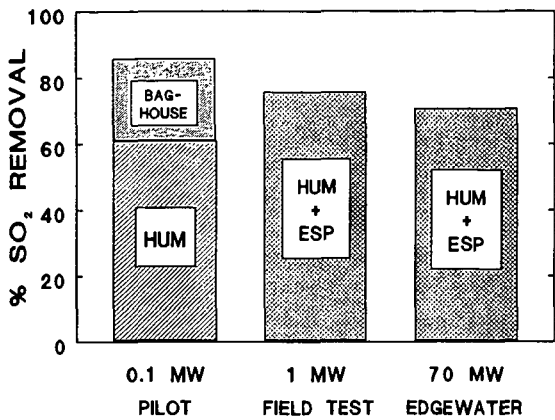


Figure 5. Comparison of Pilot, Field and Demonstration Test  
 $\text{SO}_2$  Removal Performance: Ca/S - 2 mol ratio,  
 Na/Ca = 0.19 mol ratio, 20-25°F approach  
 to adiabatic saturation.

**EVALUATION OF CALCIUM COMPOUNDS AS SORBENTS FOR IN-SITU  
DESULFURIZATION WITH TEXACO COAL GASIFICATION PROCESS**

Mitri S. Najjar and Dick Y. Jung

Texaco Inc.  
P. O. Box 509  
Beacon, NY 12508

Keywords: in-situ desulfurization; coal gasification; calcium

**SUMMARY**

The feasibility of using calcium-based compounds as potential sulfur-capturing sorbents for in-situ desulfurization in combination with partial oxidation of coal in a slagging mode was examined using thermodynamic calculations and bench-scale experimental tests. Although pure calcium compounds are excellent sorbents for capturing sulfur, problems may be encountered when other compounds which are commonly found in coal slags are present. Under the simulated reaction conditions used in Texaco coal gasifiers, calcium compounds were found to preferentially react with the silicates commonly found in coal slags rather than capture sulfur.

**INTRODUCTION**

To utilize coal in an environmentally safe manner, it is necessary to remove the gas phase sulfur compounds released during the combustion and/or gasification of coal. In recent years, integrated gasification-combined cycle (IGCC) processes have been demonstrated which gasify coal to produce synthesis gas (syngas) which is fired in a turbine to generate electrical power. Typically, these processes separate the reaction step (where coal is converted to raw syngas under reducing conditions at high temperatures) from the acid gas removal step (where physical solvents are generally used to scrub hydrogen sulfide and carbonyl sulfide from the crude syngas). This approach requires significant capital investments as well as operating utility costs since the hot syngas must be cooled to the low temperatures commonly needed for physical solvents and subsequent reheated prior to its introduction into the gas turbine.

A potentially more efficient alternative is to combine coal combustion with the sulfur removal step in the same vessel. However, the solubility of sulfur in coal slags is quite low (typically between 0.01 and 0.5 weight percent). One possible approach to enhance sulfur solubility in coal slags is the addition of sulfur-capturing sorbents along with the coal feed to the gasifier. The ideal sorbent should be an inexpensive additive that chemically reacts with the sulfur compounds in the gas (primarily hydrogen sulfide with smaller amounts of carbonyl sulfide) to form a disposable sulfide that is encapsulated in the resultant slag but this additive should not cause any complications for slag flow from the gasifier.

Although calcium-based compounds have been commercially used in fluidized bed combustion to perform in-situ desulfurization,

only bench scale work has been reported using these potential sorbents to study high temperature desulfurization in conjunction with an entrained bed coal gasifier. It was hoped that the sulfur from the gas phase would be captured in the slag as calcium sulfide under the reducing atmosphere commonly found in these coal gasifiers. Whitney, et al.<sup>1</sup> have suggested that the use of concentrated coal-water slurries mixed with finely divided lime (CaO) or limestone (CaCO<sub>3</sub>) represents a promising avenue for coal conversion with simultaneous sulfur capture but they reported evidence of mass transfer limitations. Freund and Lyon<sup>2</sup> performed thermodynamic calculations that indicate a range of attainable conditions where high levels of sulfur capture could be achieved for fuel-rich combustion of coals containing calcium-based sorbents. However, they also point out that even though the thermodynamics of sulfur sorption may be favorable, there are no assurances that the kinetics will be fast enough for practical use. In addition, neither group of researchers consider the interactions among calcium compounds and other components in the coal slag (such as aluminosilicates) or the effect of these additives on slag removal from the gasifier. To explore the possibility of using calcium-based compounds to capture sulfur in the more reducing atmosphere typically found in Texaco coal gasifiers with coal-water slurry feeds operating in a slagging mode, theoretical thermodynamic calculations as well as bench scale drop tube furnace equilibrium experimental runs were performed.

## METHODS

### Calculations

Thermodynamic equilibrium calculations were performed using a multiphase free energy minimization computer program by an in-house version of SOLGASMIX<sup>3</sup> augmented with additional thermodynamic data<sup>4</sup>. The systems considered in this study include calcium compounds alone as well as with inorganic species (e. g. silicon-, iron- and aluminum-based compounds) commonly found in coal slags under simulated syngas compositions expected in Texaco coal gasifiers with coal-water slurry feeds operating in a slagging mode.

### Experiments

To validate these equilibrium predictions, bench scale drop tube furnace equilibrium experiments were performed for selected coal slag-additive systems. These tests were conducted at atmospheric pressure using temperatures and gas compositions selected to simulate gasifier conditions using the apparatus shown schematically in Figure 1. The principal units for high temperature testing are two identical LeMont Scientific quench furnaces capable of reaching 3000°F. Samples of the slag and sorbent (50-100 mg) were placed in a crucible that is suspended in the furnace by a thin platinum wire which is then equilibrated by exposure to a flowing gas mixture for at least 18 hours. Gaseous mixtures of CO, CO<sub>2</sub> and 1 vol %SO<sub>2</sub> in Argon were selected to simulate the S<sub>2</sub> and O<sub>2</sub> partial pressures at the desired temperatures and ambient pressure based on the thermodynamic equilibrium calculations using an in-house version of SOLGASMIX<sup>3</sup>. The suspended slag-sorbent sample was then rapidly quenched by dropping the crucible into a pool of water or simulated syngas. This was

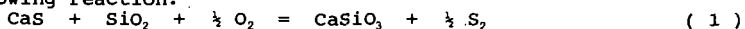
accomplished by passing an electrical current through the suspending platinum wire which causes the wire to break.

The quenched sample was recovered and characterized by petrographic examination using a Leitz Orthoplan microscope and electron microprobe analysis. An Amray 1645 scanning electron microscope equipped with secondary and backscattered electron detectors for imaging as well as a Tracor Northern TN-5500 energy dispersive X-ray microanalysis system with 40 MByte data storage capacity and color display were used to obtain SEM photomicrographs to show phase morphologies as well as EDX multielement semiquant chemical analysis to confirm phase identifications.

## RESULTS

Equilibrium calculations based on the calcium oxide/calcium sulfide system with simulated syngas from a Texaco coal gasifier initially looked quite promising for sulfur capture. Phase diagrams indicate that calcium sulfide (in the absence of other coal slag compounds) is stable over the temperature range as well as oxygen and sulfur partial pressures commonly expected in Texaco coal gasifiers. The calculations suggest that in-situ sulfur capture with calcium (when there is no interactions with the coal slag) is favored by lower temperatures and/or more reducing conditions.

However, when other compounds from the coal slag are incorporated into these calculations, the situation is now altered. For example, if silica ( $\text{SiO}_2$ ) is added to this calcium oxide/sulfide system, new phases must now be taken into account which form via chemical reactions. Consider  $\text{CaSiO}_3$  which is formed by the following reaction:



Note CaS is now stable only below the CaS-SiO<sub>2</sub>-CaSiO<sub>3</sub> region shown in Figure 2. The now smaller CaS stability region would translate into a reduced sulfur capture for this system in comparison to the system without silica added. Note that a much lower oxygen partial pressure is now needed for a stable CaS phase which may not be possible for a Texaco coal gasifier with a coal-water slurry feed operating in a slagging mode. If one now further considers the addition of iron and aluminum compounds (which are commonly found in most coal slags) to this system, the situation becomes even more complex with a plethora of new phases that must now be considered. A sample calculation result is shown in Table 1 which indicates that with even a relatively high calcium additive loading, most of the calcium is predicted to appear in various aluminosilicate compounds rather than the desired CaS under oxygen and sulfur partial pressures expected in Texaco coal gasifiers. Hence, calcium would be a less effective sorbent for sulfur capture under these conditions.

To qualitatively confirm these predictions, bench scale equilibrium drop tube furnace runs were performed using simulated oxygen and sulfur partial pressures selected to match those expected in Texaco coal gasifiers. The EDX semiquant chemical analyses for several silicate phase grains from these experimental runs are listed in Table 2. Note that the sulfur content for these silicate particles is relatively low even though the calcium and silicon content were relatively high. No calcium sulfide grains were identified. Hence, these experimental data support the

prediction that under the simulated syngas conditions for a Texaco coal gasifier with a coal-water slurry feed operating in a slagging mode, calcium compounds preferentially react with the silicate compounds in the coal slag rather than the sulfur compounds in the gas phase.

#### CONCLUSIONS

The feasibility of adding calcium-based compounds as potential sulfur capturing sorbents during coal gasification is being examined using theoretical equilibrium calculations as well as bench scale equilibrium drop tube furnace experiments. Although it is predicted that calcium-based compounds can be effective agents for desulfurization when used alone under simulated syngas conditions commonly encountered in Texaco coal gasifiers with a coal-water slurry feed operating in a slagging mode, thermodynamic calculations suggest calcium compounds can preferentially interact with other common coal slag components, especially the silicates, which limit their usefulness as in-situ sulfur sorbents during coal gasification. EDX semiquant chemical analyses for silicate phase grains obtained from experimental bench scale equilibrium drop tube furnace runs are presented which are consistent with these predictions.

#### ACKNOWLEDGEMENTS

The authors gratefully acknowledge financial support for this work under the five year Texaco/Department of Energy Cooperative Program (Contract No. DE-FC21-87MC23277) on "Integration and Testing of Hot Desulfurization and Entrained Flow Gasification for Power Generation Systems" with METC's Dr. J. Beeson as Contract Manager. Uygur Kokturk assisted in designing and troubleshooting the bench scale drop tube furnace units. Ron McKeon performed most of the experimental runs while Tris Laurion provided EDX analyses of the slag samples.

#### REFERENCES

1. G. M. Whitney, Z. Yunming, M. M. Denn and E. E. Petersen, "Sulfur Capture during Partial Coal Combustion", Chem. Engineering Comm., **55** (1987) 83-93.
2. H. Freund and R. K. Lyon, "The Sulfur Retention of Calcium-Containing Coal during Fuel-Rich Combustion", Combustion and Flame, **45** (1982) 191-203.
3. G. Eriksson, Acta Chem. Scand., **25** (1971) 2651.
4. R. A. Robie, B. S. Hemingway and J. R. Fisher, "Thermodynamic Properties of Minerals and Related Substances at 298.15 K and 1 Bar ( $10^5$  Pascals) Pressure and at Higher Temperatures", U. S. Geological Survey Bulletin 1452, U. S. Government Printing Office, Washington (1979).
5. J. W. Larimer, "An experimental investigation of oldhamite, CaS; and the petrologic significance of oldhamite in meteorites", Geochimica et Cosmochimica Acta, **32** (1968) 965-82.

**TABLE 1**

Calculated equilibrium compositions at 1600 K (2420 F) and 38 atm. to check for stable phases in a system with coal slag and calcium additive under simulated Texaco coal gasifier syngas conditions

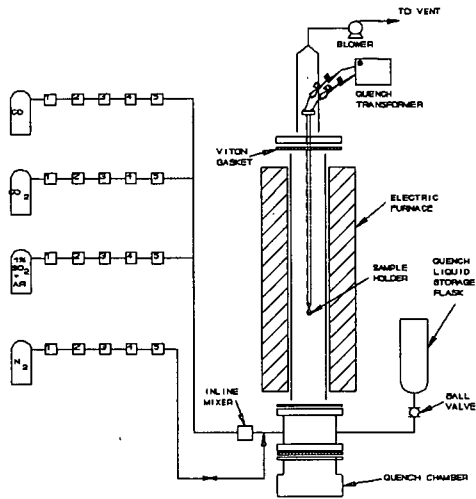
| <u>GAS PHASE COMPOSITION</u> |                      |             |                               |
|------------------------------|----------------------|-------------|-------------------------------|
| <u>Gases</u>                 | <u>Mole Fraction</u> | <u>Mole</u> | <u>Partial Pressure (atm)</u> |
| CO                           | 0.410                | 0.687       | 15.6                          |
| CO <sub>2</sub>              | 0.0987               | 0.165       | 3.75                          |
| H <sub>2</sub>               | 0.278                | 0.466       | 10.6                          |
| H <sub>2</sub> O             | 0.199                | 0.334       | 7.58                          |
| COS                          | 1.38E-04             | 2.32E-04    | 5.26E-03                      |
| H <sub>2</sub> S             | 2.79E-03             | 4.67E-03    | 0.106                         |
| O <sub>2</sub>               | 5.98E-13             | 1.00E-12    | 2.27E-11                      |
| N <sub>2</sub>               | 0.0102               | 0.0170      | 0.386                         |
| SO <sub>2</sub>              | 2.52E-07             | 4.21E-07    | 9.56E-06                      |

| <u>EQUILIBRIUM SOLID PHASES</u> |             |  |             |   |             |
|---------------------------------|-------------|--|-------------|---|-------------|
| <u>Solid</u>                    | <u>Mole</u> | <u>Solid</u>                                     | <u>Mole</u> | <u>Solid</u>  | <u>Mole</u> |
| FeO                             | 0.00400     | CaS  | 0.00270     | Ca <sub>3</sub> Al <sub>2</sub> Si <sub>3</sub> O <sub>12</sub> | 0.0         |
| FeS                             | 0.0         | CaSiO <sub>3</sub>                               | 0.0         | Fe <sub>2</sub> SiO <sub>4</sub>                                | 0.0         |
| Fe                              | 0.0         | Ca <sub>2</sub> Al <sub>2</sub> SiO <sub>7</sub> | 0.00180     | Al <sub>2</sub> SiO <sub>5</sub>                                | 0.0         |
| CaO                             | 0.0161      | Ca <sub>2</sub> SiO <sub>4</sub>                 | 0.00490     | CaAl <sub>2</sub> Si <sub>2</sub> O <sub>8</sub>                | 0.0         |
| SiO <sub>2</sub>                | 0.0         | Al <sub>2</sub> O <sub>3</sub>                   | 0.0         | Ca <sub>2</sub> Fe <sub>2</sub> O <sub>5</sub>                  | 0.0         |

**TABLE 2**

EDX chemical analysis for particles from bench scale drop tube furnace runs at 2200°F with calcium added to Pittsburgh #8 slag

| <u>Grain</u> | <u>Na</u> | <u>Al</u> | <u>Si</u> | <u>S</u> | <u>Ca</u> | <u>Fe</u> |
|--------------|-----------|-----------|-----------|----------|-----------|-----------|
| 1            | 1.40      | 21.02     | 43.97     | 0.32     | 19.23     | 11.91     |
| 2            | 3.14      | 12.87     | 54.01     | 0.34     | 12.13     | 14.50     |
| 3            | 3.23      | 13.34     | 53.39     | 0.25     | 12.84     | 13.50     |
| 4            |           |           | 40.93     |          | 58.87     |           |
| 5            | 0.64      | 12.15     | 34.86     |          | 43.80     | 4.28      |



1. FRONT PRESSURE REGULATOR
2. SHUT-OFF VALVE
3. ROTAMETER
4. FILTER
5. MASS FLOW CONTROLLER

FIGURE 1 Schematic for Equilibrium Furnace

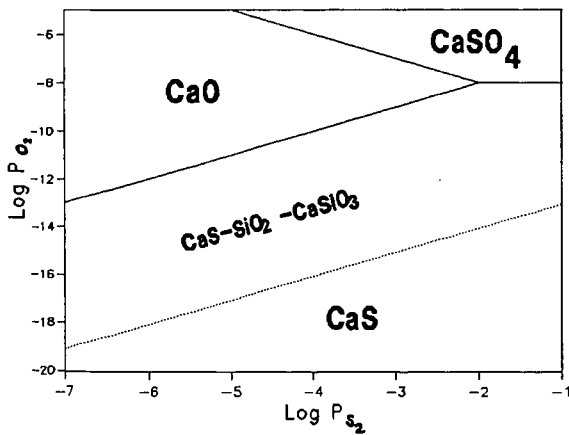


FIGURE 2 Silicate-sulfide-oxide equilibrium for Calcium at 2200°F

**PREDICTION OF SO<sub>2</sub> REMOVAL FOR POWER PLANTS  
USING INDUCT INJECTION OF LIME SLURRY**

**\*Peter Harriott, John Ruether and\*\*Fred Sudhoff**

**U.S. Department of Energy  
Pittsburgh Energy Technology Center  
Pittsburgh, PA 15236**

\*At Cornell University, Ithaca, NY  
\*\*Burns and Roe Services Corporation

Keywords: duct, lime, sulfur dioxide

More than half of SO<sub>2</sub> emissions in the United States come from older coal-fired power plants that have no scrubbers or other devices for SO<sub>2</sub> removal. Pending legislation may require at least 50 percent SO<sub>2</sub> reduction, but it would be difficult to retrofit many of these older plants with large scrubbers of the type used for new plants. Induct injection of lime slurry is a promising method for achieving moderate SO<sub>2</sub> removal by simply spraying lime slurry into the flue gas between the air preheater and the solids collection equipment. The SO<sub>2</sub> is absorbed and neutralized in the short time that it takes for the drops to evaporate, and the nearly dry solids are collected with the fly ash in the existing electrostatic precipitator or baghouse. A flow diagram is shown in Figure 1.

Simple Model for SO<sub>2</sub> Removal

Several studies of induct sorbent injection were recently carried out in pilot units using a slipstream of flue gas from an operating coal-fired utility boiler (Murphy and Samuel, 1988; Murphy et al., 1988; Drummond and Babu, 1988). Extent of SO<sub>2</sub> removal depends on the approach to adiabatic saturation temperature of the flue gas and on parameters describing the reaction of lime and SO<sub>2</sub>. The results were correlated using a simple model based on the fundamentals of mass and heat transfer to and within the drops plus some empirical factors (Harriott, 1989a). The equation for fractional removal of SO<sub>2</sub> is:

$$E_{SO_2} = 1 - e^{-X} \quad (1)$$

where

$$X = \frac{A(SR)}{B+SR} \ln \frac{T_{in} - T_{as}}{T_{out} - T_{as}} \quad (2)$$

SR = stoichiometric ratio =  $Ca(OH)_2/SO_2$  (molar)

$T_{AS}$  = adiabatic saturation temperature, °F

The factors A and B were obtained by fitting the data and depend on the type of lime and the  $SO_2$  concentration in the gas. A value of A = 1.25 was found for calcitic lime. Based on limited data, B was found to depend on the  $SO_2$  content of the entering flue gas and was correlated as:

$$B = 0.05 (\text{ppm } SO_2)^{0.5} \quad (3)$$

The predicted  $SO_2$  removal for different values of SR,  $T_{in}$ , and  $(T_{out} - T_{as})$  for 1600 ppm  $SO_2$  is shown in Figure 2.

For given inlet conditions, the  $SO_2$  removal can be improved by increasing the stoichiometric ratio or by decreasing the approach to the saturation temperature. However, too close an approach will lead to incomplete drying and deposition of wet solids in the duct or the particulate collection device. Plants that have long ducts or low flue gas velocities to give 2-3 seconds residence time in the longest straight duct could operate with a close approach to saturation and achieve good  $SO_2$  removal with moderate excess of lime. Plants with less than 1 second residence time in a straight length of duct would have to use a larger approach to insure dry solid at the exit and might not get 50%  $SO_2$  removal even with a large excess of lime.

### Duct Survey and FORTRAN Program for Utility Boilers

Data on duct dimensions, flue gas velocities, and gas temperatures are available for 316 utility boilers in a Duct Survey data base at PETC (Sarkus and Henzel, 1988). The units surveyed have capacities of at least 50 MWe and SO<sub>2</sub> emissions of 1.8 lb SO<sub>2</sub>/MM Btu or greater and are less than 35 years old. Further information on the size rating of the boilers, the coal used, and the coal properties are contained in the ORACLE data base at PETC. This information was used along with the simple model (Equations 1-3) to develop a FORTRAN program for predicting the expected SO<sub>2</sub> removal for each boiler in the survey at different operating conditions and stoichiometric ratios.

A key part of the computation is estimating the permissible approach to saturation. A typical spray was assumed to have a surface mean droplet size of 30 microns and a maximum size of 70 microns. The calculated drying times based on plug flow of gas and zero slip was correlated with the equations:

$$t_{\text{dry}} = \frac{60 F_D F_S}{\Delta T_{\text{lm}}} \quad (4)$$

where

$$F_D = 1 + 0.05 \frac{(T_{\text{in}} - T_{\text{as}})}{(T_{\text{out}} - T_{\text{as}})} \quad (5)$$

$$F_S = \left( \frac{d_{\text{max}}}{70} \right)^2 \quad (6)$$

and  $T_{\text{lm}}$  is the log mean temperature difference between the spray and flue gas at the beginning and end of the straight length of duct. The factor  $F_D$  allows for the effect of drop size distribution, which makes the largest drops evaporate more slowly than they would in a monodispersion (Harriott, 1989b). The factor  $F_S$  is used if the largest drop size is greater than 70 microns.

The first step in the program is the calculation of the approximate gas residence time based on the inlet velocity and the longest straight duct length. Space in the straight duct required for atomization equipment is neglected, and the complete gas residence time is assumed to be available for droplet drying. Then the outlet gas temperature is calculated by trial to make the drying time from Eq. (4) match the residence time. The approach to saturation is specified to be at least 20 F° to insure that the particles are dry enough to prevent sticking on the duct walls. The closest approach to adiabatic saturation that will yield stable operation is yet to be firmly established in full scale operation. The amount of water to be added is then determined by a heat balance. The Ca/S ratio is set at arbitrary values such as 1.5 or 1.8 and the SO<sub>2</sub> removal calculated, or the SO<sub>2</sub> removal is fixed and the Ca/S ratio determined.

#### Results for Normal and Part-Load Operation

The distribution of residence times in the longest straight duct at full load for the boilers in the survey is shown in Figure 3. Residence time for most boilers falls in the range 0.4 - 1.6 seconds. The projected SO<sub>2</sub> removals for a few plants with residence times ranging from 0.40 - 1.98 seconds at full load are given in Table 1. Over 50% SO<sub>2</sub> removal is possible at SR = 1.8 except for the two plants with the lowest residence times.

To illustrate how SO<sub>2</sub> removal depends on some of the independent variables, a typical boiler has been chosen as a baseline for a process variable study. The boiler chosen, at the Genoa Station in Wisconsin, has a capacity of 350 MWe and a straight duct residence time of 0.60 seconds at full load. Its flue gas contains about 1395 ppm SO<sub>2</sub>. The effect of residence time on SO<sub>2</sub> is shown in Figure 4, where the residence time at Genoa Station is treated as if it were an independent variable. The calculations have been performed such that the maximum amount of water was injected

subject to the drying conditions and minimal allowable approach to adiabatic saturation described above. It is seen that for all stoichiometries considered, the SO<sub>2</sub> removal would increase significantly at Genoa Station if the duct residence time were increased from 0.60 s to about 1.0 s. The increased removal is due not only to longer reaction time, but also to a closer approach to saturation that is possible with the longer drying time. For times above about 1.2 s little additional SO<sub>2</sub> removal is predicted. This is because the system at 1.2 s residence time is already operating at the closest approach to saturation permitted, and the model predicts little further reaction with almost dry lime particles.

The importance of the approach to saturation is further illustrated in Table 2, where the effect of operating under reduced load conditions is shown for the Genoa Station. Operation of a boiler at part load increases the gas residence time but decreases the gas temperature at the injection point. The increased gas residence time permits operation at a closer approach to adiabatic saturation as well as providing longer reaction time. Both effects improve SO<sub>2</sub> removal. Compared to full load, operation at 80% load is predicted to increase the SO<sub>2</sub> removal by 7 percent absolute.

The increase in SO<sub>2</sub> removal with decreasing approach to saturation is similar to that observed in the dry scrubbing process, where flue gas is contacted with lime slurry in a spray dryer. However, the contact time in the spray dryer is about 10 seconds, in contrast to the typical residence times of 0.5-2 seconds in the duct. When the residence time in the duct is sufficient to allow a 20 F° approach to saturation, the predicted SO<sub>2</sub> removal is still less than that reported for a spray dryer. The difference is probably caused by additional SO<sub>2</sub> absorption in the almost dry solid during the last 8-9 seconds of residence time.

#### Total Emissions Reduction

The 316 power plant boilers in the survey data base have a total capacity of 85,400 MWe and had uncontrolled emissions of 7.9

million tons SO<sub>2</sub>/year in 1985. Using induct injection of lime slurry at Ca/S = 1.8, the model was used to estimate SO<sub>2</sub> removal in each boiler. The total SO<sub>2</sub> removed is computed to be 4.7 million tons/year for an average removal of 57 percent.

The predictions given here are estimates based on limited data. A more thorough laboratory, pilot-plant, and modeling study of the induct process is now being carried out under DOE sponsorship, and a design handbook for the process will be prepared. However, the simple model used here, with corrections to fit current data, may still be useful for quick comparisons or for predicting the effects of changes in plant operation on SO<sub>2</sub> removal.

#### REFERENCES

1. Harriott, P., "A Simple Model for the Induct Injection Process for SO<sub>2</sub> Removal," 1989a, submitted to JAPCA.
2. Harriott, P., "Drying Times for Slurry Droplets in the Duct Injection Process," 1989b, U.S. Department of Energy.
3. Murphy K.R., and E.A. Samuel, "In-duct Scrubbing Pilot Study," Fourth Annual Coal Preparation, Utilization, and Environmental Control Contractors Conference, Pittsburgh, PA, August, 1988.
4. Murphy, K.R., E.A. Samuel, and A. Demian, "In-duct Scrubbing Process," First Combined FGD and Dry SO<sub>2</sub> Control Symposium, St. Louis, MO, Oct. 1988.
5. Drummond, C.J., and M. Babu, "Duct Injection Technologies for SO<sub>2</sub> Control," ibid.
6. Sarkus, T.A. and D.S. Henzel, "DOE's Duct Injection Survey," presented at Fourth Annual DOE Coal Preparation, Utilization, and Environmental Control Contractor's Conference, Pittsburgh, Aug. 8-11, 1988.

TABLE 1

Predicted SO<sub>2</sub> Removal for Selected Plants at SR= 1.8

| Station     | MWe | PPM  | T <sub>in</sub><br>°F | T <sub>out</sub> -T <sub>as</sub><br>°F | t<br>sec | ESO <sub>2</sub><br>% |
|-------------|-----|------|-----------------------|---|----------|-----------------------|
| Gibson      | 688 | 1874 | 320                   | 51                                      | 0.68     | 53                    |
| Hutsonville | 81  | 1927 | 300                   | 48                                      | 0.73     | 52                    |
| JM Stuart   | 610 | 1032 | 288                   | 29                                      | 1.00     | 70                    |
| Joppa       | 183 | 1337 | 320                   | 84                                      | 0.50     | 40                    |
| JP Pullian  | 125 | 1526 | 350                   | 108                                     | 0.40     | 34                    |
| Lansing     | 38  | 2165 | 305                   | 40                                      | 0.77     | 58                    |
| New Castle  | 105 | 1008 | 256                   | 20                                      | 1.98     | 72                    |

TABLE 2

SO<sub>2</sub> REMOVAL EFFICIENCY AT REDUCED FIRING RATES\*

| Firing<br>Rate | Inlet<br>Temp °F | Residence<br>Time, Sec | Approach<br>to TAS °F | SO <sub>2</sub> Removal<br>Efficiency % |
|----------------|------------------|------------------------|-----------------------|---|
| Full           | 380              | 0.6                    | 54                    | 54                                      |
| 80%            | 348**            | 0.75                   | 37                    | 61                                      |
| 50%            | 330              | 1.2                    | 20                    | 71                                      |

Notes:

\*SO<sub>2</sub> Concentration 1395 PPM, Ca/S Ratio = 1.4.

\*\*Estimated Values

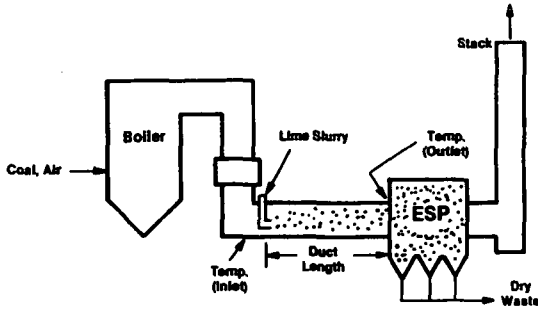


**FIGURE 1. INDUCT LIME SLURRY INJECTION PROCESS FLOW DIAGRAM.**

J/19,378

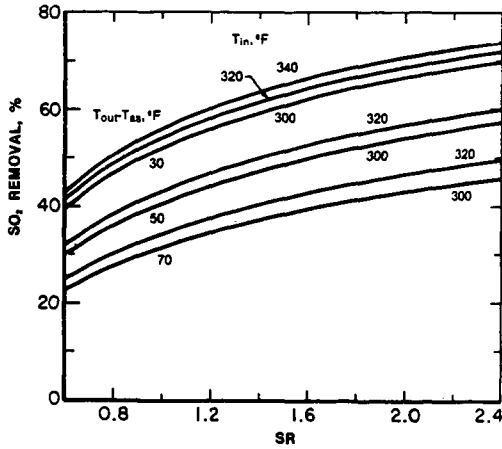


**Figure 2. Dependence of SO<sub>2</sub> Removal on Stoichiometric Ratio.**

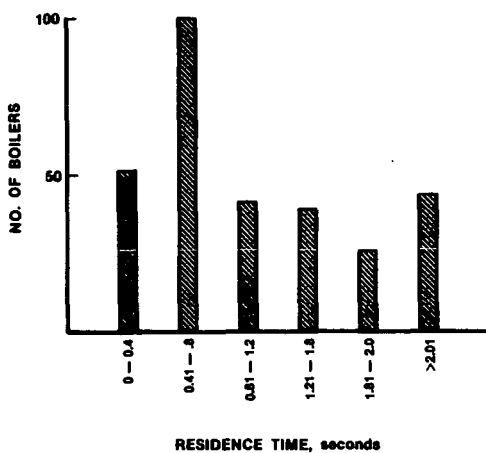


Figure 3. Residence Times in Longest Straight Duct at Full Load for Survey Data.

NO/19,565

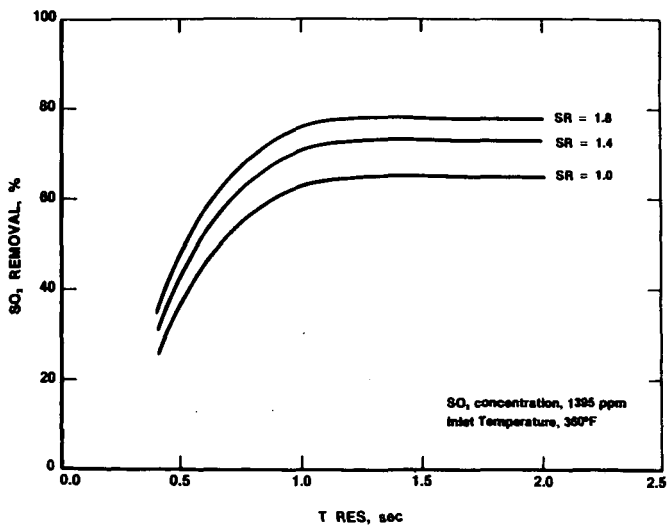


Figure 4. Dependence of SO<sub>2</sub> Removal on Residence Time.

NO/19,564